

FABRICATION AND EVALUATION OF A NOVEL BI-LAYER TISSUE-ENGINEERED SCAFFOLD FOR IMPROVED BIO SEAL AND ANTIMICROBIAL PROPERTIES OF DENTAL IMPLANTS: AN IN VITRO STUDY

A Dissertation submitted by

DR. GEETHU VENUGOPALAN
(US No.: NU21DPER04)

To



(Estd under Section 3, UGC Act 1956)
(Placed under Category 'A' by MHRD., Govt. of India; Accredited as 'A+' Grade University by NAAC)

In partial fulfilment of the requirements for the award of

MASTER OF DENTAL SURGERY (PERIODONTOLOGY)

DEPARTMENT OF PERIODONTOLOGY

A.B. SHETTY MEMORIAL INSTITUTE OF DENTAL SCIENCES

DERALAKATTE, MANGALURU-575018

KARNATAKA, INDIA

MARCH, 2024

FABRICATION AND EVALUATION OF A NOVEL BI-LAYER TISSUE-ENGINEERED SCAFFOLD FOR IMPROVED BIO SEAL AND ANTIMICROBIAL PROPERTIES OF DENTAL IMPLANTS: AN IN VITRO STUDY

A Dissertation submitted by

Dr. GEETHU VENUGOPALAN
(US No. NU21DPER04)

Under the Guidance of
PROF. (DR.) RAHUL BHANDARY

To



(Estd under Section 3, UGC Act 1956)
(Placed under Category 'A' by MHRD., Govt. of India; Accredited as 'A+' Grade University by NAAC)

In partial fulfilment of the requirements for the award of

MASTER OF DENTAL SURGERY (PERIODONTOLOGY)

DEPARTMENT OF PERIODONTOLOGY

A.B. SHETTY MEMORIAL INSTITUTE OF DENTAL SCIENCES

DERALAKATTE, MANGALURU-575018

KARNATAKA, INDIA

MARCH, 2024

CERTIFICATE

This is to certify that the dissertation titled “**Fabrication and evaluation of a novel bi-layer tissue-engineered scaffold for improved bio seal and antimicrobial properties of dental implants: An in vitro study**” is a bonafide research work carried out by **Dr. Geethu Venugopalan (NU21DPER04)** under the guidance of **Prof. (Dr.) Rahul Bhandary** in the **Department of Periodontology** of **A.B. Shetty Memorial Institute of Dental Sciences**.

The same is being submitted to the Nitte (Deemed to be University) in partial fulfillment of the requirements for the award of **Master of Dental Surgery (Periodontology)**

Prof. (Dr.) Rahul Bhandary

Guide

Dr. RAHUL BHANDARY

Professor

Department of Periodontology

A B Shetty Memorial Institute of Dental Sciences

Nitte (Deemed to be University)

Deralakatte, Mangalore - 575018

Prof. (Dr.) Amitha Ramesh

Head of the Department

Dr. AMITHA RAMESH
Professor and Head of the Department
Department of Periodontology
A B Shetty Memorial Institute of Dental Sciences
Nitte (Deemed to be University)
Deralakatte, Mangalore - 575 018

Prof. (Dr.) U. S. Krishna Nayak

Head of the Institution

Principal, A.B. Shetty Memorial Institute of Dental Sciences
Nitte (Deemed to be University)
Deralakatte, Mangalore - 575 018

DECLARATION

I, **Dr. Geethu Venugopalan (NU21DPER04)** hereby declare that the Dissertation work titled "**Fabrication and evaluation of a novel bi-layer tissue-engineered scaffold for improved bio seal and antimicrobial properties of dental implants: An in vitro study**" is my original work and has been carried out under the guidance of **Prof. (Dr.) Rahul Bhandary, Department of Periodontology, A.B. Shetty Memorial Institute of Dental Sciences** is being submitted to the **Nitte (Deemed to be University)** in partial fulfillment of the requirements for the award of **Master of Dental Surgery (Periodontology)**.

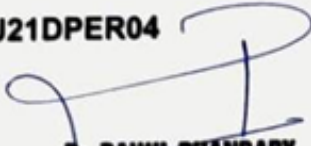
I also hereby declare that this work in part or full has not been submitted to any other University/Institution for any Degree/Diploma.

I hereby declare that Nitte (Deemed to be University) Mangalore, Karnataka shall have all the copyrights to preserve, use, and disseminate this dissertation /thesis in print or electronic format for academic/research purpose.

Date of Submission: 02.03.2024


Dr. Geethu Venugopalan

NU21DPER04


Dr. RAHUL BHANDARY
Professor
Department of Periodontology
A B Shetty Memorial Institute of Dental Sciences
Nitte (Deemed to be University)
Deralakatte, Mangalore -575018

The completion of this project would not have been possible without the invaluable support of numerous individuals and institutions.

*I am deeply indebted to my esteemed guide, **Prof.(Dr.) Rahul Bhandary**, whose unwavering support has been the cornerstone of my success. Sir's unwavering trust in my intellectual curiosity granted me the freedom and encouragement to explore a relatively new topic of tissue engineering in Periodontology for my research. His approachability, willingness to go above and beyond and consistent provision of prompt and insightful guidance significantly contributed to the success of this project. I am particularly grateful for how, during a critical juncture, he accompanied me to NITK, Suratkal, to help resolve the issue, demonstrating his unwavering dedication to the study. Furthermore, his attention to detail, even with the seemingly minor aspects of my research, set a high standard for excellence and instilled in me a commitment to thoroughness. Sir's invaluable advice was a guiding light and significantly improved the clarity and direction of my work. I am deeply grateful for his guidance and the positive impact he has had on my academic journey.*

*I am grateful for the enriching intellectual environment provided by the **Prof.(Dr.) Anandhan S** at the National Institute of Technology Karnataka, Suratkal. A special thank you for generously offering your expertise and guidance, particularly in the area of electrospinning. Your insights and willingness to share your knowledge were invaluable.*

*I also offer my sincerest gratitude to **Dr. Harsha G. Patil** who despite his own demanding Ph.D. workload, consistently made time to help me, patiently guiding me from the fundamental principles of mathematics to the intricacies of tissue engineering. I am deeply indebted to **Dr. Abhipreeth Mohapatra** for his invaluable assistance in preparing my FTIR results. I am grateful to **Dr. Govind Ekbote, Dr. Satish,** and **Dr. Harisha G** for their insightful feedback and words of encouragement throughout my research journey.*

*I extend my sincere acknowledgment to **Prof. (Dr.) Amitha Ramesh**, Head of the Department of Periodontology, for her unwavering support and motivation throughout my journey.*

*I am also grateful to **Prof.(Dr.) Biju Thomas, Prof.(Dr.) Nina Shenoy, Prof.(Dr.) Santhosh Shenoy, Prof.(Dr.) Avaneendra Talwar, Prof.(Dr.) Mamatha Shetty, Dr. Smitha Shetty, Dr. Amita Rao, Dr. Akshatha Shetty,** and **Dr. Reema Rao** for their willingness to impart knowledge and constructive criticism.*

*I would like to express my sincere gratitude to **Prof. (Dr.) U.S Krishna Nayak**, Principal and Dean of AB Shetty Memorial Institute of Dental Sciences. His leadership in consistently providing excellent research facilities was instrumental in my success.*

*My sincere appreciation extends to **Fernanda Condi De Godoi, and Carlos Mandolesi** at Tessengerlo Innovation Centre for their invaluable contribution. Their generous provision of materials for my research was pivotal in advancing my project and allowed me to delve deeper into the unexplored territories of this*

field. I am particularly grateful to Fernanda for her incredible support throughout this process. She was always just a question away, no matter how small or complex it seemed. Fernanda truly went beyond her usual duties by actively helping me navigate the initial formulations and assisting me with the shipping documents. Her dedication was invaluable.

*My deepest gratitude goes to the **American Academy of Implant Dentistry (AAID)** for their generous AAIDF Student Research Grant, which made this research endeavor possible. The AAIDF's unwavering commitment to fostering scientific exploration and innovation in implant dentistry is truly commendable, and I am incredibly grateful for their belief in my work.*

*I extend my sincere gratitude to **Dr. Mohana Kumar** and **Dr. Veena Kumari** for their invaluable contributions to my research. Their willingness to share their expertise and insights significantly enriched my research and ultimately strengthened my thesis.*

*I am deeply grateful to **Mr. Rajesha P** and **Mr. Jayaprakash Shetty** for their critical support in the laboratory. Their assistance was instrumental in ensuring I completed my thesis on time and to a high standard.*

*I extend my sincere gratitude to **Dr. Sri Vidya Bhatt** for her invaluable assistance with the statistical analysis of my research data. Her in-depth knowledge of Statistical Inference and meticulous guidance were instrumental in identifying key trends and optimizing my data analysis, ultimately strengthening the conclusions of my dissertation. I am particularly grateful for her willingness to go the extra*

mile, even answering my queries outside of office hours and explaining complex concepts clearly.

To my dearest co-pgs.' and friends, **Dr. Karthika Nair, Dr. Gauri, Dr. Bharathi, and Dr. Akriti**, I extend my heartfelt gratitude for your invaluable support throughout this journey.

I am deeply grateful to my amazing juniors and friends, **Dr. Khushi Shukla, Dr. Putta Uday Simha, Dr. Ayush Gupta, Dr. Subhash Chandra, Dr. Karthika G, and Dr. Bhaskarya Bhaskar Bora** for being the most fun and supportive juniors I could ask for. They were always willing to lend a helping hand and their friendship and support made this journey truly unforgettable.

I would also like to thank my senior, **Dr. Dipanjan Das**, for his **unwavering encouragement and timely words of advice**. I am equally grateful to **Dr. Sreeja Reddy, Dr. Meghana, and Dr. Surabhi** for their **help and support** throughout my postgraduation.

I would be remiss not to acknowledge the unwavering love and encouragement from my friends. To my dear friends, **Dr. Nandita Sorte, Dr. Akshata Rao, Dr. Vinay Kumar, Dr. Ananya Rao, Dr. Sreelakshmi S, Dr. Garima Karn, Dr. Anoopkrishna, Dr. Shawn, Dr. Joel, Dr. Karthika Nambiar, Dr. Dhvani Tanna, Dr. Hari, Parul Yadav, Dr. Jidna P, Dr. Anju, Dr. Jitin, Dr. Prathul, Dr. Tanu, Dr. Arvind, and Dr. Kevin**. Thank you for your laughter, support, and understanding, even during the most stressful moments. You have been my source of strength and joy.

I wish to acknowledge and express my gratitude to **Ms Sreedevi, Ms. Asha, Ms. Harini, Mr. Naveen, and Mr. Rajesh**. Each of you has contributed in unique ways to my journey, and I am deeply grateful for your support.

*To my parents, **Mr. Venugopalan K** and **Ms. Jyothi**, and my loving sister **Devika**, thank you for your unwavering faith in me throughout this challenging journey. I will never forget the countless sacrifices you made, to ensure I had the opportunity to pursue my academic dreams. Your unconditional love provided a haven throughout this challenging journey. Thank you for always encouraging me to give my best and it is your happiness that makes me strive for my success.*

*I am deeply indebted to **Mr. Sundaran K**, who has been a father figure throughout my journey. His unwavering belief in me, and willingness to go above and beyond, even going as far as restudying chemistry to help me, with even the simplest of chemical formulations, has truly been a source of strength for me. I am incredibly grateful for his commitment to my success. I would also like to express my sincere gratitude to **Ms. Raji M** who provided invaluable encouragement and support throughout my journey.*

To all of you, I offer my sincerest thanks. Your contributions have made this achievement possible, and I will forever cherish the memories and lessons learned along the way.

I also thank the Almighty, for the wisdom he bestowed upon me, the strength, the stability, and good health to finish the work on time. His blessings have always helped me overcome all the challenges and obstacles I've faced during this journey.

%	Percentage
µg	Microgram
Ag ⁺	Silver ions
AK.	Amikacin
ANOVA	Analysis of variance
ATCC	American Type Culture Collection
ATP	Adenosine triphosphate
BHI	Brain Heart Infusion
C	Carbon
CAS No.	Chemical Abstracts Service Registry Number (CAS Number)
CFU	Colony Forming Units
CIP.	Ciprofloxacin
CLSI	The Clinical & Laboratory Standards Institute
cm	Centimetre
CS	Collagen scaffold
Cu	Copper
Cu ²⁺	Copper ions
CuNPs	Copper Nanoparticles
DA	Dopamine
DI	Double distilled water
DMEM	Dulbecco's Modified Eagle Medium
DMF	N, N-Dimethylformamide
D-PHI	Degradable Polyurethane

ECM	Extracellular matrix
EDS	Energy-Dispersive X-Ray Spectroscopy
EDTA	Ethylenediaminetetraacetic acid
FBS	Fetal bovine serum
FTIR	Fourier Transform Infrared Spectroscopy
g.	Gram
GE/HA/PDA/CuNPs	Gelatin/Hyaluronic acid/Polydopamine/Copper nanoparticles
GelMA	Methacrylated Gelatin
HA	Hyaluronic acid
HCl	Hydrochloride
HGFs	Human Gingival Fibroblasts
HRP	Horseradish Peroxidase
hrs.	Hours
IAI	Implant-Abutment Interface
IBL	Internal Basal Lamina
IL-1 β	Interleukin-1 beta
JE	Junctional Epithelium
kV	Kilovolt
M	Molarity
MCA	Micro contact angle
MEW	Melt Electro-Writing
mg	Milligram
MH	Muller-Hinton

MIC	Minimal Inhibitory Concentration
ml	Millilitre
mol	Mole (unit)
M _r	Relative Molar Mass
MTT	3-(4,5-Dimethylthiazol-2-yl)-2,5-diphenyltetrazolium bromide
N	Nitrogen
Na	Sodium
NaCl	Sodium Chloride
nm	Nanometre
NO	Nitric oxide
O	Oxygen
°C	Degree Celsius
PBS	Phosphate-buffered saline
PCNU	Polycarbonate urethane
PDA	Polydopamine
<u>PDAM@Cu</u>	Polydopamine-Copper coating
pH	Potential of Hydrogen
PIE	Peri-Implant epithelium
QAS	Quaternary Ammonium Salt
RGD	Arginine–Glycine–Aspartic Acid
s.	Second(s)
Saos-2	Sarcoma osteogenic-2
SEM	Scanning Electron Microscopy

ABBREVIATIONS

SiC	Silicon Carbide
Ti	Titanium
Ti-6Al-4V	α - β titanium alloy
TNF- α	Tumor necrosis factor-alpha
Tris-HCl	(Tris(hydroxymethyl)aminomethane, Hydrochloric Acid)
Tukey's HSD	Tukey's HSD (honestly significant difference)
UV	Ultraviolet
w/v	Weight/Volume
wt. %	Weight percent
XTT	Methoxynitrosulfohenyl-tetrazolium carboxanilide
Zn ²⁺	Zinc ions

LIST OF TABLES

Sl. No.	Table No.	Page No.
1	Table 1: The table presented shows the quantitative analysis results for copper (Cu) using the eZAF correction method	45
2	Table 2: eZAF Quantitative Analysis of Elements in the GE/HA/PDA/CuNPs mat scaffold	48
3	Table 3: This table summarizes the antimicrobial activity of titanium (Ti) discs coated with varying CuNPs percentages against <i>Pseudomonas aeruginosa</i> , compared to a control group treated with the antibiotic Amikacin.	59
4	Table 4: One-Way ANOVA results for the effect of CuNPs concentration on <i>P. aeruginosa</i>	60
5	Table 5: This table summarizes the results of post-hoc comparisons conducted using Tukey's HSD test following a one-way ANOVA to assess the antimicrobial efficacy of different concentrations of CuNPs against dependent variable i.e., <i>P aeruginosa</i>	61
6	Table 6: This table summarizes the antimicrobial activity of titanium (Ti) discs coated with varying CuNPs percentages against <i>Staphylococcus aureus</i> , compared to a control group treated with the antibiotic Ciprofloxacin	63
7	Table 7: One-Way ANOVA Results for the Effect of CuNPs Concentration on <i>S.aureus</i>	64

8	Table 8: This table summarizes the results of pairwise comparisons using Tukey's HSD test following a one-way ANOVA to assess the antimicrobial efficacy of different concentrations of copper nanoparticles (CuNPs) against <i>Staphylococcus aureus</i> .	65
9	Table 9: Bacterial Survival after Exposure to GE/HA/CuNPs Scaffold	69

LIST OF FIGURES

Sl. No.	Figure No.	Page No.
1	Figure1: Image showing the electrospinning apparatus setup used in the study	23
2	Figure 2: This digital image depicts a GE/HA /CuNPs electrospun scaffold formed over PDA coated Ti alloy disc placed on a collector plate.	24
3	Figure 3: Representative image of the front-view image of a JEOL JSM-7610FPLUS scanning electron microscope (SEM) equipped with an Energy Dispersive Spectroscopy (EDS) detector.	26
4	Figure 4: The representative figure depicts a Jasco FTIR 4200 spectrometer employed in this study for the identification of functional groups in biological samples.	28
5	Figure 5: Optical image showing titanium discs before and after coating with GE/HA/PDA/CuNPs electrospun scaffold.	37
6	Figure 6: SEM images of the GE/HA/CuNPs electrospun scaffold at 1000 x magnification showing an interconnected network of fibers and porous morphology.	39
7	Figure 7: SEM images of the GE/HA/CuNPs electrospun scaffold at 2,500x and 2,700x magnification.	40
8	Figure 8: Figure showing Scanning electron microscopy (SEM) images of the electrospun GE/HA/CuNP scaffold at magnifications of 5000x (A) and 10,000x (B)	40

9	Figure 9: Scanning electron microscopy (SEM) image of the electrospun GE/HA/PDA/CuNPs composite scaffold with the corresponding histogram (B) illustrates the diameter distribution of the fibers.	41
10	Figure 10: Scanning electron microscopy (SEM) image (1000x magnification) of the electrospun nanofiber scaffold alongside its corresponding energy-dispersive X-ray spectroscopy (EDS) analysis	43
11	Figure 11: EDS live map demonstrating the presence and distribution of copper nanoparticles (CuNPs), indicated by yellow dots.	44
12	Figure 12: EDS spectrum of the electrospun scaffold, indicating the presence of CuNPs (CuL α) through the characteristic peak at X-ray energy (keV).	45
13	Figure 13: EDS overlay map of the electrospun GE/HA/PDA/CuNPs scaffold, displaying the elemental distributions of carbon (C - blue), nitrogen (N - green), oxygen (O - red), and copper (Cu - yellow).	46
14	Figure 14: Live EDS elemental map of the electrospun GE/HA/PDA/CuNPs scaffold, depicting the spatial distribution of carbon (C - blue), nitrogen (N - green), oxygen (O - red), and copper (Cu - yellow).	47
15	Figure 15: This figure presents an energy-dispersive X-ray spectroscopy (EDS) spectrum of the GE/HA/PDA/CuNPs mat scaffold.	48
16	Figure 16: FTIR Spectra of various scaffold components	52

17	Figure 17: Water contact angles of unmodified Ti-alloy disc, PDA coated Ti-alloy disc, and GE/HA/PDA/CuNPs scaffold coated Ti-alloy disc at various time points.	55
18	Figure 18: This figure presents the antimicrobial activity of GE/HA/PDA/CuNPs coated discs with varying copper nanoparticle (CuNP) concentrations (5%, 10%, 15%, and 20%) against <i>Pseudomonas aeruginosa</i>	62
19	Figure 19: This figure illustrates the antimicrobial activity of GE/HA/PDA/CuNPs coated discs with varying copper nanoparticle (CuNP) concentrations (15% and 20%) against <i>Staphylococcus aureus</i> .	66
20	Figure 20: Broth Microdilution Assay for Antibacterial Susceptibility Testing of CuNPs-Incorporated GE/HA Polymer Solution	68
21	Figure 21. Line graph depicting the percent reduction in bacterial count over varying contact times for two representative bacterial samples (<i>P.aeruginosa</i> and <i>S.aureus</i>)	70
22	Figure 22: Representative image of HGFs exhibiting their characteristic fibroblastic morphology	72
23	Figure 23: Representative image of cell culture plate used for testing the cytotoxicity of selected materials on human gingival fibroblasts (HGFs) by MTT and proliferation assay	73
24	Figure 24: Viability values of human gingival fibroblasts exposed to Ti-coated and Ti-uncoated materials.	74
25	Figure 25: Proliferation of human gingival fibroblasts exposed to Ti-coated and Ti-uncoated materials.	75

BACKGROUND AND OBJECTIVE:

Dental implants have revolutionized oral healthcare for decades, yet the specter of peri-implantitis continues to cast a shadow on their long-term success. Despite significant research efforts dedicated to surface modifications aimed at enhancing osseointegration, the critical role of the "biological seal" formed by soft tissue around the implant often remains overlooked. This multi-functional barrier guard the implant-bone interface from pathogenic invasion, and restricts the apical progression of marginal inflammation, ultimately preventing peri-implantitis. However, the current approaches to dental implant soft tissue integration target isolated aspects of implant healing, neglecting the interconnectedness of key phases like fibroblast adhesion, proliferation, and soft tissue attachment while simultaneously preventing microbial growth. This fragmented approach hampers the development of a truly comprehensive and optimized healing strategy.

Therefore, this study aims to fabricate a tissue-engineered scaffold that may be easily replicated over the neck of a dental implant and/or abutment, to provide optimal conditions for healing at the implant-soft tissue with enhanced soft tissue integration, and anti-bacterial colonization to provide biologically stable implants.

MATERIALS AND METHODS:

A polymer solution containing Gelatin (20 wt.%) embedded with 5-10nm Copper nanoparticles (20 % wt./v of Gelatin) and hyaluronic acid (3 wt.%) in the ratio of 6:4 was electrospun onto polydopamine-coated Titanium alloy disc to form a Gelatin-Hyaluronic acid-Polydopamine-copper nanoparticles (GE/HA/PDA/CuNPs) mat scaffold. The microstructure, morphology, fiber diameter, nanoparticle(s) distribution, composition, and wettability were studied

through SEM, EDS, FTIR, and Contact angle analysis. The antimicrobial activity of the CuNPs-impregnated scaffolds was evaluated against representative samples of Gram-negative (*Pseudomonas aeruginosa*) and Gram-positive (*Staphylococcus aureus*) bacteria by disc diffusion and broth microdilution methods. Cytotoxicity analysis (MTT assay) and cell proliferation were assessed at 24 and 72 hours for three groups: control (Gingival fibroblasts cultured alone), Ti-coated (GE/HA/PDA/CuNPs scaffold coated Ti-alloy discs); and Ti un-coated Ti alloy discs.

RESULTS:

SEM revealed a well-defined porous morphology with an average fiber diameter of 280 ± 60 nm in the electrospun GE/HA/CuNPs nanofibers. EDS confirmed the presence and uniform distribution of CuNPs throughout the scaffold. FTIR verified the successful incorporation and integrity of all constituent materials; Gelatin, hyaluronic acid, Polydopamine, and copper nanoparticles as confirmed by the spectral peaks observed. Contact angle analysis revealed a reduced contact angle for GE/HA/PDA/CuNPs modified Ti disc showing enhanced cell adhesion properties of the scaffold. The GE/HA/PDA/CuNPs scaffold exhibited significant antimicrobial activity against both Gram-negative (*P. aeruginosa*) and Gram-positive (*S. aureus*) bacteria. Cell viability and proliferation over the GE/HA/PDA/CuNPs modified Ti discs were seen to be significantly increased ($P < 0.05$) at 72 hours as compared with the unmodified Ti disc.

Conclusion:

The study findings highlight the promise of the novel bioengineered scaffold as a comprehensive strategy, for simultaneously modulating early cell adhesion and

proliferation while enhancing antimicrobial/antibiofilm properties on titanium dental implants, ultimately promoting effective soft tissue healing on the implant surface. Further investigations are warranted to explore the long-term stability and in vivo performance of these scaffolds for their potential translation to clinical practice and improved patient outcomes.

Keywords: Dental implants, peri-implantitis, biological seal, soft tissue attachment, surface modification, nanofibers, tissue engineering, nanofiber scaffold, electrospinning.

TITLE		PAGE NO
CHAPTER I: INTRODUCTION		1-16
1.1	PREAMBLE	1-8
1.2	AIMS AND OBJECTIVES	9
1.3	LITERATURE SURVEY	10-16
CHAPTER II: METHODOLOGY		17-36
CHAPTER III: RESULTS		37-75
CHAPTER IV: DISCUSSION		76-84
CHAPTER V: CONCLUSIONS, SUMMARY, LIMITATIONS, AND SCOPE FOR FUTURE WORK		85-92
REFERENCES		93-109
APPENDIX		110-111
ANNEXURES		
ANNEXURE I- Ethical Clearance Certificate		112
ANNEXURE II- Synopsis		113-130
ANNEXURE IV- Consent Forms		131-138
ANNEXURE V- 'TURNITIN' Originality Report		139-141
ANNEXURE VI- NITK Certificate		142
ANNEXURE VII- Permission letter NUCSReM		143
ANNEXURE VIII- Tukey's multiple Comparisons test data- Cell Viability and Proliferation		144-147

Dental implants constitute the current gold standard treatment for the rehabilitation of missing teeth, providing patients with an improved oral health-related quality of life with long-term functional outcomes.^[1] In the preceding decades, there has been a marked surge in the application of Titanium implants as the preferred therapeutic modality in addressing partial or complete edentulism, with an estimated one million dental implant procedures conducted annually.^[2] Projections indicate a prospective increase in the adoption of dental implants, with an anticipated expansion to encompass as much as 23% of the global population.^[3]

Nevertheless, despite the revolutionization of dental rehabilitation by osseointegrated implants, offering significant functional and aesthetic improvements, a looming shadow has emerged in the form of escalating peri-implant diseases, particularly peri-implantitis. These inflammatory conditions jeopardize the long-term success and patient well-being associated with implant supported rehabilitation, despite demonstrably high initial success rates. This growing burden of peri-implant diseases presents a significant challenge, demanding a deeper understanding of their etiology and novel approaches for prevention and treatment.^[4,5]

The inflammation-associated lesions that arise in the tissues surrounding implants are commonly referred to as Peri-implant diseases^[6]. Within the spectrum of severity of peri-implant diseases, a classification reflective of periodontal conditions in natural dentition delineates two discrete categories: peri-implant mucositis, equivalent to gingivitis, and peri-implantitis, analogous to

periodontitis.^[6, 7] Peri-implant mucositis is delineated as a reversible inflammatory response occurring in the soft tissues surrounding a functional implant. Peri-implantitis, in contrast to peri-implant mucositis, is characterized by inflammation extending beyond the soft tissues to involve the deeper connective tissues surrounding the osseointegrated implant. This progressive inflammation triggers a gradual resorption of the supporting bone, potentially leading to implant failure if left untreated.^[8, 9]

The prevailing model for peri-implant diseases posits a sequential progression akin to the well-established gingivitis-periodontitis paradigm in natural teeth. This model proposes that peri-implant mucositis, confined to the soft tissue around the implant, precedes the development of more severe peri-implantitis, characterized by inflammation extending to the underlying bone and connective tissue.^[10] Hence, the pivotal strategy for averting peri-implant diseases lies in the effective prevention of peri-implant mucositis and its subsequent progression to more advanced stages of the pathological continuum, culminating in the outcome of implant failure.^[11]

This underscores the importance of the peri-implant mucosal region, as it plays a vital role in establishing a strong physiological and biological barricade against the external environment, effectively impeding the ingress of bacterial plaque and safeguarding the integrity of the implant-site interface. This protective mechanism is achieved through the attachment of epithelial and connective tissues, effectively shielding the implant and underlying bone from the oral environment.^[12, 13]

The absence of a periodontal ligament at the implant-gingival interface, a key distinction from natural tooth structure, contributes to compromised biological properties, particularly manifested in inadequate and potentially dysfunctional soft tissue attachment.^[14] Moreover, the epithelial attachment structure, comprised of the basal lamina and hemidesmosomes, is localized predominantly in the apical third of the Peri-Implant Epithelium (PIE), diminishing its resilience and structural integrity, thereby rendering it vulnerable to bacterial infiltration. ^[12, 14, 15, 16, 17]

Additionally, in instances of delayed or improper attachment, opportunistic bacteria have the potential to infiltrate the interstitial space between the implant and gingival mucosa, thereby precipitating peri-implant infections ^[16, 17, 18]

Thus, there exists a critical need to overcome the limitation of inadequate soft tissue integration, which impedes the successful replication of the physiological milieu surrounding natural teeth.

Recent research endeavors have unveiled that the physicochemical attributes of implant materials play a pivotal role in shaping the soft tissue responses at the interface, exerting a considerable impact on the efficacy and quality of soft tissue seals. ^[19, 20] Diverse techniques have been explored for the modification of implant surfaces, encompassing physical, chemical, and biological methodologies. These targeted interventions seek to optimize the titanium (Ti) surface, thereby facilitating enhanced cellular adhesion and proliferation, culminating in improved soft tissue integration. ^[20]

Functionally-tailored biopolymers designed to mimic the native extracellular matrix: extracellular matrix (ECM) offer promising potential as surface coatings for metal implants. These constructs, applied directly to the metallic surface, can mimic the microenvironment surrounding biological entities, potentially promoting targeted cellular reactions that promote healing at the site of injury, ultimately resulting in an improved soft-tissue response. ^[21]

Polydopamine (PDA), representing the ultimate oxidation product of dopamine or other catecholamines, has emerged as a focal point for biomaterial modification due its notable capability to bind strongly to a wide array of substrates and offer secondary reactivity for biomolecule conjugation. ^[22, 23]

The polydopamine coating strategy has the potential to facilitate cell attachment and proliferation, thereby offering an additional dimension to augment cellular interactions on implant surface with good hydrophilicity, surface topography, structural integrity, biocompatibility, antimicrobial activity, cellular adhesion, and enhanced bone regeneration. ^[24,25,26,27,28]. Beyond promoting improved soft tissue response, the adhesive properties exhibited by PDA suggest its potential as a versatile intermediate layer to facilitate the integration of diverse functional materials, such as nanoparticles for targeted drug delivery, peptides for modulating cellular responses, growth factors, and hydrogels, involved in both soft tissue and bone remodeling. This ability to integrate materials enables the creation of "dual modifications," offering synergistic effects for tissue regeneration. ^[29]

Gelatin incorporates the arginine–glycine–aspartic acid (RGD) sequence, a motif known to augment cell adhesion by interacting with integrin.^[30] This biopolymer

effectively mimics RGD bio-signaling, creating a conducive site for cell attachment while inducing diverse cellular responses, including the facilitation of cellular proliferation, differentiation, and migration. Additionally, it promotes cell adhesion, spreading, and activation.^[31,32]

Hyaluronic acid (HA), a naturally occurring polysaccharide found throughout the human body, is a critical component of the ECM.^[34,35] HA significantly contributes to modulating the initial phases of inflammation and serves as an effective scavenger of reactive oxygen species.^[36] Its multifaceted properties extend beyond its anti-inflammatory functions, encompassing bacteriostasis^[37,38] and the alleviation of pain and swelling^[39]. Additionally, HA acts as a cellular modulator, influencing diverse biological responses such as angiogenesis, cell adhesion, proliferation, and differentiation through interactions with surface receptors on target cells.^[40,41,42]

The long-term success of dental implants is also intricately linked to a competitive process known as the "race for the surface." This dynamic interplay involves a race between tissue integration and bacterial colonization, both vying for dominance on the implant surface.^[43] Successful tissue integration around the implant results in its encapsulation by native host cells, thereby minimizing the susceptibility to infection. Conversely, if bacterial growth prevails, the likelihood of infection, potentially leading to peri-implantitis, is significantly heightened.^[43, 44]

Hence, the optimal approach to address peri-implantitis involves preventing biofilm formation on the implant material and creating an environment conducive to the proliferation of native cells.^[44] While systemic antibiotics are frequently employed for this purpose in practice, the associated risks of systemic toxicity

and microbial resistance have prompted the exploration of alternatives, including antimicrobial metal nanoparticles.^[45]

Several metal ions, including Cu^{2+} , Ag^{+} , and Zn^{2+} , are recognized for their antibacterial properties, presenting the possibility of deposition onto implant surfaces.^[46] Nonetheless, the reduced toxicity, enhanced cytocompatibility, and the capability for metabolic processing within the body make copper a favorable option for deposition on implant surfaces.^[47] Additionally, copper exhibits inherent antimicrobial properties, contributing to effective biofilm control by acting on dispersed bacteria.^[47,48]

Thus, it can be hypothesized that the use of three-dimensional porous scaffold matrices fabricated from various biocompatible polymers possessing tailored properties, including cell migration, proliferation, and inherent anti-inflammatory and antimicrobial functionalities, could offer a strategic advantage in preventing the onset of peri-implant mucositis and its progression to peri-implantitis.^[49]

The realization of biomimetic dental implant coatings hinges on a meticulous orchestration of the Tissue Engineering Triad.^[50] This triumvirate, encompassing cellular constituents, ingenious engineering methodologies, and the strategic integration of biochemical and physicochemical cues, paves the way for the development of intricate surface architectures, known as scaffolds that emulate the native extracellular matrix. This synergistic interplay fosters a microenvironment conducive to cellular adhesion, proliferation, and differentiation, ultimately leading to functional and durable tissue integration.^[50,51]

In tissue engineering, scaffolds serve as crucial temporary matrices, fostering cellular proliferation until achieving functional autonomy.^[52] These scaffolds require meticulously designed interconnected pore networks with optimal dimensions to facilitate efficient diffusion of essential growth factors.^[53] Additionally, ideal scaffolds possess commendable attributes like mechanical strength,^[54] biodegradability, bioactivity,^[55,56] hydrophilicity,^[57] and biocompatibility, while promoting tissue-inductive properties.^[57,58,59,60]

A versatile array of techniques is presently employed for scaffold fabrication.^[58,61,62] These include electrospinning for generating highly porous nanofibrous scaffolds^[63]; phase separation offering precise control over pore size and distribution^[64]; solvent casting commonly used for drug delivery and cell culture applications; particulate leaching that allows tailoring porosity and pore interconnectivity by incorporating and subsequently removing sacrificial particles., gas foaming which introduces bubbles into the material to create lightweight scaffolds with interconnected pores,^[65,66] rapid prototyping that utilizes computer-aided design and additive manufacturing for intricate geometries and functionalities, bioprinting, decellularization, melt electro-writing (MEW) and others.^[67,68,69]

Electrospinning employs an electrohydrodynamic process where an electric field induces the formation of a charged polymer jet. This jet undergoes stretching and solvent evaporation, resulting in the production of nanofibrous scaffolds with a high surface area-to-volume ratio^[70,71]

These electrospun fibrous scaffolds characterized by nanoscale/microscale

structures and interconnected pores mirroring the natural extracellular matrix in tissues, exhibit considerable promise in fostering the development of functional tissues. This potential is attributed to their notable features, including high porosity, specific surface area, favorable cell adhesion, and controlled drug release.^[70, 71, 72]

Therefore, this study aims to fabricate a novel tissue-engineered scaffold that may be seamless replicability over three-dimensional surfaces, such as dental implant necks and abutments, to create a microenvironment conducive to optimal tissue healing at the implant-soft tissue with enhanced cell proliferation, and anti-bacterial colonization to provide biologically stable implants.

RESEARCH GAPS:

The integral aspect of dental implant integration, the 'biological seal' encircling a dental implant, serving as a crucial physiological and biological barrier against the external environment, is frequently disregarded. The existing approach to healing lacks comprehensiveness, omitting critical phases such as coagulation, inflammation reduction, cell proliferation, heightened soft tissue attachment, and biofilm formation prevention, all of which play pivotal roles in implant integration. Notably, there is a current absence of micro or macrostructural surface modifications capable of facilitating perpendicularly directed collagen attachment of gingival fibers onto the implant surface. This underscores the need for a more holistic and tailored approach to enhance the efficacy of dental implant integration.

AIM

Fabrication and characterization of a bilayer tissue-engineered scaffold incorporating Polydopamine and Gelatin-hyaluronic acid-copper nanofibers, for enhanced bio seal and antimicrobial properties of dental implants

OBJECTIVES

1. To synthesize and characterize a tissue-engineered bi-layer scaffold containing polydopamine and Copper nanoparticle embedded Gelatin-Hyaluronic acid electrospun mat.
2. To evaluate the cell proliferation, attachment, and cytotoxicity of this tissue-engineered bilayer scaffold against gingival fibroblasts
3. To investigate the antimicrobial efficacy of the tissue-engineered bilayer scaffold-coated titanium Dental implant surface

NULL HYPOTHESIS (H_0):

The biomodification of the surface of Grade V titanium alloy with tissue-engineered bi-layer scaffold does not improve cell proliferation and attachment at the implant site and promotes microbial activity, resulting in an incomplete implant bio-seal.

ALTERNATE HYPOTHESIS (H_1):

The biomodification of Grade V titanium alloy surface with bilayer tissue-engineered scaffold enhances cell proliferation and attachment at the implant site while providing anti-microbial action, thereby improving the peri-implant mucosal seal.

1.3.1 PERI-IMPLANT MUCOSA IN PERI-IMPLANT DISEASE PATHOGENESIS:

1. Ikeda et al. (2000) employed a rat maxilla implantation model to investigate the ultrastructural features of the peri-implant epithelium (PIE) interface. The authors advocated the application of horseradish peroxidase (HRP) as a tracing agent in the mucosal region surrounding dental implants or teeth, as a means to visually demonstrate the distribution patterns observed at each transmucosal interface. In the natural interface, it was discerned that copious amounts of HRP were retained at the coronal region of the Junctional Epithelium (JE) and Internal Basal Lamina (IBL). In contrast, elevated concentrations of HRP were evident from the upper to middle regions of the PIE encircling dental implants. Thus, it was discerned that only the lower region exhibited a resilient epithelial attachment structure, while such structural integrity was notably absent in the middle and upper portions.^[73]
2. Atieh et al. (2013) conducted a systematic review and meta-analysis to assess the prevalence of peri-implant diseases in both general and high-risk populations. Their analysis of nine studies, encompassing 1,497 participants and 6,283 implants, revealed that peri-implant mucositis affected 63.4% of participants (30.7% of implants) and peri-implantitis affected 18.8% of participants (9.6% of implants). The authors concluded that peri-implant diseases are a common complication following implant therapy.^[74]
3. Matteo Albertini et al. (2014) conducted an assessment of periodontal and opportunistic flora in individuals diagnosed with peri-implantitis, identifying specific microorganisms such as *Candida albicans*, *Pseudomonas*

aeruginosa, *Staphylococcus aureus*, and *Staphylococcus warneri* in the context of peri-implantitis. The study's findings led to the noteworthy conclusion that the implant surface may be colonized by pathogens distinct from those commonly associated with periodontal bacteria. The presence of opportunistic pathogens, notably *P. aeruginosa*, *S. aureus*, and *C. albicans*, was observed, prompting the authors to suggest a potential association between these opportunistic pathogens and the occurrence of implant failure^[75]

4. Wang et al. (2015) reviewed soft tissue healing around dental implants, highlighting potential shortcomings in peri-implant soft tissue integration compared to natural teeth. Their analysis revealed a less favorable alignment of gingival fibers and diminished vascular supply at the implant interface, leading to reduced resistance against bacterial invasion. This vulnerability predisposes the peri-implant region to complications like peri-implant disease and bone loss. Notably, the authors observed significant differences in fibroblast and collagen fiber alignment compared to natural teeth. In natural dentition, collagen fibers exhibit a perpendicular orientation providing strength, while around implants, they align parallel to the surface, making them weaker and more susceptible to breakdown and bacterial invasion.^[76]
5. Shibli et al. (2015) identified key factors influencing osseointegration, peri-implant disease, and treatment. Their consensus report highlighted the critical role of the soft tissue seal, encompassing the junctional epithelium and connective tissue adaptation, for implant success. They emphasized the

importance of preserving the peri-implant biologic width and avoiding its disruption. Additionally, the report stressed the significance of the abutment-implant seal in minimizing mechanical and biological complications, maintaining marginal bone levels, and ultimately contributing to long-term implant success.^[77]

6. Ivanovski et al. (2017) compared healthy and diseased peri-implant and periodontal marginal soft tissues, concluding that maintaining the integrity of the peri-implant soft-tissue seal is crucial for peri-implant health. Their study revealed that specific implant design features, such as the connection between the implant and abutment and the surface characteristics of both elements, may influence the long-term health of the surrounding soft tissues.^[78]
7. Lafaurie et al. (2017) undertook a comprehensive systematic review to evaluate the microbial diversity in peri-implantitis, periodontitis, and healthy implant sites. The review encompassed investigations of microbial biofilms and whole microbiomes to elucidate similarities and discrepancies in microbial community. The review identified peri-implantitis as a diverse and mixed infection, incorporating periodontopathic microorganisms, non-cultivable anaerobic Gram-positive rods, as well as other non-cultivable Gram-negative rods. Additionally, opportunistic microorganisms, including enteric rods and *Staphylococcus aureus*, were identified, albeit infrequently.^[79]

1.3.2 TISSUE-ENGINEERED SCAFFOLDS FOR DENTAL APPLICATIONS

8. Hatayama et al. (2017) investigated the use of collagen scaffolds for in-situ tissue engineering for gingival tissue regeneration. They compared two scaffolds, CS-pH7.4 and CS-pH3.0, derived from atelocollagen treated at different pH levels. The study assessed epithelial and submucosal tissue lengths at the wound site compared to the control. They found that CS-pH7.4 significantly increased epithelial and submucosal tissue regeneration, leading to restored gum thickness. This led the authors to conclude that CS-pH7.4 holds promise as a scaffold for gingival tissue regeneration.^[80]
9. In 2018, Makita et al. conducted an investigation exploring the impact of micro/nanopatterned gelatins crosslinked with genipin on the biocompatibility of dental implants. The study elucidated that the intricate design of the gelatin surface pattern can effectively modulate both the attachment and proliferation of Saos-2 cells. Consequently, gelatin surfaces patterned through genipin crosslinking emerge as a viable option for the deliberate patterning of biocompatible materials, demonstrating their potential as a valuable choice in this regard.^[81]
10. Jitendra Sharan et al. (2018) investigated the impact of bio-functionalization on grade V titanium alloy by incorporating type I human collagen for enhancing and promoting human periodontal fibroblast cell adhesion. The study's findings led to the conclusion that bio-functionalization significantly contributes to the improvement of cell growth, consequently fostering the formation of a gingival seal-like structure in soft tissues. This enhancement is anticipated to positively influence the dynamic interaction between soft

tissues and the customized surface of titanium grade V alloy, ultimately augmenting its survivability within the biological system. ^[82]

11.Hameed et al., (2018) studied antibacterial properties of copper nanoparticles surface coating on titanium dental implant. The results revealed that Cu²⁺ released from Ti Cu and Ti Cu/HA exerted a strong antibacterial effect against *P. gingivalis* suggesting that Cu²⁺ showed good antibacterial activity against the microorganism. The antibacterial efficiency of Cu nanoparticles was dependent on the quantities of Cu²⁺. According to this study, copper ion doped hydroxyapatite (Cu/HA) in nanoparticles is considered highly effective as an antibacterial agent and Titanium surface modification with this material can be recommended as an attractive coating for local control of infection around dental implant. ^[83]

12.Thanh Dinh et al. (2018) conducted a study on the enhancement of tissue integration for medical implants using a novel approach. The authors proposed a method involving the combination of an enzyme-crosslinked gelatin hydrogel with polydopamine (PDA) coating to improve integration between any implant material and various tissues. The enzyme-crosslinked gelatin hydrogel demonstrated non-cytotoxicity to human dermal fibroblasts, facilitating cell adhesion and proliferation. The collective findings suggest that the synergistic application of PDA coating with a gelatin hydrogel holds promise for augmenting the integration of diverse medical implants. ^[84]

13.Jayanti Mendhi et al., (2021) studied Endogenous nitric oxide-generating surfaces via polydopamine-copper coatings for preventing biofilm dispersal and promoting microbial killing. NO generated from the PDAM@Cu coatings

effectively induced the dispersal of biofilms shown by the reduction in biofilm biomass as well as reduced biofilm attachment in samples prepared with blood and NO donors. Cu ions released from the PDAM@Cu coatings resulted in the killing of the dispersed bacteria, which was evidenced by the live/dead cell staining and reduced metabolic activity noted from the XTT assay. The authors concluded that PDAM@Cu coatings with NO-generating surfaces have a dual anti-biofilm function, with a synergistic effect on biofilm dispersal from regulated NO generation and bactericidal effects from Cu ions from the coatings. ^[85]

14. Fernández et.al, (2021) investigated the effects of hyaluronic acid (HA) on peri-implant clinical variables and crevicular concentrations of the proinflammatory biomarkers interleukin (IL)-1 β and tumor necrosis factor (TNF)- α in patients with peri-implantitis. The HA treated group showed lower Probing pocket depth (PPD) and less bleeding on probing compared to the control group. This study demonstrates for the first time that the topical application of a HA gel in the peri-implant pocket and around implants with peri-implantitis may reduce inflammation and crevicular fluid IL-1 β levels. ^[86]

15. In the year 2023, Lin et al. conducted an in vivo investigation focusing on a biodegradable bilayer polyurethane fibrous membrane manufactured through uniaxial electrostatic spinning. This innovative approach aimed to establish dual-sided Janus properties by incorporating the bioactive compound dopamine (DA) and the antimicrobial Gemini Quaternary Ammonium Salt (QAS). The findings of the study revealed that the Janus polyurethane fibrous membrane exhibited a remarkable capacity to

significantly enhance the regeneration of periodontal defects in rat subjects. This outcome, attributed to the membrane's superior mechanical properties and biocompatibility, underscores its potential applications in the domain of periodontal regeneration.^[87]

16. Webb et al. (2024) developed composite scaffolds for gingival tissue regeneration using light-cured, electrospun materials with tunable hydrophilicity and biodegradation. They employed methacrylated Gelatin (GelMa) crosslinked with synthetic methacrylates' and defined monomers, incorporating degradable polyurethane (D-PHI) and polycarbonate urethane (PCNU) in a factorial design. The resulting materials exhibited rapid initial degradation followed by a gradual process, enabling early infiltration of human adipose-derived stromal/stem cells while maintaining graft integrity. These findings suggest the potential of these scaffolds for oral soft tissue regeneration due to their ability to balance cell infiltration with structural stability.^[88]

2.1 SAMPLE COLLECTION

Gingival tissue samples (n = 3) were collected from periodontally and systemically healthy subjects reporting to the Department of Periodontology, A.B. Shetty Memorial Institute of Dental Sciences, undergoing Premolar extraction as a part of orthodontic treatment or crown lengthening procedure after obtaining their consent.

Institutional ethical clearance was obtained before the start of the study. (Ref.No. ETHICS/ABSMIDS/250/2022)

2.1.1 CRITERIA FOR INCLUSION

- Periodontally healthy patients with probing depth $\leq 3\text{mm}$, with no clinical attachment loss and $<10\%$ bleeding on probing.*
- Systemically healthy individuals
- 18-30 years

*According to the 2017 Classification of Periodontal and Peri-implant Diseases and Conditions⁽⁸⁹⁾

2.1.2 CRITERIA FOR EXCLUSION

- Gingivitis/periodontitis patients with probing depth $>3\text{ mm}$
- Systemically compromised patients
- Pregnant and lactating women
- Patients under antibiotic drug therapy

2.2 FABRICATION OF GE/HA/PDA/CuNPs BILAYER SCAFFOLD FOR SOFT TISSUE ENGINEERING

2.2.1 MATERIALS:

Commercially available, 10 mm diameter x 2 mm thickness Grade V titanium alloy (Ti-6Al-4V) discs meeting ASTM standards served as dental implant prototypes in this study. The discs with 99.9 % purity (Young's Modulus of 104GPa, Density 4.429g/cm³) were purchased from Parshwamani Metals, Mumbai, India

Type A pure Gelatin (Bloom 280, Isoelectric point 7-8) for tissue engineering applications was graciously supplied by the Tessenderlo Innovation Centre, Belgium (PB Leiner) from their CLARO™ tissue-engineering products range. Dopamine HCl (Extra pure >98%, CAS No.: 62-31-7), N, N-Dimethylformamide (DMF, Extra pure AR >99.5%, CAS No.: 68-12-2), and 1M Tris(hydroxymethyl)amino methane, Hydrochloric Acid buffer (Tris-HCl buffer, pH 8) were procured from Sisco Research Laboratories, India.

Hyaluronic acid, Na salt ($M_r = 1.0-1.5 \times 10^6$), was obtained from Research Lab Fine Chem. Industries, Mumbai. Copper nanoparticles with a size range of 5-10nm and a purity of 99.5% were sourced from Nano Research Lab, Jamshedpur.

2.2.2 PREPARATION OF TITANIUM DISCS FOR SCAFFOLD APPLICATIONS:

Grade 5 titanium alloy (Ti-6Al-4V) discs, with a diameter of 10mm and thickness of 2 mm, were subjected to a meticulously controlled polishing process to achieve a surface finish comparable to the smooth surfaces observed on the necks/collars of dental implants. Silicon Carbide (SiC) abrasive sheets of increasing grit size 200, 320, 400, and 600 were progressively employed, followed by a final polishing step using 1-micron oil-based diamond paste.

After the polishing process, the Ti-alloy discs were subjected to an ultrasonic cleaning procedure utilizing acetone, ethanol, and deionized water sequentially to eliminate any residual polishing compounds or contaminants. The discs were air-dried and stored in a hot air oven, to ensure a sterile dry surface for subsequent utilization.

2.2.3 POLYDOPAMINE COATING TREATMENT:

2.0 grams of Dopamine HCl was dissolved in 600 ml (0.1mol/L) of Tris- HCl buffer in an open Pyrex beaker and subjected to ultrasonic agitation for 30 minutes at room temperature. The cleaned Ti discs were then immersed in the prepared dopamine/Tris-HCl buffer solution for duration of 24 hours and the self-polymerization of dopamine was verified by the discernible color change of the solution to dark gray. The PDA coated Ti discs were then removed and cleansed with deionized water, and subjected to overnight drying in a vacuum oven at room temperature.

2.2.4 FABRICATION OF NANOFIBROUS GE/HA/CUNP ELECTROSPUN MAT:

A nanofibrous scaffold composed of gelatin (GE), hyaluronic acid (HA), and copper nanoparticles (CuNPs) was fabricated via electrospinning. To determine the optimal composition for subsequent experiments, the gelation and spinnability of various combinations were assessed.

Pure gelatin at various weight percentages (8%, 9%, 10%, 15%, and 20%) and HA (sodium salt) at different weight percentages (0.01%, 1%, 2%, 3 % and 4%) were combined with various weight ratios (GE/HA = 1:1, 9:1, 8:2, 7:3, 6:4, and 5:5) and subjected to electrospinning under different controlled conditions till an optimum composition and ratio was achieved.

Following the assessment of gelation and spinnability, a 20wt. % of Gelatin and 3wt. % of hyaluronic acid in the GE/HA weight ratio of 6:4 was deemed optimal and chosen as the concentration for further investigations.

Preparation of 3wt. % HA Solution:

To prepare the solution for electrospinning, 3 wt. % of HA was combined with DMF, and double distilled water (DI) in a 1:1 ratio, resulting in a 4ml solution. This mixture was subjected to constant stirring using a magnetic stirrer for 8 hours until the solution became transparent.

Preparation of 20wt. % GE-CuNPs Solution:

Varying weight percentages of copper nanoparticles (1%, 5%, 10%, 15%, and 20%) based on the weight of Gelatin were added to a 1:1 solution of DMF and DI to obtain a 6ml solution. This mixture was then subjected to ultrasonication for 24 hours to ensure a homogeneous distribution of the Cu nanoparticles.

Following this, a 20% w/v gelatin was dissolved in the 1:1 solution of DMF and DI containing homogeneously distributed CuNPs at 40°C for 20 minutes. The dissolution process was expedited through constant stirring to achieve a homogeneous solution.

Preparation of GE /HA/ CuNPs polymer solution for electrospinning:

To promote optimal interaction and minimize air bubble formation, the prepared CuNPs dissolved Gelatin (GE/CuNPs) solution was gradually introduced drop wise at a controlled rate into the HA solution under continuous stirring at 40°C. This process was continued for approximately 30 minutes, until the solution achieved a uniform dark grey color, confirming the successful amalgamation of the components and the formation of a homogeneous and well-integrated biopolymer solution ideally suited for subsequent electrospinning.

Electrospinning of GE/HA/CuNPs nanofibrous mat scaffold:

The GE/HA/CuNPs nanofibers were fabricated using a commercially available electrospinning system (E-spin-Nano V1-VHC, Physics Equipment Co., India) under precisely controlled environmental conditions.

Precise thermostatic control of the electrospinning chamber environment, maintained at approximately 40°C with humidity <50%, ensuring both the retention of targeted solution viscosity and the promotion of consistent fiber morphology. This optimal temperature facilitated the efficient evaporation of the DMF solvent, further ensuring the successful formation of nanofibers with the desired characteristics. A dedicated heating lamp positioned within the chamber facilitated precise temperature control.

A 10-mL syringe, equipped with a 0.8 mm inner diameter capillary tip possessing a 6% luer taper, served as the polymer solution reservoir. A dedicated syringe pump facilitated the precise delivery of the polymer solution through the needle tip at a controlled flow rate of 0.5 ml/hour. For optimal fiber morphology and uniformity, a constant voltage of 22 kV was applied, and the needle-to-collector distance was maintained at 12 cm throughout the electrospinning process.

The electrospun nanofibers were collected onto the PDA-coated Ti-alloy discs strategically arranged on a 200x200mm plate collector. Subsequently, the GE/HA/CuNPs/PDA-coated Ti-discs underwent crosslinking via exposure to 1% glutaraldehyde vapors for 30 minutes within a sealed chamber.

To ensure the complete elimination of any residual solvents and glutaraldehyde vapors, the discs were subjected to a vacuum oven treatment at ambient temperature overnight. Finally, the discs were transferred to a dedicated UV chamber (254nm/8W) for targeted cross-linking of the gelatin component and concurrent sterilization.



Figure 1: Image showing the electrospinning apparatus setup used in the study

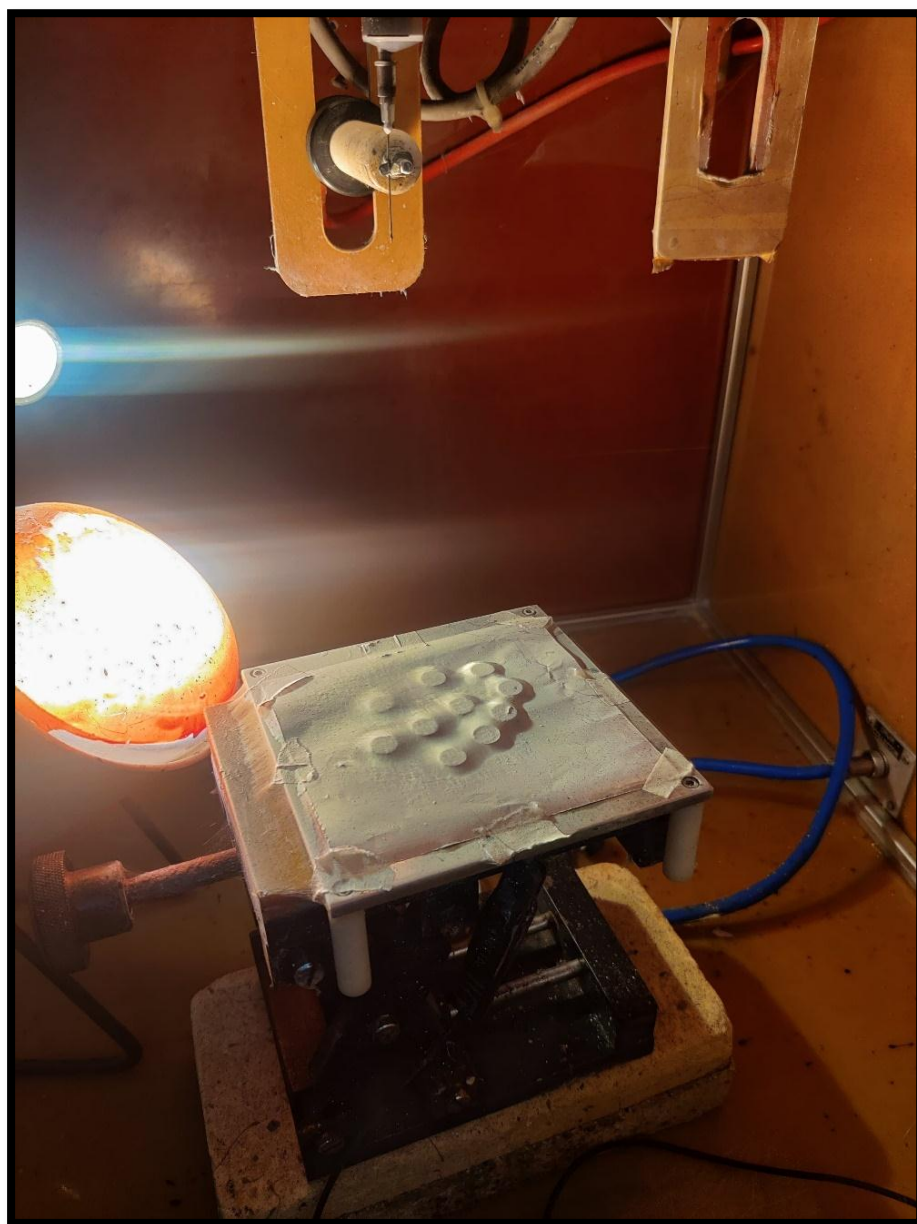


Figure 2: This digital image depicts a GE/HA /CuNPs electrospun scaffold formed over PDA coated Ti alloy disc placed on a collector plate.

2.3 CHARACTERIZATION OF THE BILAYER SCAFFOLD

2.3.1 Scanning Electron Microscopy (SEM) and Energy-Dispersive X-Ray Spectroscopy (EDS)

A high-resolution Field Emission Scanning Electron Microscope (FESEM) was employed to analyze the morphological characteristics of the electrospun nanofibers.

The instrument used was a JEOL JSM-7610FPLUS (Japan), equipped with an Energy Dispersive X-ray Spectroscopy (EDS) system. The accelerating voltage during analysis was set at 10 kV. A thin layer of gold was coated to the samples using the JFC 1600 auto fine coater from JEOL Ltd., Japan, before conducting SEM imaging.

To ensure comprehensive and statistically relevant data, various parameters like fiber diameter, particle distribution, and uniformity were quantitatively assessed using the dedicated image analysis software. Subsequently, fiber diameter measurements were performed on 50 randomly selected fibers, with each fiber analyzed at three distinct locations using ImageJ 1.5 software (National Institutes of Health, USA).



Figure 3: Representative image of the front-view image of a JEOL JSM-7610FPLUS scanning electron microscope (SEM) equipped with an Energy Dispersive Spectroscopy (EDS) detector. The cylindrical EDS detector, positioned above the specimen chamber, facilitates elemental analysis of microscopic samples

2.3.2 Fourier-transform infrared spectroscopy

Fourier Transform Infrared (FTIR) spectroscopy was employed for the recording of spectra, utilizing a Jasco FTIR 4200 spectrometer. The objective of this analysis was to discern the surface composition of the mats. By utilizing FTIR, information about the functional groups formed and the nature of bonding on Titanium (Ti) alloy discs, both before and after surface modifications, was elucidated. The analysis was done in attenuated mode for the GE/HA/PDA/CuNPs coated Ti-disc, PDA-coated Ti-disc, and in transmission mode for the other samples.

This spectroscopic technique enabled a detailed examination of the molecular composition and bonding characteristics, shedding light on the chemical changes brought about by the surface modifications on the Ti alloy discs.



Figure 4: The representative figure depicts a Jasco FTIR 4200 spectrometer employed in this study for the identification of functional groups in biological samples. The spectrometer operates by directing infrared radiation through the sample, causing specific absorption based on its molecular composition. The resulting spectrum, generated by interferometer modulation and detected by a sensitive detector, provides a unique fingerprint for the identification and quantification of targeted functional groups.

2.3.3 Contact angle analysis:

To assess the hydrophilicity of the modified titanium surface for improved cell adhesion, the contact angle was measured using a Krüss Advance instrument (Krüss, Germany). After cleaning the surface to remove contaminants, a 50 μ L droplet of distilled water was deposited. Images were captured at 5-second intervals for 2 minutes, and the contact angle between the surface and the droplet edge was automatically determined using Drop Shape Analysis software.

2.4 ANTIMICROBIAL STUDIES:

2.4.1 DISC DIFFUSION METHOD:

The procedural approach undertaken in this investigation adheres to the guidelines set forth by the Clinical Laboratory Standard Institute (CLSI) for the disc diffusion method employed in antimicrobial susceptibility testing.^[90] The experiment was conducted in triplicates, with meticulous measurement of each inhibition zone to the nearest millimeter using a calibrated caliper.

Inoculum preparation:

Freeze-dried pellets of *Staphylococcus aureus* (ATCC-29213) and *Pseudomonas aeruginosa* (ATCC 27853) were obtained from the American Type Culture Collection (ATCC). The pellets were inoculated into Brain-Heart Infusion (BHI) broth and incubated at 37°C for 4 hours for each bacterial species. A comparison with a 0.5 McFarland standard solution was conducted to confirm the density of the suspension.

Plate Inoculation and Disc Application

Following McFarland standard 0.5 turbidity adjustments, of the inoculum suspension a sterile cotton swab was employed to inoculate Mueller-Hinton agar plates. Each plate was then systematically swabbed with the inoculum solution within 15 minutes of preparation, to obtain a uniform lawn of microorganisms. After the inoculation process, UV-sterilized GE/HA/PDA/CuNPs scaffold coated Ti alloy discs were positioned onto the surface of the growth plates.

As a reference, Ciprofloxacin (CIP, 5mcg) HiMedia discs were chosen as a control agent for *S. aureus*, while Amikacin (AK, 30mcg) HiMedia disc served as the control for *P. aeruginosa*. The inclusion of these control agents facilitated a comparative assessment of the antimicrobial activity of the scaffold against standard antibiotics.

Incubation and Plate Reading

The Muller-Hinton agar plates were incubated at 37°C, for 16-24 hours. Following this incubation period, the agar plates were positioned with the lids removed on a dark background illuminated by reflected light and the diameters of the zones of inhibition were measured. A pair of calipers was employed for precision in measurement, with the plates held at an approximate distance of 30 cm from the observer's eye during the measurement process

2.4.2 BROTH MICRODILUTION METHOD:

The antibacterial efficacy of polymer solutions formulated with 20 wt.% gelatin, 3 wt.% hyaluronic acid (6:4 ratio), and varying copper nanoparticle (CuNPs) concentrations (15 wt.% and 20 wt.% relative to weight of gelatin) were investigated against *Pseudomonas aeruginosa* and *Staphylococcus aureus* using the broth microdilution method to determine their minimum inhibitory concentration (MIC).

An inoculum suspension of *P.aeruginosa* and *S.aureus* (prepared in 0.85% NaCl) was standardized to 0.5 McFarland standards, further diluted 1:100 in broth, and added to each well, yielding a final inoculum of 1.5×10^6 CFU/mL.

In a sterile 96-well microplate, column 1 received 200 μ L of broth medium, followed by the addition of 100 μ L of the polymer solution (20 wt.% gelatin, 3 wt.% HA, 6:4 ratio) containing either 15% or 20% CuNPs. Subsequent columns (2-11) received 200 μ L of broth initially. Serial two-fold dilutions were performed from columns 1 to 11, resulting in a gradient of polymer concentrations. Following incubation at 37°C for 24 hours, the MIC was defined as the lowest concentration exhibiting no visible microbial growth, confirmed by the absence of both turbidity and precipitation.

2.5 CYTOTOXICITY AND CELL PROLIFERATION

2.5.1 ISOLATION AND CULTURE OF HUMAN GINGIVAL FIBROBLASTS

Human gingival fibroblasts were procured with approval from the institutional ethical committee, and sourced from healthy subjects undergoing orthodontic tooth extraction or crown lengthening procedures. The gingival tissues acquired were promptly and meticulously preserved in a sterile saline solution, ensuring the maintenance of their physiological integrity and viability for subsequent investigative procedures.

The gingival samples collected underwent thorough rinsing with phosphate-buffered saline (PBS) for 3 to 4 cycles. Subsequently, the gingival samples were sectioned into 1×1 mm dimensions and placed onto a 4 mm diameter petri dish. After allowing the tissues to settle in the Petri dish for 5-10 minutes, they were supplied with Dulbecco's modified eagle's medium (DMEM) culture media, maintained at a pH of 7.2, and enriched with 10% fetal bovine serum (FBS), 100µg/ml penicillin, and 100mg/ml streptomycin to prevent microbial growth.

The culture plates were incubated in a humidified environment at 37°C with 5% CO₂ and 95% air to mimic physiological conditions and promote optimal cell growth.

Cultured cells were subsequently harvested through treatment with 0.25% trypsin-0.025% EDTA in PBS. Subculturing of gingival fibroblasts was performed weekly at a 1:4 ratio, with a change in the culture medium between subcultures.

2.5.2 CELL VIABILITY DETERMINATION BY MTT ASSAY

To evaluate the cytotoxicity of the materials, triplicate samples ($n = 3$) were prepared for each experimental group:

Control (C): Cultured gingival fibroblasts were maintained in their standard culture medium without any additional treatment. This group served as the baseline for cell viability.

Test group 1 (Ti-coated): Titanium alloy discs coated with polydopamine and embedded with a gelatin-hyaluronic acid electrospun scaffold containing CuNPs at the previously determined highest antimicrobial activity (20wt. %)

Test group 2 (Ti-Coated): Unmodified titanium alloy discs

The samples underwent toxicity assessment using the 3-(4,5-dimethylthiazol-2-yl)-2,5-diphenyl-2H-tetrazolium bromide (MTT) assay. In a 96-well plate, gingival fibroblasts at a frequency of 5×10^4 were evenly seeded. UV-sterilized Ti-coated and Ti- uncoated discs were introduced into the medium. The assay was performed at four time points: 0, 24, 48, and 72 hours.

At each time point, cells were rinsed with PBS, followed by incubation with 5mg/ml MTT solution for 4 hours at 37°C. Subsequently, dimethyl sulfoxide was introduced to each well to dissolve the chromogenic products formed through the reduction of tetrazolium salts by dehydrogenases and reductases. The absorbance was measured using a microplate reader (Thermo Fisher Scientific, USA) at a wavelength of 570nm. Control cells, left untreated, served as a baseline with their viability set at 100%.

2.5.3 CELL PROLIFERATION:

A 24-well tissue culture plate (Thermo Scientific, USA) was used for cell proliferation assay. Cell-substrate interactions were evaluated using three distinct substrates, each tested in triplicate (n=3).

Control Group: HGFs directly seeded onto the culture plate surface

Study Group 1 (Ti-coated): HGFs seeded onto tissue-engineered titanium alloy discs coated with polydopamine and embedded with a gelatin-hyaluronic acid electrospun scaffold containing CuNPs at the previously determined highest antimicrobial activity (20wt. %)

Study group 2 (Ti-uncoated): Unmodified titanium alloy disc

Cells were seeded at a density of 1×10^4 cells per well and cultured in triplicate for each time point (0, 24 hours, 48 hours, and 72 hours). At each designated time point, cells from individual wells were harvested, counted using a hemacytometer under a phase-contrast microscope (Olympus, Japan), and the mean count for triplicate wells was calculated.

2.6 STATISTICAL ANALYSIS:

The data were entered in MS Excel and then exported to SPSS version 22 for statistical analysis. All experiments were performed in triplicates. For the data on antibacterial activity, reduction in the CFUs and zone of inhibition for *S.aureus* and *P.aeruginosa* was summarised using mean and standard deviation. Inter-group comparisons were performed using ANOVA, and Tukey's post-hoc test. The confidence interval was considered at 95% and $p \leq 0.05$ was considered statistically significant.

For the cell proliferation and cytotoxicity analysis, the assay was performed in triplicates for each group. Statistical analyses were performed using two-way analysis of variance (ANOVA) (GraphPad Prism, USA). Any p-value below 0.05 was considered statistically significant. Tukey's test was used as the follow-up post hoc comparison method. The results were presented as mean \pm standard deviation.

3.1 CHARACTERIZATION OF GE/HA/PDA/CuNPs SCAFFOLD:

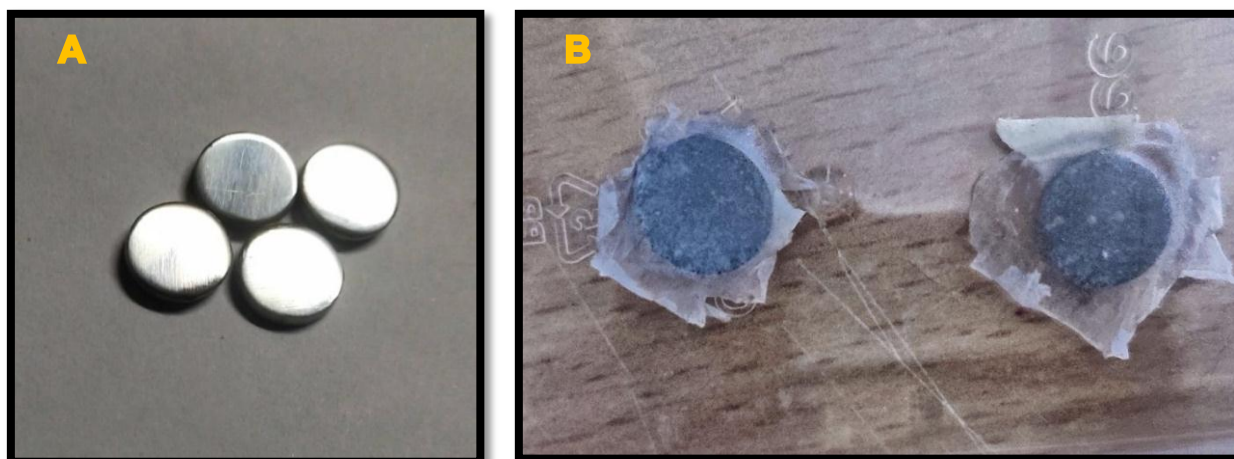


Figure 5: Optical image showing titanium discs before and after coating with GE/HA/PDA/CuNPs electrospun scaffold.

A. Unmodified titanium disc displaying a smooth, textured surface.

B. Titanium disc coated with GE/HA/PDA/CuNPs electrospun mat scaffold.

3.1.1 SCANNING ELECTRON MICROSCOPY (SEM) CHARACTERIZATION OF GE/HA/CuNPs ELECTROSPUN MAT

Scanning Electron Microscopy (SEM) analysis of the GE/HA/CuNPs electrospun mats revealed a uniform and interconnected network of nanofibers with smooth, bead-free morphology. The average fiber diameter, measured from high-resolution SEM images using ImageJ software, was 284 ± 60 nm, indicating a narrow and consistent size distribution across the mat.

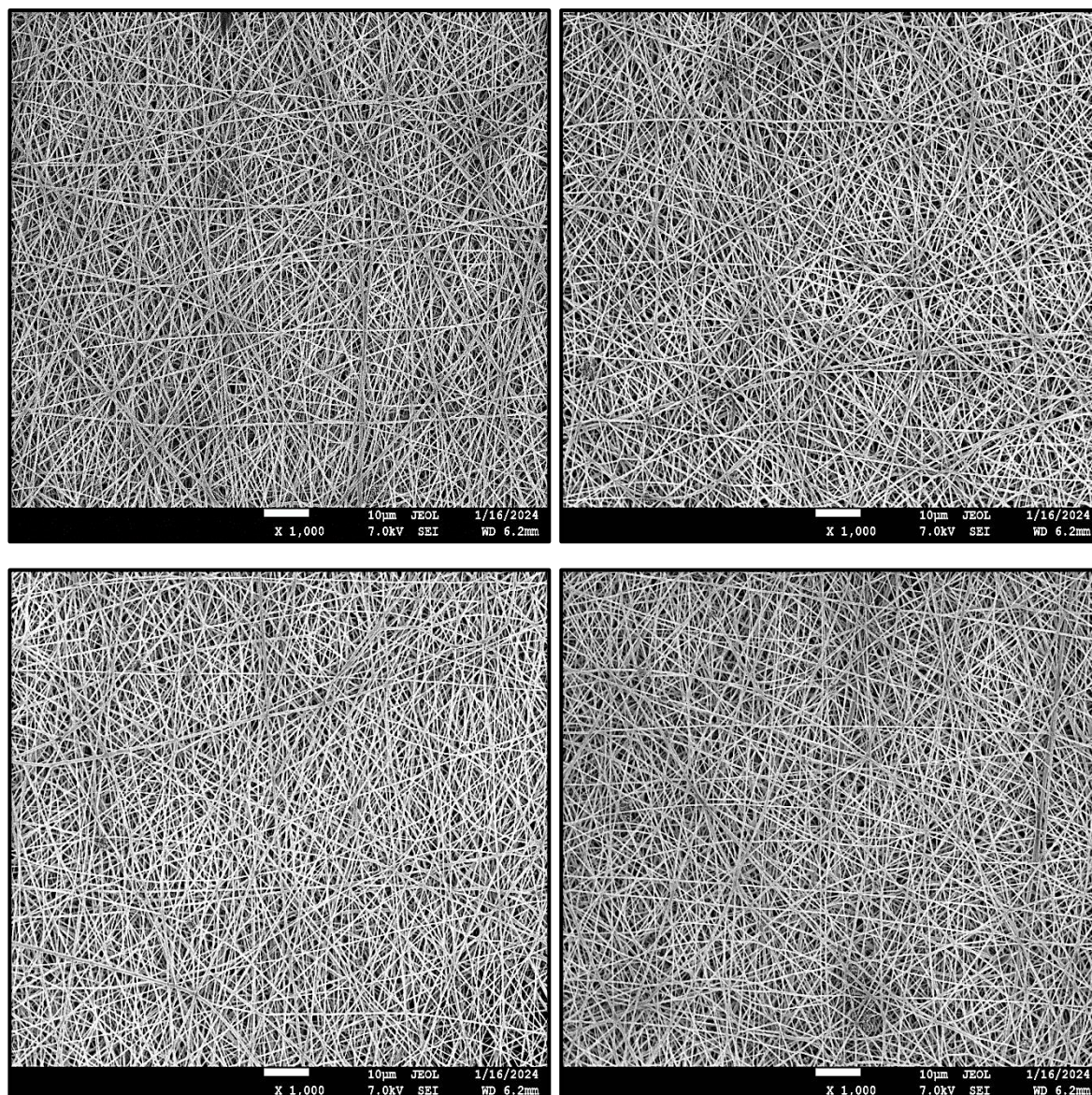


Figure 6: SEM images of the GE/HA/CuNPs electrospun scaffold at 1000 x magnification showing an interconnected network of fibers and porous morphology.

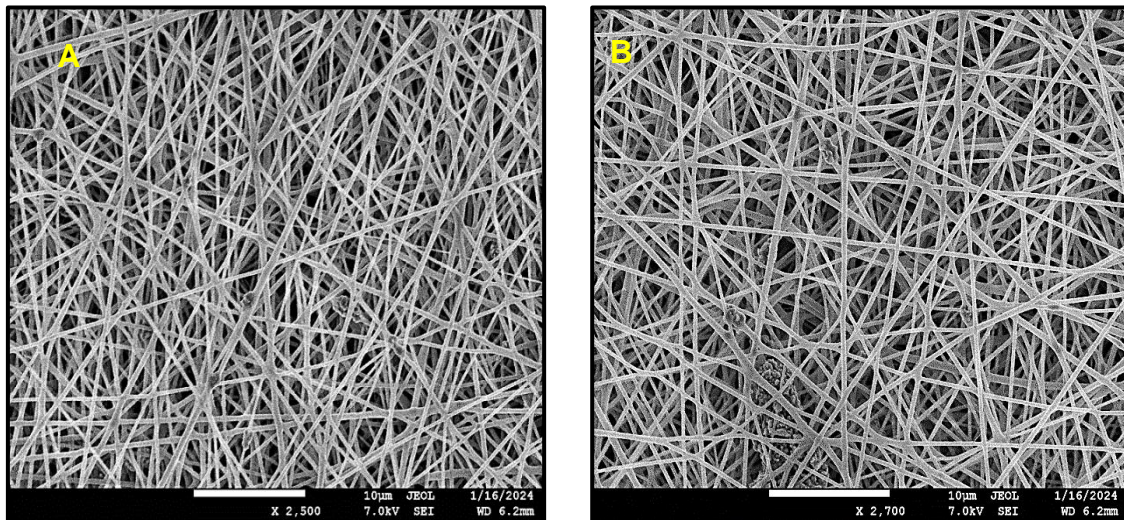


Figure 7: SEM images of the GE/HA/CuNPs electrospun scaffold

A: At 2,500x magnification

B: At 2,700x magnification.

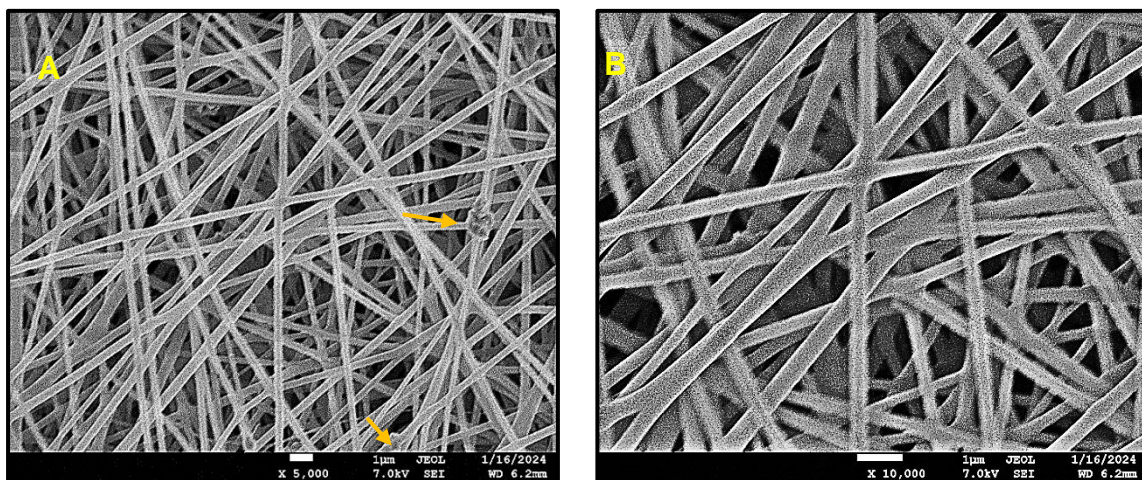


Figure 8: Figure showing Scanning electron microscopy (SEM) images of the electrospun GE/HA/CuNPs scaffold at:

A. Magnification of 5000x reveals regions of copper nanoparticle (CuNPs) aggregation, highlighted by yellow arrows.

B. Magnification of 10,000x

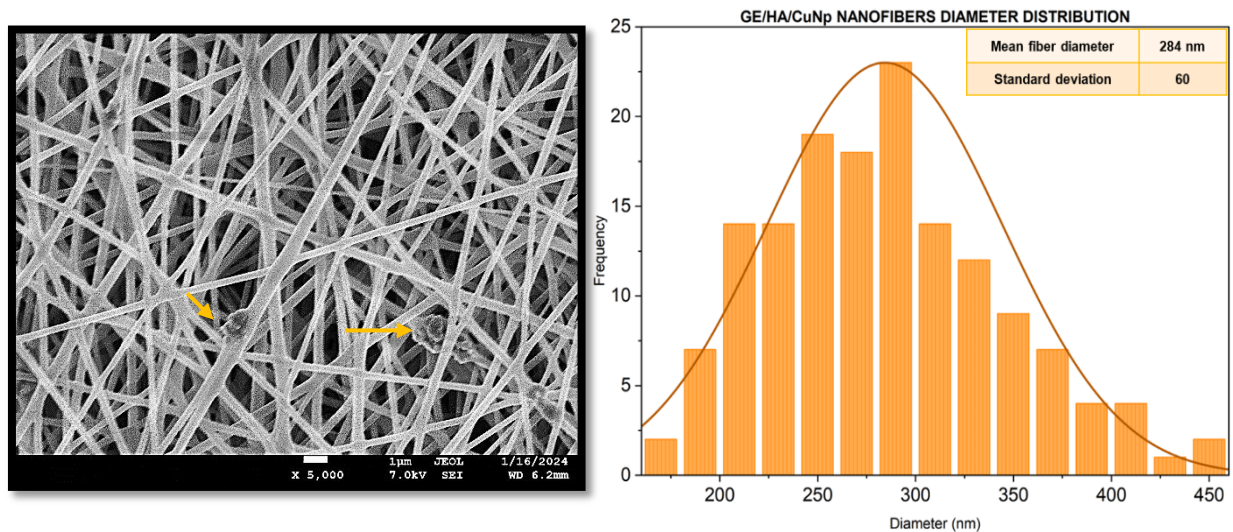


Figure 9: Scanning electron microscopy (SEM) image of the electrospun GE/HA/PDA/CuNPs composite scaffold with the corresponding histogram illustrating the diameter distribution of the fibers. The mean fiber distribution is 284nm with standard deviation of 60nm.

Regions of copper nanoparticle (CuNPs) aggregation are highlighted by yellow arrows.

3.1.2 EDS ANALYSIS

Energy-dispersive X-ray spectroscopy (EDS) analysis confirmed the successful integration of copper nanoparticles (CuNPs) within the GE/HA/PDA coating on the titanium substrate. The EDS spectra revealed characteristic copper peaks, solidifying the presence and distribution of CuNPs throughout the scaffold structure. Distinct spectral signatures corresponding to Carbon (C), Nitrogen (N), Oxygen (O), and Copper (Cu) demonstrated the presence and close association of Gelatin, Hyaluronic acid, and Copper with the electrospun scaffold matrix.

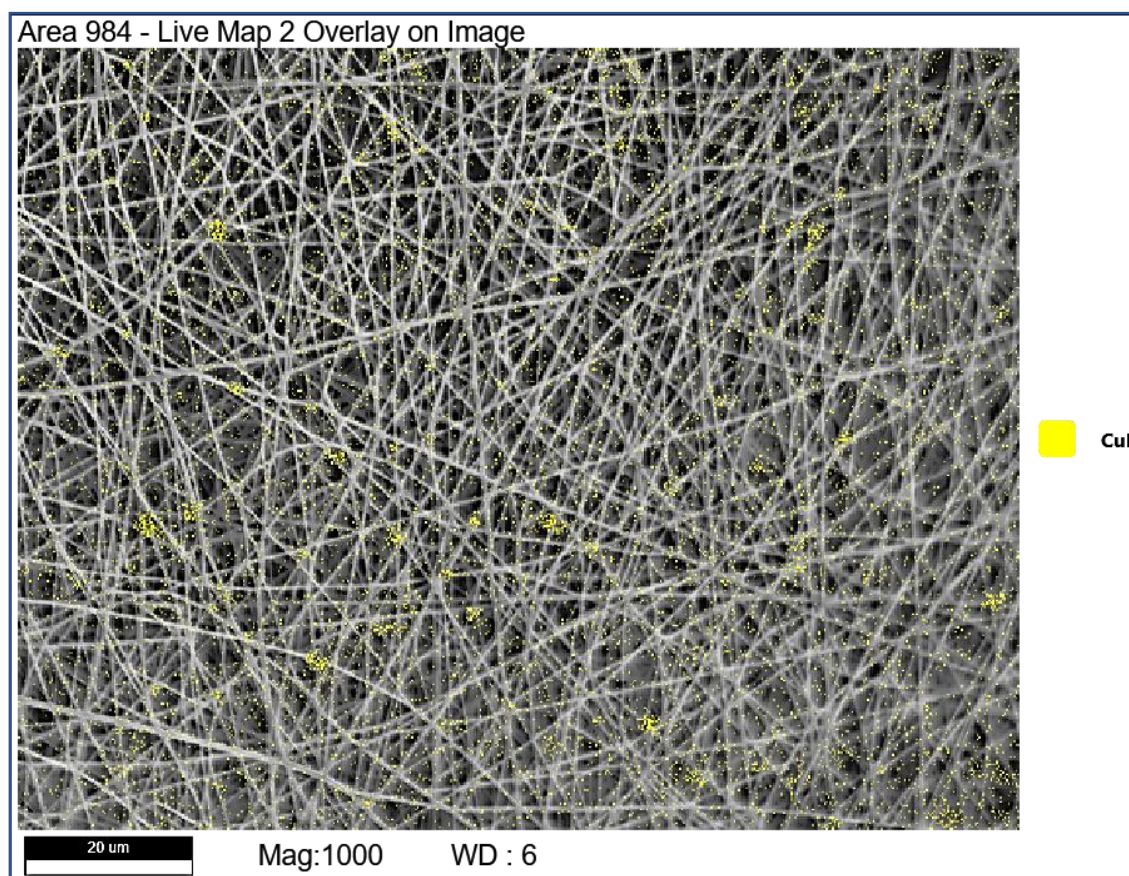


Figure 10: An integrated figure presents a Scanning electron microscopy (SEM) image (1000x magnification) of the electrospun nanofiber scaffold alongside its corresponding energy-dispersive X-ray spectroscopy (EDS) analysis. Yellow dots on the SEM image highlight the distribution of copper nanoparticles (CuNPs) within the scaffold, as confirmed by the EDS data.

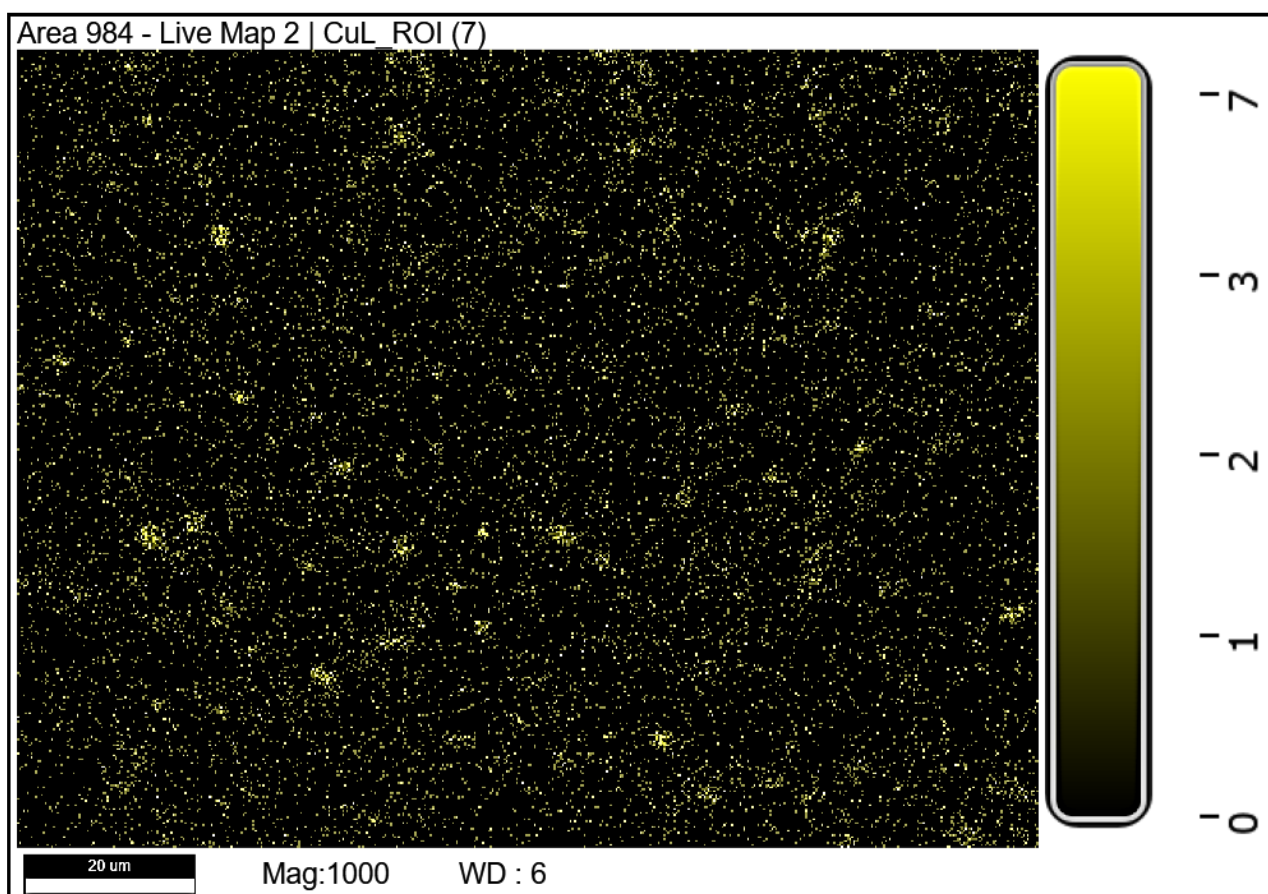


Figure 11: EDS live map demonstrating the presence and distribution of copper nanoparticles (CuNPs), indicated by yellow dots.

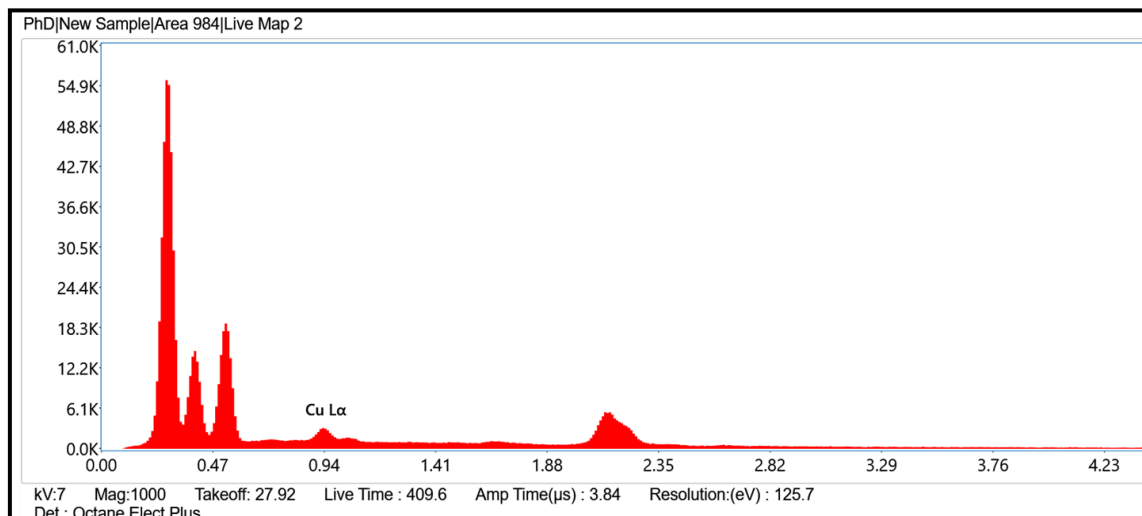


Figure 12: EDS spectrum of the electrospun scaffold, indicating the presence of CuNPs (CuLα) through the characteristic peak at X-ray energy (keV).

eZAF Quant Result - Analysis Uncertainty: 99.00 %		
Element	Weight %	Atomic %
Cu L	100.0	100.0

Table 1: The table presented shows the quantitative analysis results for copper (Cu) using the eZAF correction method

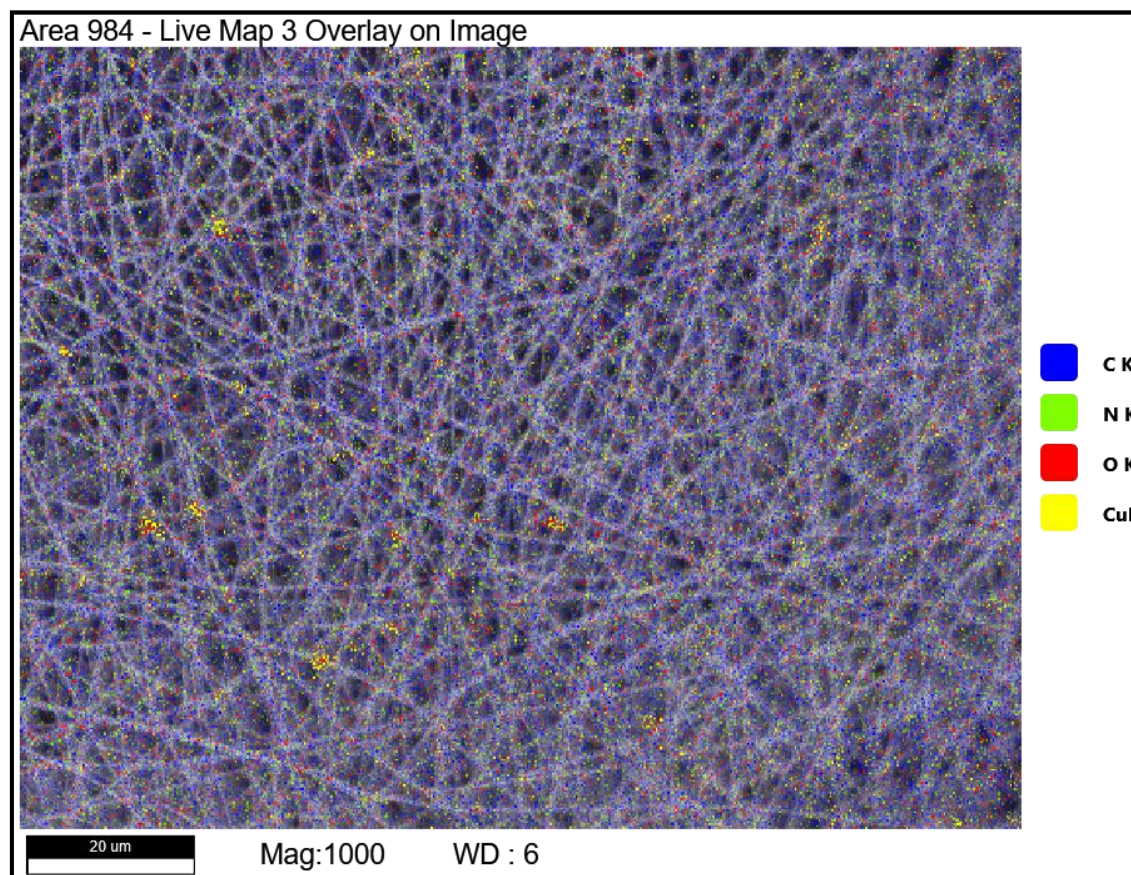


Figure 13: EDS overlay map of the electrospun GE/HA/PDA/CuNPs scaffold, displaying the elemental distributions of carbon (C - blue), nitrogen (N - green), oxygen (O - red), and copper (Cu - yellow).

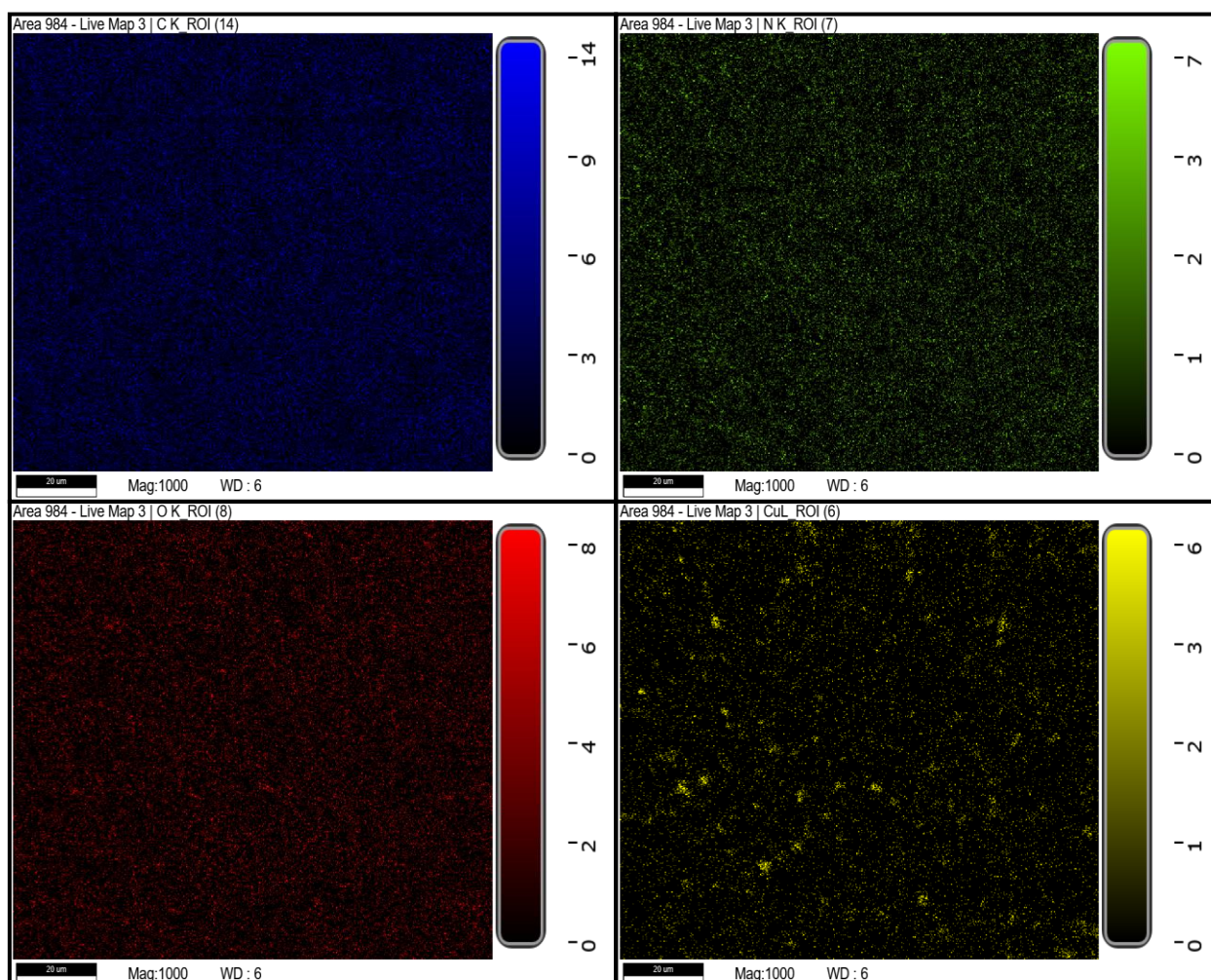


Figure 14: Live EDS elemental map of the electrospun GE/HA/PDA/CuNPs scaffold, depicting the spatial distribution of carbon (C - blue), nitrogen (N - green), oxygen (O - red), and copper (Cu - yellow).

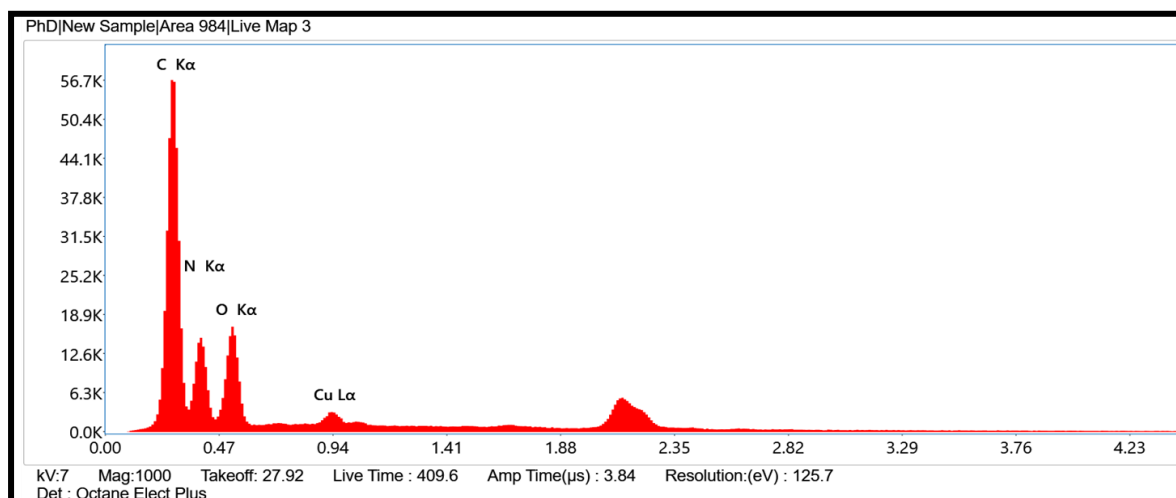


Figure 15: This figure presents an energy-dispersive X-ray spectroscopy (EDS) spectrum of the GE/HA/PDA/CuNPs mat scaffold. The graph displays characteristic peaks corresponding to the presence of carbon (C), nitrogen (N), oxygen (O), and copper (Cu) in the sample.

eZAF Quant Result - Analysis Uncertainty: 99.00 %		
Element	Weight %	Atomic %
C K	61.9	67.3
N K	22.0	20.5
O K	14.5	11.9
Cu L	1.6	0.3

Table 2: eZAF Quantitative Analysis of Elements in the GE/HA/PDA/CuNPs mat scaffold

3.1.3 FOURIER TRANSFORM INFRARED SPECTROSCOPY ANALYSIS

FTIR analysis was conducted on various samples, including hyaluronic acid, gelatin, copper nanoparticles, GE/HA/PDA/CuNPs bilayer scaffold fabricated on Ti alloy disc, and polydopamine coated Ti alloy disc to study their chemical compositions and bonding interactions. A plot of % transmittance was generated by correlating it with the wavenumber to visualize the characteristic functional groups and interactions of covalent bonds present within each sample.

FTIR Spectra of hyaluronic acid:

A broadband of around 3258 cm^{-1} was assigned to the O–H groups in HA. Two bands at 1604 , 1688 , and 1540 cm^{-1} corresponded to carbonyl stretching bands of carboxylic acid and amide I and amide II, respectively. Ether bands were assigned at 1151 and 1032 cm^{-1} . Bands at 1517 and 1320 cm^{-1} are indicative of the amide groups in N-acetyl- β -d-glucosamine units, and the bands at 1260 and 1032 cm^{-1} are assigned to the vibrations of the carboxylic groups in β -d-glucuronic acid units. A small peak around 1150 shows C-O-C bonds of the polysaccharides. Two bands around 1604 and 1415 cm^{-1} corresponding to the antisymmetric and symmetric valence vibration COO^- are present. A peak at 673 conforms to the out-of-plane aromatic band as well as -CO bands.

FTIR spectra of Gelatin:

The bands of gelatin in the IR spectra are situated in the amide band region; amide-I represents C=O stretching/hydrogen bonding couple with COO^- , amide-II

represents bending vibration of N-H groups and stretching vibrations of C-N groups, Amide-III is related to the vibrations in plane of C-N and N-H groups of bound amide. Gelatin peaks at 3466 cm^{-1} attributed to the presence of hydrogen bond water and amide A, 1658 cm^{-1} peaks correspond to the occurrence of amide I, at 1565 cm^{-1} indicates amide-II, band at 1240 cm^{-1} indicates the amide-III, peaks range from 1460 V to 1380 cm^{-1} were attributed to the symmetric and asymmetric bending vibrations of the methyl group. A small peak at 1445 represents -C=O stretching of the carbonate group. A peak at 673 cm^{-1} conforms to the out-of-plane aromatic band and the peak at 1032 cm^{-1} indicates C-N stretching of the pyrrolidine.

FTIR spectrum of copper nanoparticles:

This analysis was used to determine the functional organic groups on the surface of the nanoparticles generated by oleic acid. A broad peak at 3457 cm^{-1} conforms to OH stretching. The peaks at 1614 and 1399 cm^{-1} correspond to C=C bonds of unsaturated compounds and bending of aliphatic C-H respectively. A peak at 673 conforms to the out-of-plane aromatic band as well as -CO bands.

FTIR spectrum of Ge-HA-Cu nanofibers:

Observation of the FTIR spectrum shows various peaks confirming the presence of the constituent materials. The broad peaks at 3280 and 2930 conform to the OH stretching and -CH stretching of aliphatic groups respectively. Bands at 1632 , 1525 , and 1239 cm^{-1} correspond to stretching bands amide I, amide II, and amide III, respectively. A peak at 1442 represents -C=O stretching of the carbonate group. The bands at 1239 and 1078 cm^{-1} conform to the vibrations of the

carboxylic groups in β -d-glucuronic acid units.

FTIR spectra of GE/HA/PDA/CuNPs mat scaffold coated on the Ti-alloy discs:

Observation of the FTIR spectrum represented shows various peaks confirming the presence of the constituent materials. The broad peaks at 3341 conform to the OH stretching. Bands at 1632, 1528, and 1260 cm^{-1} correspond to stretching bands amide I, amide II, and amide III, respectively. A peak at 1462 represents -C=O stretching of the carbonate group. The bands at 1239 and 1078 cm^{-1} conform to the vibrations of the carboxylic groups in β -d-glucuronic acid units.

FTIR spectra of polydopamine-coated Ti-alloy disc

Vibrations associated with C=C functional groups were attributed to peaks at 1632 cm^{-1} . PDA exhibited peaks at 2941 cm^{-1} and 3347 cm^{-1} corresponding to C-H and O-H vibrations respectively. Bands at 1519 and 1260 cm^{-1} correspond to stretching bands of amide II and amide III, respectively. A peak at 1467 represents -C=O stretching of the carbonate group. A band at 1078 cm^{-1} conforms to the vibrations of the carboxylic (-C=O) groups.

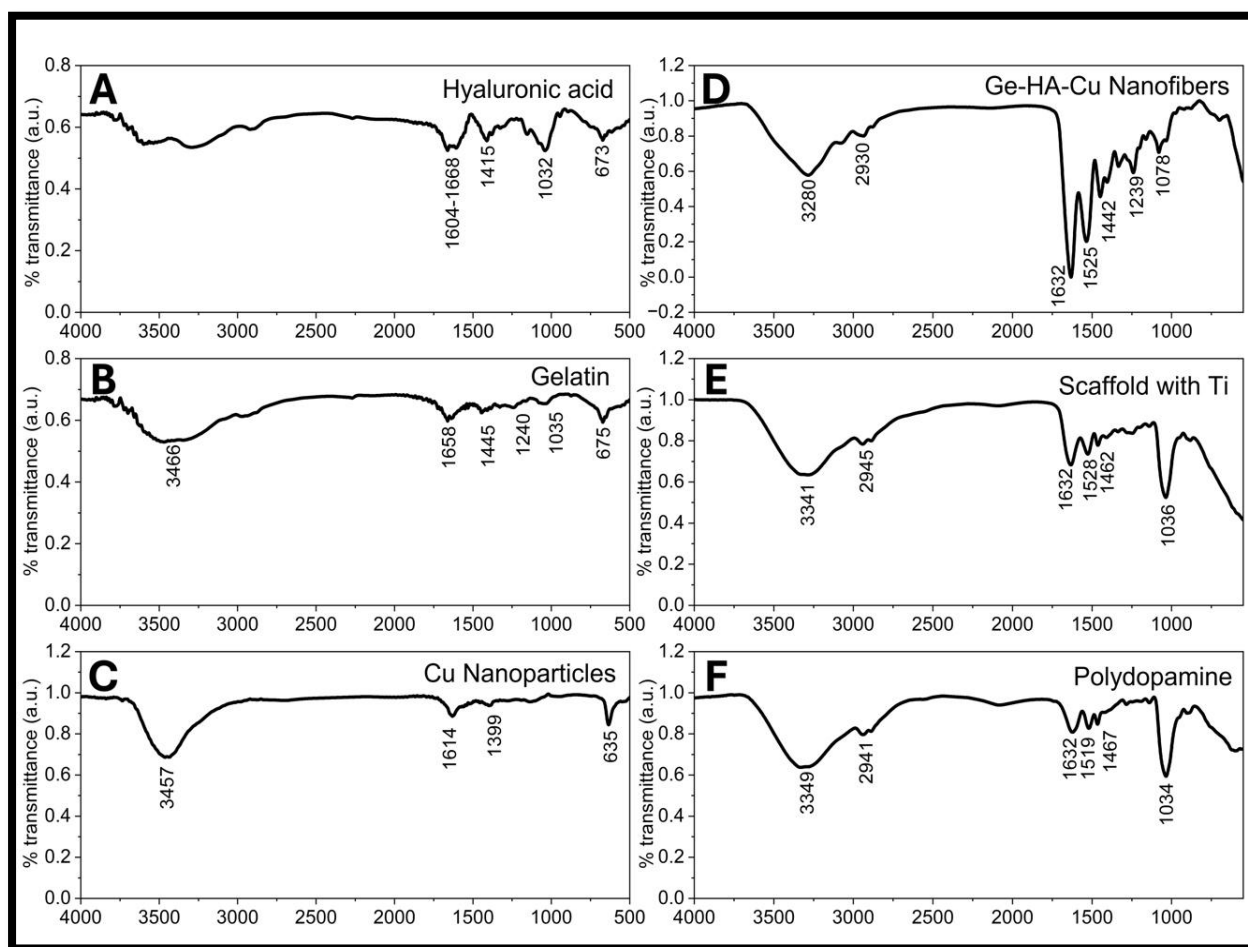


Figure 16: FTIR Spectra of various scaffold components

A: FTIR spectrum of Hyaluronic acid

B: FTIR spectrum of Gelatin

C; FTIR spectrum of Cu Nanoparticles

D: FTIR spectrum of GE/HA/CuNPs electrospun mat scaffold

E: FTIR spectrum of GE/HA/PDA/CuNPs COATED Ti alloy disc

F: FTIR spectrum of Polydopamine coated Ti-alloy disc.

The x-axis represents wavenumber (cm^{-1}), and the y-axis represents % transmittance.

3.1.4 CONTACT ANGLE ANALYSIS:

The influence of surface chemistry on water interaction was investigated by evaluating the wettability of the unmodified Ti-alloy disc, polydopamine (PDA)-coated Ti- alloy disc, and GE/HA/PDA/CuNPs-coated Ti-alloy disc using a Krüss Advance contact angle goniometer (Krüss GmbH, Germany.)

The initial water contact angle of unmodified titanium implants was measured to be 77°. This angle gradually decreased over time, reaching 52° within the first 80 seconds. This initial, relatively high contact angle indicates that water droplets initially bead up on the unmodified titanium surface, signifying poor wettability. However, the observed decrease in contact angle suggests a gradual improvement in wettability over time.

The micro contact angle (MCA) on titanium surfaces coated with polydopamine (PDA) exhibited a significant reduction from 17° to 12° within the initial 4 seconds of contact. This rapid decrease indicates a marked improvement in surface wettability compared to the unmodified titanium implants. The observed enhancement can be attributed to the presence of hydroxyl (–OH) and amino (–NH₂) groups within the PDA structure. These functional groups readily participate in hydrogen bonding with water molecules, leading to a stronger interaction and lower contact angle. Furthermore, the presence of aromatic rings in the PDA structure facilitates π - π stacking interactions with nonpolar molecules, further contributing to the overall enhanced wettability of the coated surface.

The MCA of the GE/HA/PDA/CuNPs scaffold exhibited an intermediate behavior between the unmodified titanium and polydopamine-coated surfaces, initially measuring 67° and gradually decreasing to 42° within 80 seconds. This suggests the scaffold possesses an intermediate level of wettability, likely influenced by the combined effects of the scaffold's material composition, containing both hydrophilic and hydrophobic components, and its surface topography with inherent porosity.

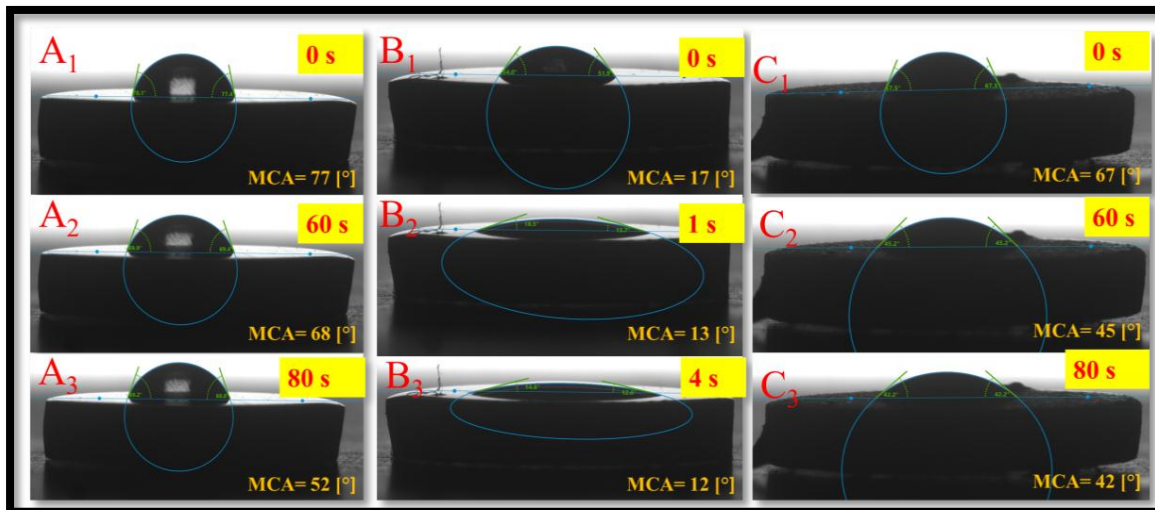


Figure 17: Water contact angles of

- A. Unmodified Ti-alloy disc (A_1 to A_3 showing a reduction in MCA from 77° to 52° over 80 seconds)
- B. Polydopamine-coated Ti-alloy disc (B_1 to B_3 showing a reduction in MCA from 17° to 12° over 4 seconds)
- C. GE/HA/PDA/CuNPs scaffold coated Ti-alloy disc (C_1 to C_3 showing a reduction in MCA from 67° to 42° over 80 seconds)

3.2 ANTIMICROBIAL ACTIVITY:

3.2.1 DISK DIFFUSION:

The antibacterial activity of GE/HA/PDA/CuNPs scaffolds against *Pseudomonas aeruginosa* (gram-negative) and *Staphylococcus aureus* (gram-positive) was evaluated using the Kirby-Bauer disc diffusion method. Scaffolds loaded with varying copper nanoparticle (CuNPs) concentrations (1 wt.%, 5 wt.%, 10 wt.%, 15 wt.%, and 20 wt.%) were prepared and placed on standardized agar plates inoculated with the respective bacterial strains. The diameter of clear inhibition zones formed around the scaffolds after incubation was measured and interpreted according to established standards.

Incorporating copper nanoparticles (CuNPs) into GE-CuNp/HA/PDA scaffolds demonstrated varying degrees of antibacterial efficacy against *Pseudomonas aeruginosa* (gram-negative) and *Staphylococcus aureus* (gram-positive), as evaluated by the Kirby-Bauer disc diffusion method. Samples loaded with 1, 5, and 10 wt. % of CuNPs (Ti-coated 1, 2 and 3 respectively) displayed minimal to no inhibition against both bacterial strains. This was evidenced by the absence or presence of only small inhibition zones around these samples, suggesting limited antibacterial activity at these CuNPs concentrations.

Sample 4 (Ti-coated 4), containing 15 wt. % of CuNPs, exhibited a demonstrably stronger antibacterial effect against *P. aeruginosa* compared to lower CuNPs concentrations. This was evident by the presence of a measurable inhibition zone, indicating the suppression of bacterial growth. However, its efficacy against *S. aureus* remained limited, as evidenced by the minimal inhibition zone.

In stark contrast to the minimal to no activity observed at lower CuNPs concentrations, sample 5 (Ti-coated 5, 20 wt.% of CuNPs) demonstrated a broad-spectrum and potent antibacterial effect. This was evident by the presence of clear inhibition zones against both *P. aeruginosa* and *S. aureus*, suggesting significant growth inhibition for both bacterial strains.

The disc diffusion assay demonstrated significantly larger zones of inhibition surrounding the GE/HA/PDA/CuNPs scaffolds against *P. aeruginosa* (gram-negative) compared to *S. aureus* (gram-positive). This observation signifies a greater susceptibility of *P. aeruginosa* to the antibacterial effects of the scaffolds.

Susceptibility against *Pseudomonas aeruginosa*:

A clear concentration-dependent trend emerged for the antibacterial activity against *Pseudomonas aeruginosa* across all CuNPs-loaded scaffolds. Notably, all except one (1 wt. % of CuNPs) tested CuNPs concentrations (5, 10, 15, and 20 wt. %) showed growth inhibition, as evidenced by measurable inhibition zones. Among these, Ti-coated discs incorporated with 20 wt. % CuNPs (Ti-coated 5) displayed the largest inhibition zone, followed by the 15 wt. % CuNPs (Ti-coated 4) group. This unequivocal observation underscores a direct correlation between increasing CuNPs concentration and enhanced antibacterial efficacy against *P. aeruginosa*.

Post hoc analysis using Tukey's honest significant difference (HSD) test revealed no statistically significant difference ($p = > 0.05$) in the antimicrobial efficacy of the 20 wt. % CuNPs-loaded scaffolds (Ti-coated 5) compared to the Amikacin control group. This finding suggests that the 20 wt. % CuNPs-loaded scaffold exhibits an equivalent level of antimicrobial activity against the tested *Pseudomonas aeruginosa* as the clinically established antibiotic Amikacin.

SAMPLE ID	CuNPs concentration (wt.%)	Zone of inhibition (in mm)
Ti coated 1	1%	0
Ti coated 2	5%	10±0.30
Ti coated 3	10%	11±0.59
Ti coated 4	15%	17±1.03
Ti coated 5	20%	27±1.98
CONTROL-Amikacin		30±1.05

Table 3: This table summarizes the antimicrobial activity of titanium (Ti) discs coated with varying CuNPs percentages against *Pseudomonas aeruginosa*, compared to a control group treated with the antibiotic Amikacin.

ANOVA					
<i>P aeruginosa</i>					
	Sum of Squares	df	Mean Square	F	Sig.
Between Groups	2237.111	5	447.422	96.885	.000
Within Groups	55.417	12	4.618		
Total	2292.528	17			

Table 4: One-Way ANOVA results for the effect of CuNPs concentration on *P. aeruginosa*

Multiple Comparisons					
(I) Cu Concentration wt. %	(J) Cu Concentration wt. %	Mean Difference (I- J)	Sig.	95% Confidence Interval	
				Lower Bound	Upper Bound
Amikacin	1%	33.33333 [*]	.000	27.4397	39.2270
	5%	23.33333 [*]	.000	17.4397	29.2270
	10%	22.33333 [*]	.000	16.4397	28.2270
	15%	16.33333 [*]	.000	10.4397	22.2270
	20%	6.00000 [*]	.045	.1063	11.8937
1%	Amikacin	-33.33333 [*]	.000	-39.2270	-27.4397
	5%	-10.00000 [*]	.001	-15.8937	-4.1063
	10%	-11.00000 [*]	.000	-16.8937	-5.1063
	15%	-17.00000 [*]	.000	-22.8937	-11.1063
	20%	-27.33333 [*]	.000	-33.2270	-21.4397
5%	Amikacin	-23.33333 [*]	.000	-29.2270	-17.4397
	1%	10.00000 [*]	.001	4.1063	15.8937
	10%	-1.00000	.991	-6.8937	4.8937
	15%	-7.00000 [*]	.017	-12.8937	-1.1063
	20%	-17.33333 [*]	.000	-23.2270	-11.4397
10%	Amikacin	-22.33333 [*]	.000	-28.2270	-16.4397
	1%	11.00000 [*]	.000	5.1063	16.8937
	5%	1.00000	.991	-4.8937	6.8937
	15%	-6.00000 [*]	.045	-11.8937	-.1063
	20%	-16.33333 [*]	.000	-22.2270	-10.4397
15%	Amikacin	-16.33333 [*]	.000	-22.2270	-10.4397
	1%	17.00000 [*]	.000	11.1063	22.8937
	5%	7.00000 [*]	.017	1.1063	12.8937
	10%	6.00000 [*]	.045	.1063	11.8937
	20%	-10.33333 [*]	.001	-16.2270	-4.4397
20%	Amikacin	-6.00000 [*]	.045	-11.8937	-.1063
	1%	27.33333 [*]	.000	21.4397	33.2270
	5%	17.33333 [*]	.000	11.4397	23.2270
	10%	16.33333 [*]	.000	10.4397	22.2270
	15%	10.33333 [*]	.001	4.4397	16.2270

Table 5: This table summarizes the results of post-hoc comparisons conducted using Tukey's HSD test following a one-way ANOVA to assess the antimicrobial efficacy of different concentrations of CuNPs against the dependent variable i.e., *P. aeruginosa*.

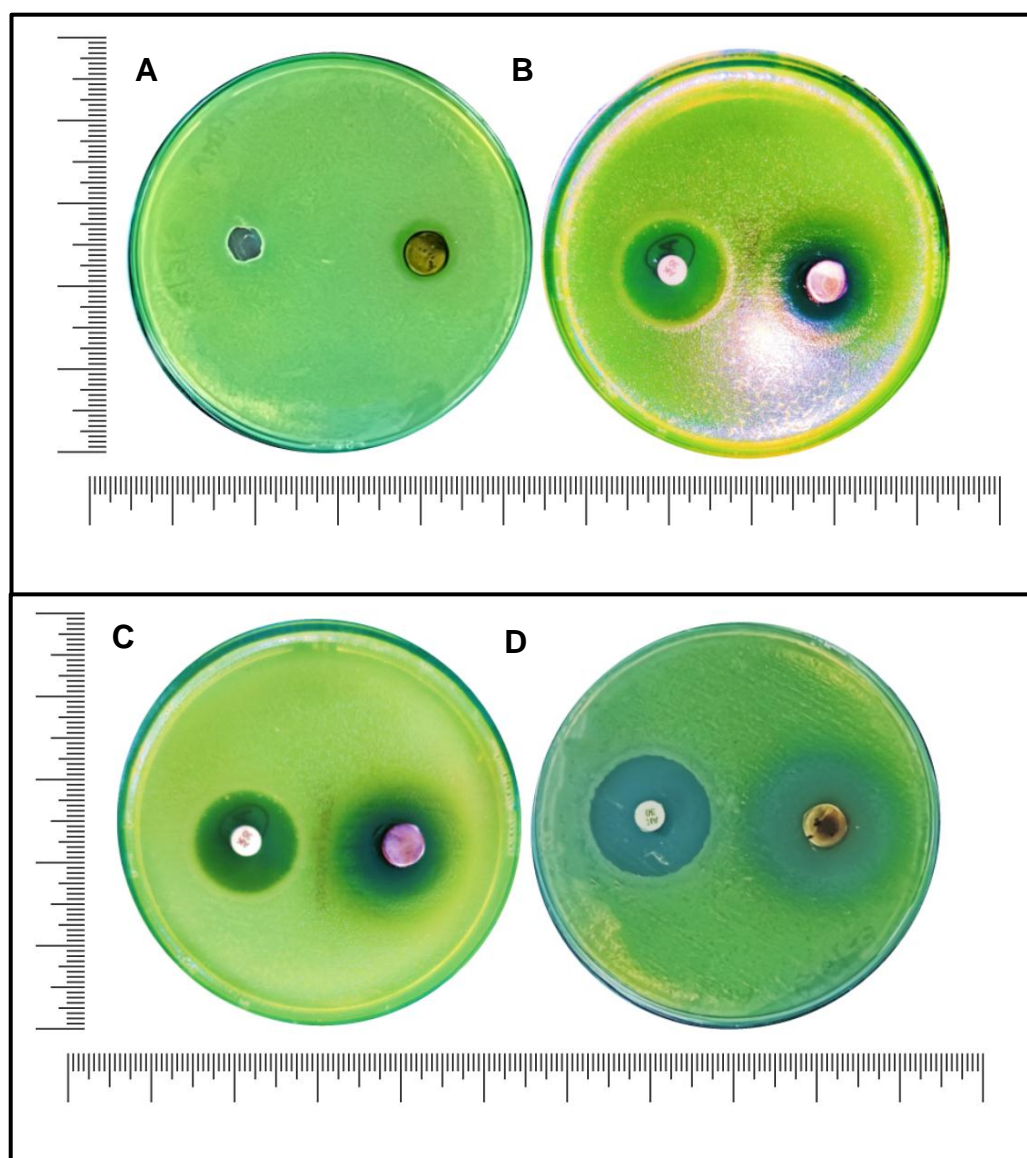


Figure 18: This figure presents the antimicrobial activity of GE/HA/PDA/CuNPs coated discs with varying copper nanoparticle (CuNPs) concentrations against *Pseudomonas aeruginosa*. Each disc is depicted within its respective zone of inhibition, representing the clear area surrounding the disc where bacterial growth is inhibited due to the antimicrobial effect of the scaffold coated discs.

- A. Zone of inhibition around Ti-coated disc 2 (5 wt.% CuNPs)
- B. Zone of inhibition around Ti-coated disc 3 (10 wt.% CuNPs)
- C. Zone of inhibition around Ti-coated disc 4 (15 wt.% CuNPs)
- D. Zone of inhibition around Ti-coated disc 5 (20 wt.% CuNPs)

Susceptibility against *Staphylococcus aureus*:

The study revealed a limited concentration-dependent effect of CuNPs on the antibacterial activity against *Staphylococcus aureus*. Only scaffolds loaded with 15% and 20 wt. % CuNPs exhibited measurable inhibition zones (average diameters of 10 ± 0.15 and 12 ± 0.64 , respectively), indicating an absence of activity at lower concentrations (1, 5 and 10 wt.%). Notably, the 20% CuNPs group displayed the largest inhibition zone, suggesting a threshold effect at this concentration.

SAMPLE ID	CuNPs Concentration (wt. %)	Zone of inhibition (in mm)
Ti coated 1	1%	0
Ti coated 2	5%	0
Ti coated 3	10%	0
Ti coated 4	15%	10 ± 0.15
Ti coated 5	20%	12 ± 0.64
CONTROL- Ciprofloxacin		20 ± 0.50

Table 6: This table summarizes the antimicrobial activity of titanium (Ti) discs coated with varying CuNPs percentages against *Staphylococcus aureus*, compared to a control group treated with the antibiotic Ciprofloxacin.

ANOVA					
S aureus					
	Sum of Squares	df	Mean Square	F	Sig.
Between Groups	1050.000	5	210.000	1847.236	.000
Within Groups	1.364	12	.114		
Total	1051.364	17			

Table 7: One-Way ANOVA Results for the Effect of CuNPs Concentration on *S.aureus*

Multiple Comparisons					
(I) Cu Concentration wt.%)	(J) Cu Concentration (wt.%)	Mean Difference (I-J)	Sig.	95% Confidence Interval	
				Lower Bound	Upper Bound
Amikacin	1%	33.33333 [*]	.000	27.4397	39.2270
	5%	23.33333 [*]	.000	17.4397	29.2270
	10%	22.33333 [*]	.000	16.4397	28.2270
	15%	16.33333 [*]	.000	10.4397	22.2270
	20%	6.00000 [*]	.045	.1063	11.8937
1%	Amikacin	-33.33333 [*]	.000	-39.2270	-27.4397
	5%	-10.00000 [*]	.001	-15.8937	-4.1063
	10%	-11.00000 [*]	.000	-16.8937	-5.1063
	15%	-17.00000 [*]	.000	-22.8937	-11.1063
	20%	-27.33333 [*]	.000	-33.2270	-21.4397
5%	Amikacin	-23.33333 [*]	.000	-29.2270	-17.4397
	1%	10.00000 [*]	.001	4.1063	15.8937
	10%	-1.00000	.991	-6.8937	4.8937
	15%	-7.00000 [*]	.017	-12.8937	-1.1063
	20%	-17.33333 [*]	.000	-23.2270	-11.4397
10%	Amikacin	-22.33333 [*]	.000	-28.2270	-16.4397
	1%	11.00000 [*]	.000	5.1063	16.8937
	5%	1.00000	.991	-4.8937	6.8937
	15%	-6.00000 [*]	.045	-11.8937	-.1063
	20%	-16.33333 [*]	.000	-22.2270	-10.4397
15%	Amikacin	-16.33333 [*]	.000	-22.2270	-10.4397
	1%	17.00000 [*]	.000	11.1063	22.8937
	5%	7.00000 [*]	.017	1.1063	12.8937
	10%	6.00000 [*]	.045	.1063	11.8937
	20%	-10.33333 [*]	.001	-16.2270	-4.4397
20%	Amikacin	-6.00000 [*]	.045	-11.8937	-.1063
	1%	27.33333 [*]	.000	21.4397	33.2270
	5%	17.33333 [*]	.000	11.4397	23.2270
	10%	16.33333 [*]	.000	10.4397	22.2270
	15%	10.33333 [*]	.001	4.4397	16.2270

Table 8: This table summarizes the results of pairwise comparisons using Tukey's HSD test following a one-way ANOVA to assess the antimicrobial efficacy of different concentrations of copper nanoparticles (CuNPs) against *Staphylococcus aureus*.

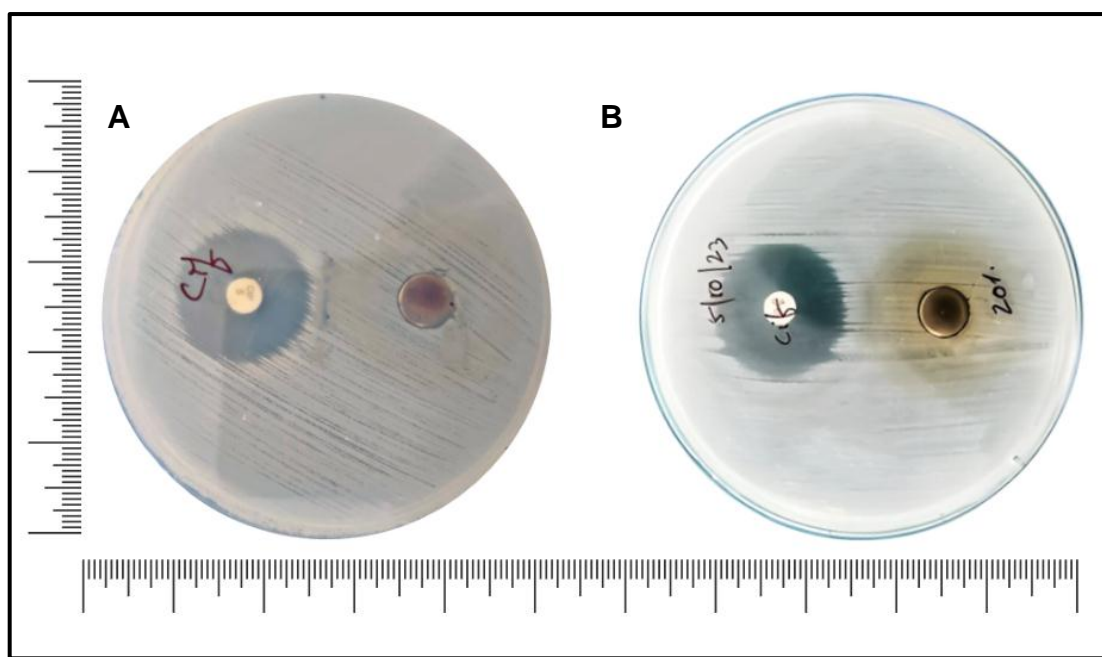


Figure 19: This figure illustrates the antimicrobial activity of GE/HA/PDA/CuNPs coated discs with varying copper nanoparticle (CuNPs) concentrations (15% and 20%) against *Staphylococcus aureus*.

- A. Zone of inhibition around Ti-coated disc 4 (15 wt.% CuNPs)
- B. Zone of inhibition around Ti-coated disc 5 (20 wt.% CuNPs)

3.2.2 BROTH MICRODILUTION

The broth microdilution method revealed the minimum inhibitory concentration (MIC) of the CuNPs-impregnated GE/HA polymer solution against *Staphylococcus aureus* to be 1200µg/ml for 15 wt. % and 600µg/ml for 20 wt. % of CuNPs. Conversely, against *Pseudomonas aeruginosa*, the MIC values were 300µg/ml and 115µg/ml for 15 wt.% and 20 wt.% of CuNPs, respectively

These results indicated a higher sensitivity of the CuNPs against *P. aeruginosa* than compared to *S. aureus*.

Data obtained from serial broth microdilution assay also showed a direct correlation between the antimicrobial effects on microbial colonies with time.

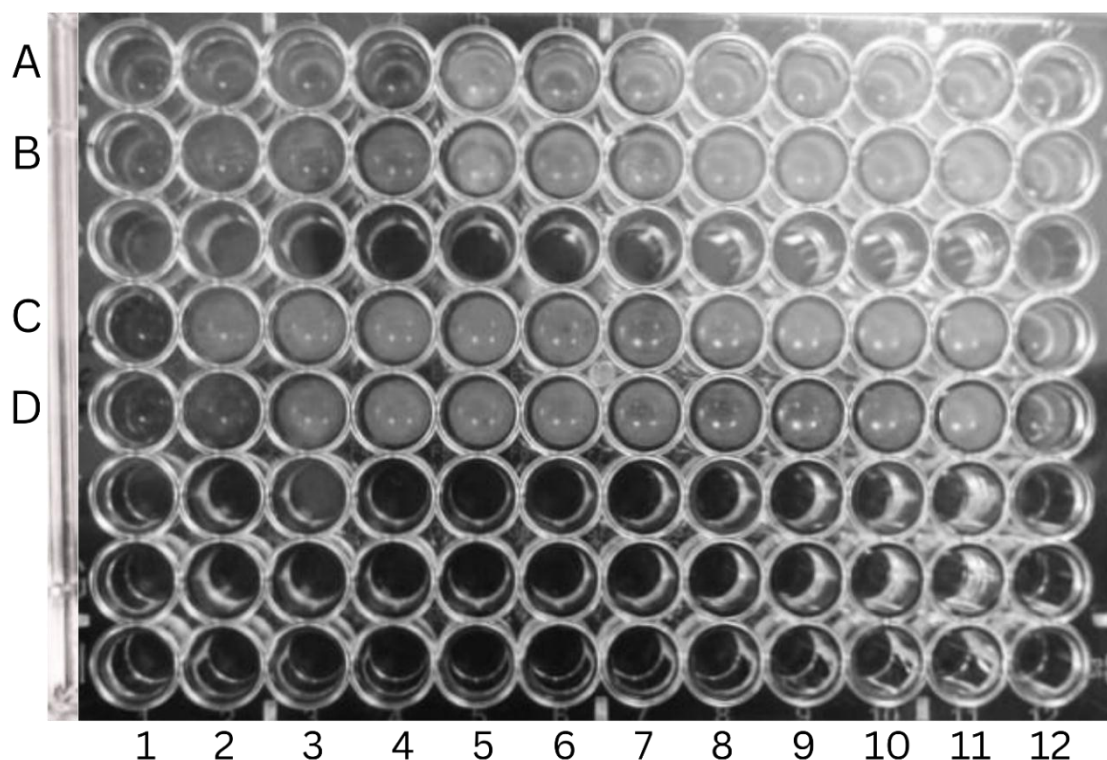


Figure 20: Broth Microdilution Assay for Antibacterial Susceptibility Testing of CuNPs-Incorporated GE/HA Polymer Solution against two bacterial strains: *P. aeruginosa* and *S. aureus*. The wells are arranged in rows, with each row containing different concentrations of the polymer solution. The 11th well serves as the positive control, and the 12th well acts as the negative control.

- A. Antibacterial susceptibility of 20wt.% CuNPs-incorporated GE/HA polymer solution against *P. aeruginosa*. Turbidity is observed starting from the 5th well, indicating bacterial growth at and below this concentration.
- B. Antibacterial susceptibility of 15wt.% CuNPs-incorporated GE/HA polymer solution against *P. aeruginosa*. Turbidity is observed starting from the 3rd well.
- C. Antibacterial susceptibility of 15wt.% CuNPs-incorporated GE/HA polymer solution against *S. aureus*. Turbidity is observed starting from the 2nd well.
- D. Antibacterial susceptibility of 15wt.% CuNPs-incorporated GE/HA polymer solution against *S. aureus*. Turbidity is observed starting from the 3rd well.

CuNPs concentration	Contact time	Colony-forming units (CFU) per milliliter (mL) of surviving microbial population following interaction with GE/HA/CuNPs		Antibacterial activity (% reduction in CFU)	
		<i>S.aureus</i>	<i>P.aeruginosa</i>	<i>S.aureus</i>	<i>P.aeruginosa</i>
20%	0 hours	1.5×10^8	1.5×10^8	-	-
	4 hours	0.5×10^7	1.5×10^6	96.6	99
	24 hours	1.0×10^5	2	99.93	99.99
15%	0 hours	1.5×10^8	1.5×10^8	-	-
	4 hours	1.2×10^8	0.2×10^8	20	86.7
	24 hours	1.0×10^7	0.3×10^7	93.3	98

Table 9: Bacterial Survival after Exposure to GE/HA/CuNPs Scaffold

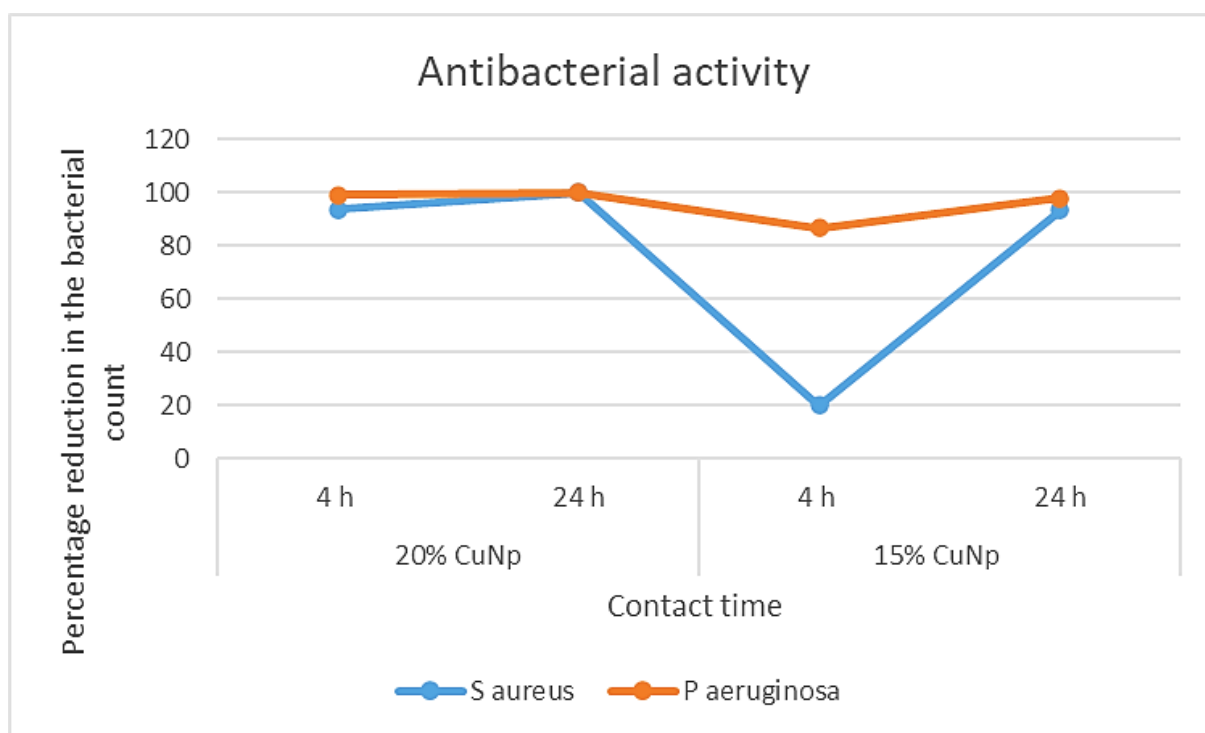


Figure 21: Line graph depicting the percent reduction in bacterial count over varying contact times for two representative bacterial samples (*P.aeruginosa* and *S.aureus*)

3.3 CELL PROLIFERATION AND CYTOTOXICITY

The viability and growth potential of human gingival fibroblasts (HGFs) were assessed in vitro to evaluate the biocompatibility of the fabricated Ti-coated (GE-CuNp/HA/PDA) scaffolds. HGFs were successfully cultured and subsequently exposed to the scaffolds for varying durations. To investigate the impact of scaffold exposure on cellular health and proliferation, both **cytotoxicity and proliferation assays** were performed.

All three groups (control, Ti-coated, and Ti-uncoated) show a similar trend of increasing cell viability over time (24 hrs., 48 hrs., 72 hrs.). At each time point, the Ti-coated group exhibits slightly higher cell viability compared to the Ti-uncoated group. Ti-coated group shows similar cell viability to the control group, particularly at 48 and 72 hours. This indicates that the Ti coating does not significantly alter cell viability compared to the standard culture conditions.

The cell proliferation analysis revealed no significant difference in cell proliferation between the control and Ti-coated alloy disc at the 24-hour time point, indicating that both groups supported initial cell attachment and spreading. Subsequent evaluation of cell proliferation demonstrated a highly statistically significant difference ($p < 0.0001$) between the GE/HA/PDA/CuNPs-coated Ti alloy disc (Ti-coated disc) and the unmodified Ti disc (ti-coated) at all time points investigated (24, 48, and 72 hours). These findings suggest that the GE/HA/PDA/CuNPs scaffold significantly enhances the attachment, migration, and proliferation of Human Gingival Fibroblasts (HGFs).

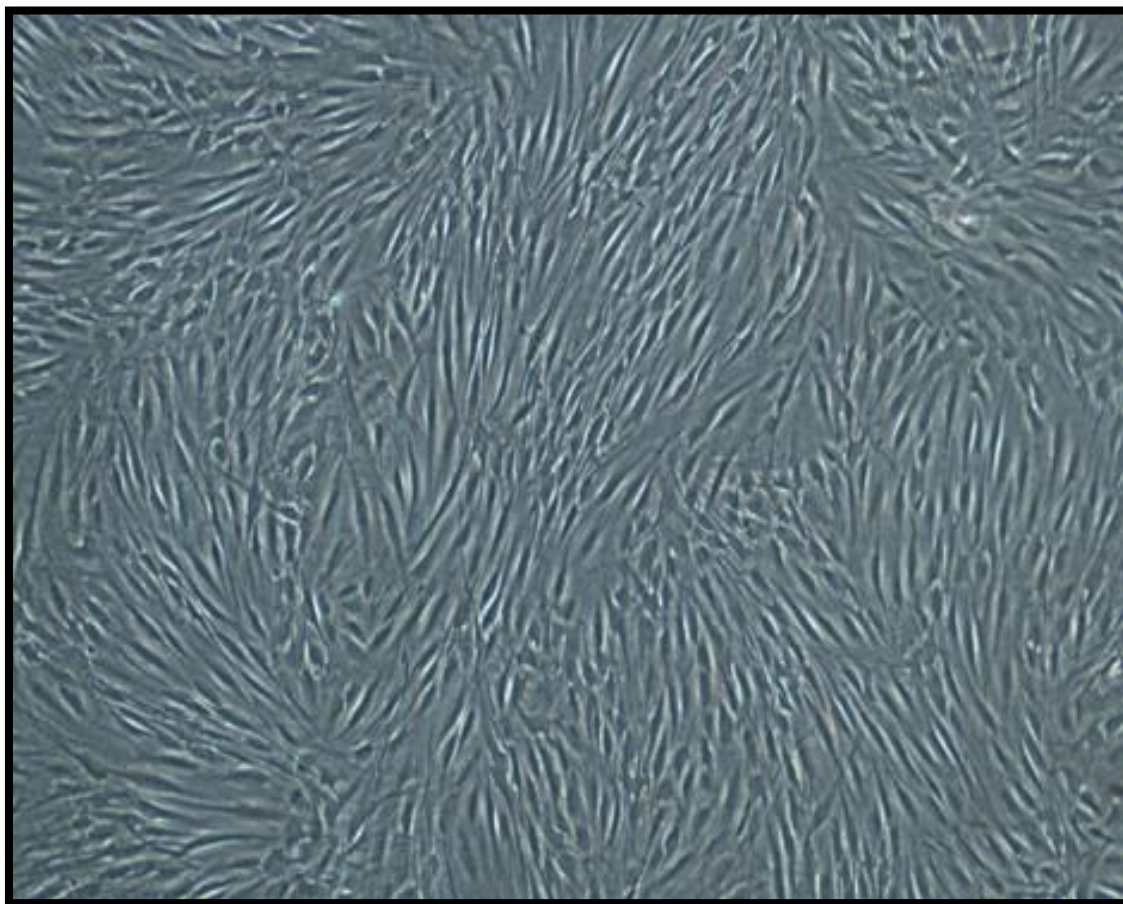


Figure 22: Representative image of HGFs exhibiting their characteristic fibroblastic morphology. This image serves as a crucial control, demonstrating the healthy and viable state of the cultured cells before interaction with the scaffolds.

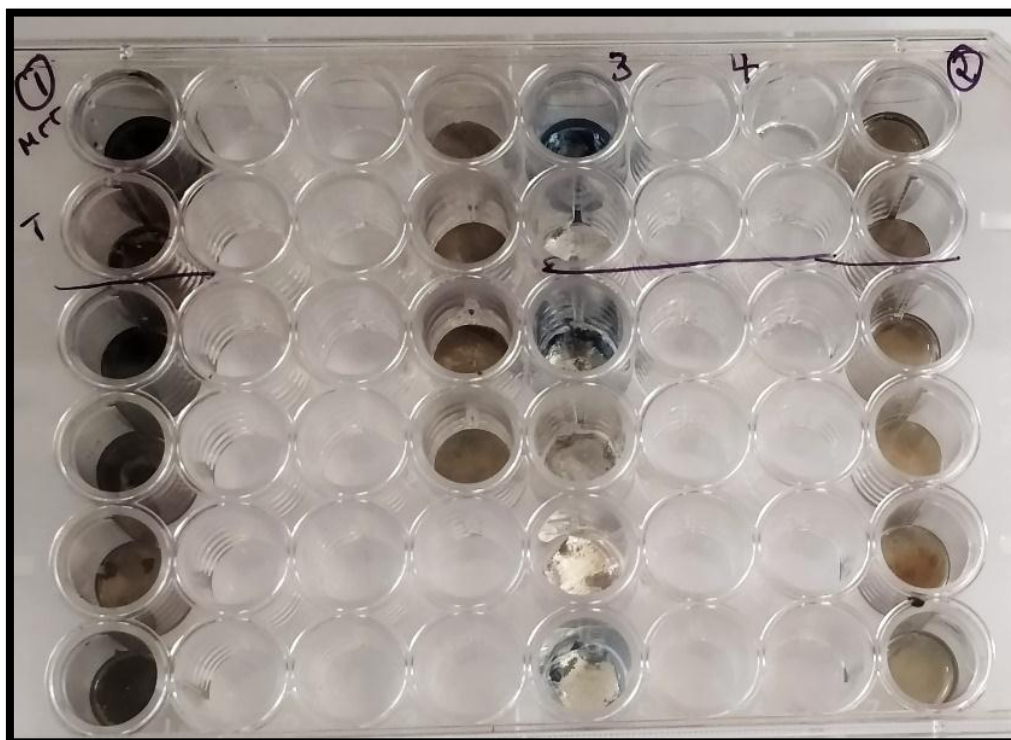


Figure 23: Representative image of cell culture plate used for testing the cytotoxicity of selected materials on human gingival fibroblasts (HGFs) by 3-[4,5-Dimethylthiazol-2-yl]-2,5 diphenyl tetrazolium bromide (MTT) and proliferation assay.

For MTT assay, the absorbance was recorded at 570 nm using a multiplate reader (Thermo Fisher Scientific, USA).

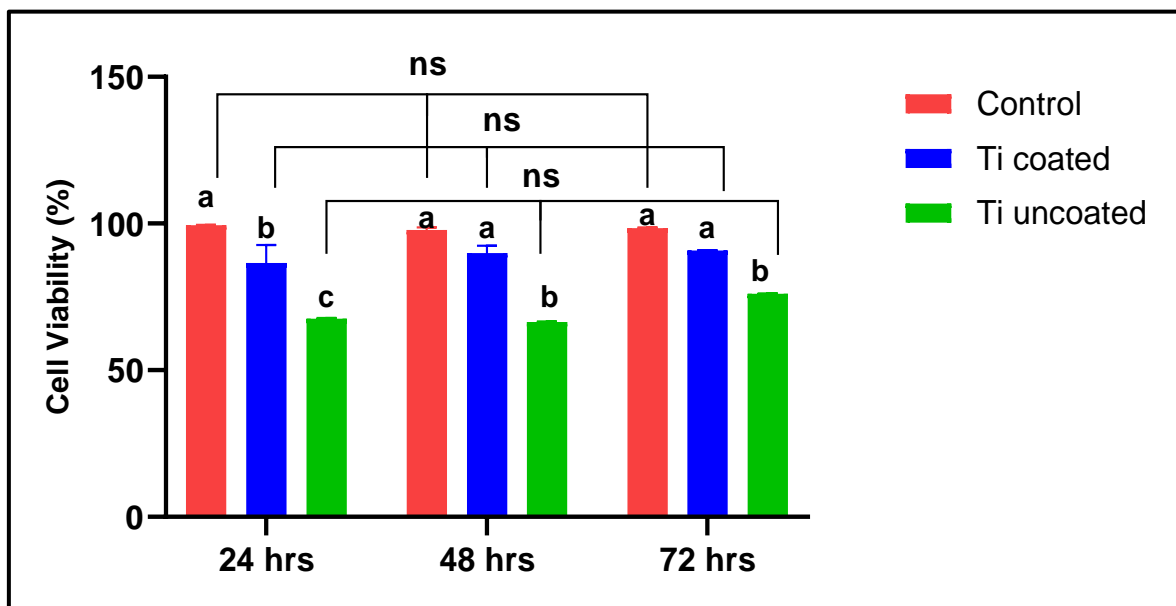


Figure 24: Viability values of human gingival fibroblasts exposed to Ti coated and Ti uncoated materials. The human gingival fibroblasts cultured alone served as a control. MTT assay was carried out at different time points, (24 hrs. 48 hrs., and 72 hrs), and the absorbance values measured at 570 nm are plotted.

Superscripts 'a, b and c' indicate statistically significant ($P < 0.05$) differences in the viability values between the control and tested materials at each time point of assay.

'ns' indicate no statistically significant ($P > 0.05$) differences for control and each tested material between the various time points as indicated.

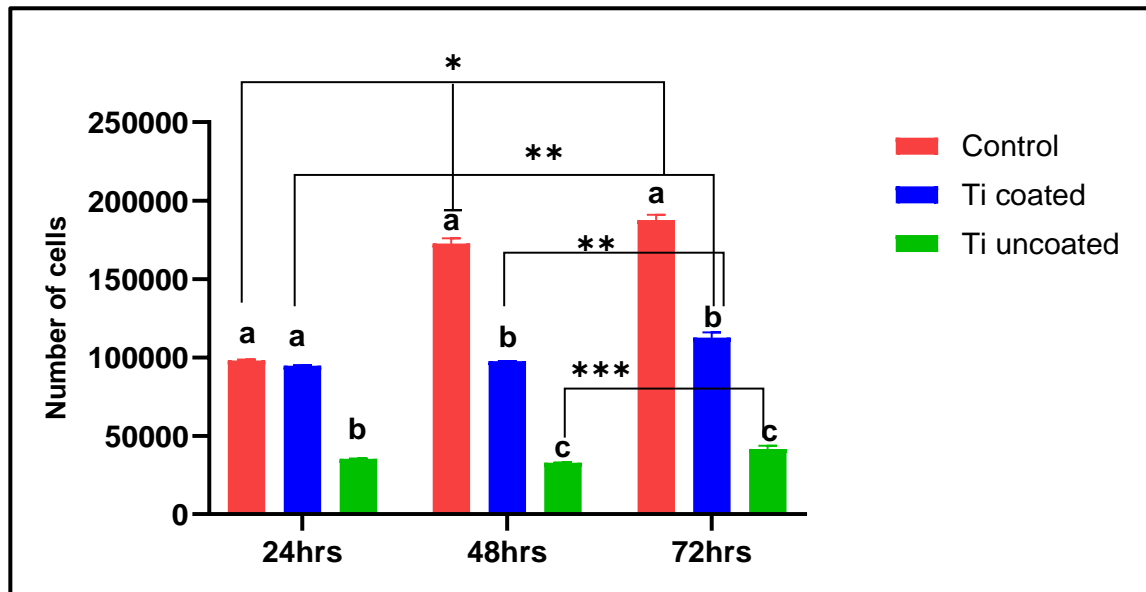


Figure 25: Proliferation of human gingival fibroblasts exposed to Ti-coated and Ti-uncoated materials. The human gingival fibroblasts cultured alone served as a control. Proliferation assay was carried out at different time points, 24 hrs., 48 hrs., and 72 hrs., and the cell numbers were plotted accordingly.

Superscripts 'a, b and c' indicate statistically significant ($P < 0.05$) differences in the number of human gingival fibroblasts between the control and tested materials at each time point of assay.

*, **, and *** indicate statistically significant ($P < 0.05$) differences for control and each tested material between the various time points as indicated in the graph.

The assay was performed in triplicates for each group.

The study explored the fabrication of a multifunctional, tissue-engineered electrospun scaffold that may be easily replicated over the complex three-dimensional topography of dental implants, such as the neck and/or abutment, to facilitate accelerated and robust soft tissue regeneration at the implant-soft tissue interface while concurrently mitigating bacterial colonization to provide biologically stable implants.

The success of dental implants hinges on their seamless integration with host tissues along with functional anti-microbial activity. While the normal oral flora is typically non-threatening, implanted biomaterials present unique challenges that can trigger bacterial virulence and biofilm formation.^[91]

The current trend in biomaterial design prioritizes either cell integration or antimicrobial activity, creating a trade-off that limits the full potential of these materials.^[91,92] However, recent advances are uncovering methods and techniques that synergistically integrate both functionalities. It is crucial to acknowledge that certain implant surfaces designed to promote cell attachment might paradoxically facilitate biofilm formation. Conversely, surfaces engineered for antimicrobial efficacy may exhibit cytotoxicity or fail to stimulate tissue attachment.^[93]

The omnipresence of peri-implant biofilm formation and microbial colonization poses a significant challenge to long-term implant success, irrespective of implant design or disease status.^[94,95] Mounting evidence unequivocally demonstrates the ubiquitous infiltration of microbes into the peri-implant sulcus and the implant-abutment interface (IAI) as early as five hours after functional loading, mediated

by microleakage through micro gaps inherent in various connection designs. While Morse taper connections may exhibit marginally lower bacterial burdens, they are not invincible to colonization.^[96,97]

Current strategies to mitigate this challenge, such as utilizing 0.2% chlorhexidine during two-step implant surgeries, primarily target bacterial reduction. However, these approaches fail to address the issue of bacterial endotoxin penetration, which persists even after initial disinfection.^[98]

Thus, the persistent challenge of postoperative complications associated with microbial colonization of implant surfaces also necessitates the exploration of multifaceted effective and safe antimicrobial strategies for implant surfaces. A plethora of promising approaches have been investigated, encompassing Engineered surface modifications, nano topography and antimicrobial peptide functionalization, UV-activatable surface, Drug-loaded and metal nanoparticle-polymer coating primarily silver(AgNPs).^[99, 100, 101]

Within the landscape of antimicrobial metal nanoparticle coatings, copper nanoparticles (CuNPs) present themselves as a potentially safer alternative due to several key advantages such as broad-spectrum activity against various bacteria, including multidrug-resistant strains, good biocompatibility and inherent body mechanisms to regulate copper homeostasis.^[102,103,104]

The human body possesses dedicated copper-transporting adenosine triphosphatases (Cu-ATPases) like ATP7A and ATP7B. These efficiently eliminate excess copper through the intestine (ATP7A) and bile/milk (ATP7B), mitigating the risk of long-term accumulation and associated

cytotoxicity compared to silver or other metal antimicrobial nanoparticles.^[104]

This study utilized copper nanoparticles (CuNPs) within the size range of 5-10nm embedded within the GE/HA scaffold. Energy-dispersive X-ray spectroscopy (EDS) confirmed the presence and uniform distribution of CuNPs throughout the scaffold. The selection of 5-10nm CuNPs was strategically guided by the need to achieve an optimal balance between three critical parameters: sustained antimicrobial activity, minimized cytotoxicity, and long-term scaffold stability. Extant literature confirms an inverse relationship between nanoparticle size and antimicrobial efficacy.^[104,105,106]

The antimicrobial activity of the CuNPs embedded GE/HA/PDA scaffold was confirmed by the presence of distinct inhibition zones surrounding Ti-coated discs placed on bacteria-inoculated agar plates after 24 hours. Notably, the broad-spectrum antibacterial activity of the 20 wt. % CuNPs loaded scaffolds matched that of the Amikacin control, a clinically established antibiotic effective against *Pseudomonas aeruginosa*. The lower MIC value and larger inhibition zone observed for *P. aeruginosa* relative to *S. aureus* further support this observation.

These results suggest the potential of the CuNPs embedded scaffolds as an effective antimicrobial agent, exhibiting enhanced activity against gram-negative *P. aeruginosa* compared to gram-positive *S. aureus*. This promising finding underscores the need for further investigation to explore the therapeutic potential of these scaffolds and optimize their efficacy for specific applications.

The antimicrobial activity can also be attributed to arise from the synergistic action of CuNPs with the scaffold components. The GE/HA/CuNPs electrospun

scaffold reinforced by employing Polydopamine as an intermediate bridging layer on the Ti alloy disc surface that would have prevented bacterial adhesion whilst enhancing the adhesion of CuNPs to the scaffold, potentially improving their interaction with bacteria. This would result in dual action of Cu, i.e. NO release mediated biofilm dispersion, and bacterial killing.^[102, 107]

The hyaluronic acid, can also contribute by disrupting bacterial adhesion and preventing biofilm formation, which can enhance the antimicrobial effectiveness of CuNPs.^[108] The porous nature of the GE/HA/PDA/CuNPs scaffold would have also offered a significant advantage by enabling sustained release of CuNPs potentially prolonging antimicrobial efficacy without requiring high initial doses.^[109]

Furthermore, the RGD signaling motif present within gelatin facilitates enhanced host cell infiltration into the scaffold.^[110] This influx of cells, primarily fibroblasts and immune cells, could potentially contribute to the observed antimicrobial effect by secretion of antimicrobial factors and enhanced immune response.

However, further investigations are needed to fully elucidate the specific roles and relative contributions of these mechanisms in the observed antimicrobial effect. Future studies could employ in vitro and in vivo models to quantify host cell infiltration, measure the production of specific antimicrobial factors, and assess the impact on bacterial burden and immune cell activation.

While the GE/HA/PDA/CuNPs scaffold coating offers promising antimicrobial activity, long-term success hinges not only on combating bacterial pathogens at the implant site but also on establishing a robust biological seal. This seal,

formed by the integration of soft tissue with the implant surface, plays a critical role in preventing infections and ensuring implant stability. ^[16, 111]

Our investigation established a two-step fabrication process for a bilayer scaffold coating on Ti alloy discs. This process involved meticulous cleaning and drying of the discs, followed by controlled immersion in a Dopamine-Tris HCl buffer solution to facilitate the self-polymerization and formation of a polydopamine (PDA) layer. The successful deposition of the PDA layer was then confirmed through Fourier-Transform Infrared Spectroscopy (FTIR) analysis, demonstrating the presence of characteristic functional group peaks associated with PDA.

The GE/HA/CuNPs scaffold was fabricated using a biomimetic approach, aiming to mimic the natural extracellular matrix (ECM) and provide a supportive environment for cell growth. Electrospinning a solution of gelatin and hyaluronic acid (GE: HA = 6:4) dissolved in a volatile solvent mixture (DMF: DI) yielded a porous network of interconnected fibers with an average diameter of 284 nm as confirmed by SEM analysis. FTIR analysis further confirmed the presence of the desired components (GE, HA, and CuNPs) within the scaffold.

Contact angle measurements revealed significantly lower contact angles on the GE/HA/PDA/CuNPs mat scaffold-coated Ti alloy disc compared to the uncoated Ti alloy disc, indicating enhanced hydrophilicity. This can be attributed to two key factors: The presence of hydrophilic groups and porous structure. The composite nanofibers contain functional groups like hydroxyl (-OH) and carboxyl (-COOH) present in the gelatin and hyaluronic acid components, which can readily interact with water molecules, promoting surface wetting. ^[112,113]

The interconnected pores within the scaffold create a larger surface area and provide capillary forces that draw in water droplets, further contributing to the observed hydrophilicity. This enhanced hydrophilicity is a key advantage, as it is well-documented to promote cell adhesion and proliferation. By providing a more favorable environment for cell attachment and spreading, the scaffold can potentially support tissue regeneration. ^[112,114,115]

In vitro cytotoxicity and proliferation analysis yielded promising results, demonstrating a statistically significant enhancement in cell growth and proliferation on the GE/HA/PDA/CuNPs-coated Ti alloy disc compared to the uncoated Ti discs. This observation aligns with the findings of scanning electron microscopy (SEM), which revealed extensive fibroblast alignment parallel to the substrate surface.

These observations suggest intimate cell spreading and potentially enhanced interaction with the modified topography of the scaffold coating. This can be attributed, in part, to the inherent properties of the nanofibrous structure. Compared to flat surfaces, the nanofibers offer a significantly larger surface area, providing more space for cell adhesion and spreading. Additionally, the intertwined fibers create microenvironments that mimic the natural extracellular matrix (ECM), further promoting cell attachment and growth. ^[116,117]

Gelatin, a major component of the scaffold, possesses inherent arginine-glycine-aspartic acid (RGD) sequences. These sequences act as biomimetic ligands, readily recognized by integrin receptors on fibroblast cell membranes. This interaction triggers important cell signaling pathways essential for attachment, migration, and proliferation. ^[30,118]

The synergistic combination of hyaluronic acid (HA) and gelatin within the scaffold matrix offers distinct benefits. HA contributes to tissue lubrication and hydration, reducing friction and wear while also interacting with specific receptors on cells crucial for soft tissue regeneration, such as fibroblasts and endothelial cells.^[119,120] This interaction promotes cell adhesion, migration, and proliferation, ultimately contributing to tissue repair and potentially improving the integrity of the seal.

HA plays a role in stimulating the formation of new blood vessels (angiogenesis), enhancing vascularization within the soft tissue. This improved blood supply ensures adequate delivery of nutrients and oxygen, supporting tissue viability and promoting faster healing. HA possesses inherent anti-inflammatory properties, mitigating tissue inflammation often associated with implantation.^[121] This reduced inflammatory response promotes faster healing and creates a more conducive environment for long-term implant success.

PDAs can adhere to a wide range of materials, including metals, polymers, and even biological tissues.^[22,23] This makes it a valuable tool for surface modification and enhancing the adhesion of various components within the scaffold. The resulting formation of strong covalent and non-covalent interactions with the surfaces fosters durable and long-lasting adhesion, crucial for the structural integrity and functionality of the scaffold over time.^[122]

This approach of enhancing component adhesion through surface modification offers specific advantages pertinent to scaffold performance. Firstly, it reinforces the scaffold's structural integrity, particularly during the torqueing forces

encountered during implant insertion. Secondly, it strengthens the interaction between the scaffold and surrounding tissues, potentially promoting improved tissue integration and long-term functionality.

In conclusion, this study successfully developed a novel bilayer bio-engineered scaffold with promising properties for tissue regeneration. The GE/HA/PDA/CuNPs scaffold presents a biocompatible and structurally supportive microenvironment, featuring mussel-inspired adhesion. This promotes host cell adhesion, growth, and potential differentiation, ultimately contributing to tissue regeneration. Mimicking the structure and function of the native extracellular matrix (ECM), the scaffold offers increased stability with tailored porosities. These features facilitate the self-seeding of native cells and promote the formation of a well-integrated implant-abutment interface, resembling the natural tooth. Additionally, the scaffold's inherent antimicrobial activity inhibits bacterial colonization at the implant-tissue interface within the first 24 hours, a crucial period for postoperative healing and successful cell attachment. These combined features suggest the potential of this scaffold for advancing translational and multidisciplinary implant research and promoting tissue regeneration in dental implantology.

While this study showcases promising results for the GE/HA/PDA/CuNPs scaffold in dental implant applications, several limitations hinder a definitive assessment of its clinical potential. Firstly, the study does not address the scaffold's long-term performance, neglecting crucial factors like attachment strength, degradation rate, and bio-tribocorrosion. Further exploration is required to evaluate the potential for mimicking natural tissue organization by studying perpendicular PDL

fiber insertion within the scaffold's porous structure. Thirdly, the impact of the scaffold on the immune system, specifically its potential immunomodulatory effects, remains unexplored. Investigating its influence on inflammatory responses, both anti-inflammatory and pro-inflammatory markers, could be beneficial for mitigating peri-implant complications.

Fourthly, while focusing on fibroblast migration and attachment, the study neglects the crucial interaction with epithelial tissue. Finally, the primary reliance on in vitro models necessitates further investigation through an optimized in vivo study for a definitive evaluation.

Addressing these limitations and pursuing the outlined future research directions are crucial for comprehensively understanding the GE/HA/PDA/CuNPs scaffold's potential to improve clinical outcomes and patient experience in dental implant therapy.

5.1 CONCLUSION

This study successfully developed and characterized a novel GE/HA/PDA/CuNPs electrospun scaffold, demonstrating its potential as a biocompatible coating for dental implants to enhance soft tissue integration. Despite limitations, the results indicate this scaffold could contribute to a healthy biological seal by promoting fibroblast infiltration, potentially leading to improved tissue growth and integration around the implant. This ultimately fosters a stronger and more durable seal while effectively eliminating bacteria at the implant site, minimizing infection risk and promoting tissue healing. By understanding the synergistic effects of the scaffold on both bacterial control and tissue integration, we can optimize its design and pave the way for improved clinical outcomes in dental implant therapy.

5.2 SUMMARY

This thesis aimed to develop a novel coating for dental implants that offers dual functionality: enhancing tissue integration and mitigating infection risk for long-term clinical benefit.

5.2.1 Fabrication and characterization of bi-layer GE/HA/PDA/CUNPs scaffold:

Grade 5 titanium discs, measuring 10mm in diameter and 2mm thick, were polished and then cleaned ultrasonically. These discs were subsequently coated with polydopamine (PDA) through self-polymerization of a dopamine solution.

Following optimization, a polymer solution containing 6:4 weight ratio of Gelatin (280 bloom, Type A) to hyaluronic acid, sodium salt (M_r 1.0-1.5 $\times 10^6$) was prepared for electrospinning. Copper nanoparticles (5-10nm size) were incorporated at varying concentrations according to the weight percentage of gelatin. The solutions were then carefully combined under controlled conditions.

Using a controlled electrospinning system, the optimized solution was electrospun onto the PDA-coated titanium discs under precisely controlled temperature, humidity, voltage, and distance parameters. The scaffolds underwent crosslinking with 1% glutaraldehyde vapors, followed by vacuum treatment to eliminate residual solvent and glutaraldehyde vapors. The gelatin component was further crosslinked and sterilized using UV irradiation.

This meticulous fabrication process resulted in a bilayer scaffold with a PDA-coated titanium base and a nanofibrous GE/HA/CuNPs layer. The scaffold exhibited the desired characteristics, including appropriate fiber morphology, confirmed composition, and improved hydrophilicity, as confirmed by SEM, EDS, FTIR, and Contact Angle analysis, making it suitable for potential cell adhesion and further exploration in soft tissue engineering applications.

5.2.2 Exploring the antibacterial potential of GE-CUNP/HA/PDA scaffolds:

This section delves into the antibacterial properties of GE/HA/PDA/CuNPs scaffolds against two bacterial strains: *Pseudomonas aeruginosa* (gram-negative) and *Staphylococcus aureus* (gram-positive).

The investigation employed the Kirby-Bauer disc diffusion method to evaluate the scaffolds' antibacterial effects. Scaffolds loaded with varying CuNPs concentrations were tested, starting with the lowest CuNPs concentration (1 wt.%) and progressively increasing by 5% for each subsequent test (5 wt. %, 10 wt.%, 15 wt./%, and 20 wt.%). Notably, larger zones of inhibition, indicating greater bacterial suppression, were observed against *P. aeruginosa* compared to *S. aureus*. This suggests a higher susceptibility of *P. aeruginosa* to the scaffolds' antibacterial properties.

Among the tested CuNPs concentrations, 20 wt. % exhibited the most potent activity against *P. aeruginosa*, comparable to the positive control antibiotic (Amikacin). This finding highlights the potential of these scaffolds as broad-spectrum antibacterial agents against gram-negative bacteria. However, the

efficacy against *S. aureus* remained limited, with only 15 and 20 wt. % CuNPs demonstrating measurable inhibition zones, suggesting a less pronounced concentration-dependent effect.

To further explore the selective susceptibility observed the minimum inhibitory concentration (MIC) of the CuNPs-impregnated GE/HA polymer solution was determined using the broth microdilution method. Broth microdilution testing revealed the CuNPs-impregnated GE/HA solution's MIC against *S. aureus* was decreased by increasing the CuNPs concentration (1200µg/ml at 15 wt. % and 600µg/ml at 20 wt. %). Similarly, MICs decreased with increasing concentration (112 µg/ml at 15 wt.% and 75 µg/ml at 20 wt.%) against *P. aeruginosa*.

The comparatively lower MIC of 20wt.% CuNPs reinforced the disc diffusion findings, confirming a higher sensitivity of *P. aeruginosa* to CuNPs compared to *S. aureus*. This selective susceptibility highlights the potential of tailoring CuNPs concentration to target specific bacterial strains.

A direct correlation was observed between the CuNPs concentration and the reduction in *P. aeruginosa* colonies over time, emphasizing the dynamic nature of the antibacterial activity.

5.2.3 Cell proliferation and cytotoxicity

A total of three samples were obtained from periodontally and systemically healthy individuals aged 18-30 years undergoing premolar extraction for orthodontic treatment or crown lengthening procedures following institutional and ethical approval.

The tissue was meticulously preserved in sterile saline to ensure its viability for subsequent experiments. Following thorough rinsing and sectioning, the gingival

samples were placed in Petri dishes and nourished with a specially formulated culture medium containing essential nutrients and antibiotics. The culture environment was carefully controlled with specific humidity, temperature, and carbon dioxide levels to optimize cell growth. To maintain a healthy cell population, a passaging process was performed weekly, involving the dilution and transfer of cells to a fresh medium.

To evaluate the potential cytotoxicity of the coated material, three groups were established: a control group with no intervention, a test group 1 exposed to titanium discs coated with the material containing copper nanoparticles at the highest tested minimum inhibitory concentration (MIC), and a test group 2 exposed to uncoated titanium discs. Gingival fibroblasts were seeded in a 96-well plate and co-incubated with the respective test materials. The MTT assay, a reliable indicator of metabolic activity and thus cell viability, was conducted at four-time points: 0, 24, 48, and 72 hours. Cell viability was calculated relative to the control group, representing 100%.

Encouragingly, all groups displayed an increasing trend in cell viability over time. Notably, the group exposed to the coated discs consistently exhibited slightly higher cell viability compared to the uncoated discs at each time point. Furthermore, the coated discs demonstrated comparable cell viability to the control group, particularly at later time points.

This promising result suggests that, at the tested concentration, the Ti coating with copper nanoparticles did not significantly alter the viability of human gingival fibroblasts compared to standard culture conditions and bare titanium discs. This

CONCLUSION, SUMMARY & SCOPE FOR FUTURE WORK

finding paves the way for further evaluation of the coated material's biocompatibility and potential suitability for various applications.

A statistically significant difference ($p < 0.0001$) was demonstrated between the GE/HA/PDA/CuNPs-coated Ti alloy disc and the unmodified control at all investigated time points (24, 48, and 72 hours). This finding suggests that the incorporation of CuNPs within the scaffold significantly enhances the attachment, migration, and proliferation of HGFs.

5.3 LIMITATIONS AND SCOPE FOR FUTURE WORK:

While this study offers promising results for the GE/HA/PDA/CuNPs scaffold, several key areas require further investigation to fully understand its potential for clinical application in dental implants.

Further analysis of the scaffold's integration with surrounding tissues, including attachment strength, degradation rate, and bio-tribocorrosion, was not addressed in the current work. Additionally, studying perpendicular PDL fiber insertion within the scaffold's porous structure, as suggested by its design, would be valuable to evaluate its potential for mimicking natural tissue organization.

The potential immunomodulatory effects of the scaffold were not investigated in the current study. Further investigation evaluating the Anti-inflammatory and pro-inflammatory markers could be particularly beneficial for mitigating peri-implant complications.

Tissue Regeneration vs. Repair: Peri-implant tissue healing often prioritizes repair over regeneration, potentially compromising soft tissue attachment. While this study focused on fibroblast migration, and attachment, exploring the interaction with epithelial tissue is equally important. Studying a model that incorporates both epithelial and connective tissues would provide a more comprehensive understanding of the healing process.

The current study primarily relied on in vitro models; however, an optimized in vivo study is crucial to assess the scaffold's performance in a complex biological environment. An in vivo model with single-stage implant placement would allow for long-term observation of the biological seal's stability and the impact of sustained CuNPs release on surrounding tissues. This would provide crucial insights into the scaffold's durability and potential effects over time.

By addressing these limitations and pursuing the outlined future directions, this research can pave the way for a more comprehensive understanding of the GE/HA/PDA/CuNPs scaffold's potential to improve clinical outcomes and overall patient experience in dental implant therapy.

1. Le Guéhennec L, Soueidan A, Layrolle P, Amouriq Y. Surface treatments of titanium dental implants for rapid osseointegration. *Dental Materials*. 2007 Jul;23(7):844–54.
2. Moraschini V, Poubel LA da C, Ferreira VF, Barboza E dos SP. Evaluation of survival and success rates of dental implants reported in longitudinal studies with a follow-up period of at least 10 years: a systematic review. *International Journal of Oral and Maxillofacial Surgery*. 2015 Mar;44(3):377–88.
3. Nickenig HJ, Wichmann M, Andreas SK, Eitner S. Oral health–related quality of life in partially edentulous patients: Assessments before and after implant therapy. *Journal of Cranio-Maxillofacial Surgery* [Internet]. 2008 Dec 1;36(8):477–80.
4. Smeets R, Henningsen A, Jung O, Heiland M, Hammächer C, Stein JM. Definition, etiology, prevention and treatment of peri-implantitis – a review. *Head & Face Medicine* [Internet]. 2014 Sep 3 [cited 2019 Dec 16];10(1). Available from: <https://www.ncbi.nlm.nih.gov/pmc/articles/PMC4164121/>
5. Turkyilmaz I, editor. *Implant Dentistry - The Most Promising Discipline of Dentistry* [Internet]. InTech; 2011. Available from: <http://dx.doi.org/10.5772/964>
6. J Levignac. [Periimplantation osteolysis- periimplantosis - periimplantitis]. *PubMed*. 1965 Oct 1;12(8):1251–60.
7. Gutteridge DL. Proceedings of the 1st European Workshop on Periodontology. *Journal of Dentistry*. 1996 May;24(3):235.
8. Zitzmann NU, Berglundh T. Definition and prevalence of peri-implant diseases. *Journal of Clinical Periodontology*. 2008 Sep;35:286–91.

9. Schwarz F, Derks J, Monje A, Wang HL. Peri-implantitis. *Journal of Clinical Periodontology*. 2018 Jun;45(S20):S246–66.
10. Lang NP, Berglundh T. Periimplant diseases: where are we now? - Consensus of the Seventh European Workshop on Periodontology. *Journal of Clinical Periodontology*. 2011 Feb 16;38:178–81.
11. Lindhe J, Meyle J. Peri-implant diseases: Consensus Report of the Sixth European Workshop on Periodontology. *Journal of Clinical Periodontology*. 2008 Sep;35:282–5.
12. Jepsen S, Berglundh T, Genco R, Aass AM, Demirel K, Derks J, et al. Primary prevention of peri-implantitis: Managing peri-implant mucositis. *Journal of Clinical Periodontology*. 2015 Mar 31;42:S152–7.
13. Wen Lin Chai, Masfueh Razali, Keyvan Moharamzadeh, Muhammad Sohail Zafar. *The hard and soft tissue interfaces with dental implants*. Elsevier eBooks. 2020 Jan 1;173–201.
14. Wen Lin Chai. *Dimension and Structures of Biological Seal of Peri-Implant Tissues*. IntechOpen; 2016.
15. Hämmerle CHF, Tarnow D. The etiology of hard- and soft-tissue deficiencies at dental implants: A narrative review. *Journal of Periodontology* [Internet]. 2018 Jun 1;89 Suppl 1:S291–303. Available from: <https://www.ncbi.nlm.nih.gov/pubmed/29926950>
16. Alva H, Prasad K, Prasad A. Bioseal: The physiological and biological barrier for osseointegrated supported prosthesis. *Journal of Dental Implants*. 2013;3(2):148.
17. Buser D, Sennerby L, De Bruyn H. Modern implant dentistry based on osseointegration: 50 years of progress, current trends and open questions.

- Periodontology 2000. 2016 Dec 21;73(1):7–21.
18. Resnik R. Misch's Contemporary Implant Dentistry E-Book. Elsevier Health Sciences; 2020.
 19. Kligman S, Ren Z, Chung CH, Perillo MA, Chang YC, Koo H, et al. The Impact of Dental Implant Surface Modifications on Osseointegration and Biofilm Formation. *Journal of Clinical Medicine*. 2021 Apr 12;10(8).
 20. Rausch MA, Shokoohi-Tabrizi H, Wehner C, Pippenger BE, Wagner RS, Ulm C, et al. Impact of Implant Surface Material and Microscale Roughness on the Initial Attachment and Proliferation of Primary Human Gingival Fibroblasts. *Biology*. 2021 Apr 22;10(5):356.
 21. Aamodt JM, Grainger DW. Extracellular matrix-based biomaterial scaffolds and the host response. *Biomaterials*. 2016 Apr;86:68–82.
 22. Ball V. Polydopamine Nanomaterials: Recent Advances in Synthesis Methods and Applications. *Frontiers in Bioengineering and Biotechnology*. 2018 Aug 17;6.
 23. Palladino P, Bettazzi F, Scarano S. Polydopamine: surface coating, molecular imprinting, and electrochemistry—successful applications and future perspectives in (bio)analysis. *Analytical and Bioanalytical Chemistry*. 2019 Feb 26; 411(19):4327–38.
 24. Liu Y, Ai K, Lu L. Polydopamine and Its Derivative Materials: Synthesis and Promising Applications in Energy, Environmental, and Biomedical Fields. *Chemical Reviews*. 2014 Feb 11; 114(9):5057–115.
 25. Zhu Y, Liu D, Wang XL, He Y, Luan W, Qi F, et al. Polydopamine-mediated covalent functionalization of collagen on a titanium alloy to promote biocompatibility with soft tissues. *Journal of Materials Chemistry B*. 2019

- Mar 20;7(12):2019–31.
26. He S, Zhou P, Wang L, Xiong X, Zhang Y, Deng Y, et al. Antibiotic-decorated titanium with enhanced antibacterial activity through adhesive polydopamine for dental/bone implant. *Journal of The Royal Society Interface*. 2014 Jun 6; 11(95):20140169.
 27. Sook Hee Ku, Joon Seok Lee, Chan Beum Park. Spatial Control of Cell Adhesion and Patterning through Mussel-Inspired Surface Modification by Polydopamine. *Langmuir*. 2010 Aug 31;26(19):15104–8.
 28. Jia L, Han F, Wang H, Zhu C, Guo Q, Li J, et al. Polydopamine-assisted surface modification for orthopaedic implants. *Journal of Orthopaedic Translation* [Internet]. 2019 Apr 1; 17:82–95. Available from: <https://www.sciencedirect.com/science/article/pii/S2214031X19300439>
 29. Ma T, Wang C, Ge X, Zhang Y. Applications of Polydopamine in Implant Surface Modification. *Macromolecular Bioscience*. 2023 Jun 3;23(10).
 30. D'Souza SE, Ginsberg MH, Plow EF. Arginyl-glycyl-aspartic acid (RGD): a cell adhesion motif. *Trends in Biochemical Sciences*. 1991 Jan;16:246–50.
 31. Caballero Aguilar LM, Kapsa RM, O'Connell CD, McArthur SL, Stoddart PR, Moulton SE. Controlled release from PCL–alginate microspheres *via* secondary encapsulation using GelMA/HAMA hydrogel scaffolds. *Soft Matter*. 2019;15(18):3779–87.
 32. Sachar A, Strom TA, San Miguel S, Serrano MJ, Svoboda KKH, Liu X. Cell-matrix and cell-cell interactions of human gingival fibroblasts on three-dimensional nanofibrous gelatin scaffolds. *Journal of Tissue Engineering and Regenerative Medicine*. 2012 Aug 13;8(11):862–73.
 33. Khan M, Shanmugaraj A, Prada C, Patel A, Babins E, Bhandari M. The Role

- of Hyaluronic Acid for Soft Tissue Indications: A Systematic Review and Meta-Analysis. *Sports Health: A Multidisciplinary Approach*. 2022 Feb 3;194173812110733.
34. Rahemtulla F. Proteoglycans of Oral Tissues. *Critical Reviews in Oral Biology & Medicine*. 1992 Jan;3(1):135–62.
 35. Dahiya P, Kamal R. Hyaluronic acid: A boon in periodontal therapy. *North American Journal of Medical Sciences*. 2013;5(5):309.
 36. Rice KG. *The Chemistry, Biology, and Medical Applications of Hyaluronan and Its Derivatives* Edited by T. C. Laurent. Portland Press, London, U.K. 1998. xvi + 341 pp. 17 × 25 cm. ISBN 1-85578-119-0. \$127.50. *Journal of Medicinal Chemistry*. 1998 Dec 1;41(26):5336–6.
 37. Pirnazar P, Wolinsky L, Nachnani S, Haake S, Pilloni A, Bernard GW. Bacteriostatic Effects of Hyaluronic Acid. *Journal of Periodontology*. 1999 Apr;70(4):370–4.
 38. Ardizzoni A, Neglia RG, Baschieri MC, Cermelli C, Caratozzolo M, Righi E, et al. Influence of hyaluronic acid on bacterial and fungal species, including clinically relevant opportunistic pathogens. *Journal of Materials Science: Materials in Medicine*. 2011 Sep 4;22(10):2329–38.
 39. Weigel PH, Frost SJ, McGary CT, LeBœuf RD. The role of hyaluronic acid in inflammation and wound healing. *PubMed*. 1988 Jan 1;10(6):355–65.
 40. Deed R, Rooney P, Kumar P, Norton JD, Smith J, Freemont AJ, Kumar S. Early-response gene signalling is induced by angiogenic oligosaccharides of hyaluronan in endothelial cells. Inhibition by non-angiogenic, high-molecular-weight hyaluronan. *International journal of cancer*. 1997 Apr 10;71(2):251-6.
 41. Toole BP. Hyaluronan in morphogenesis. *Seminars in Cell & Developmental Biology* [Internet]. 2001 Apr 1 [cited 2022 Jun 21];12(2):79–87. Available

from:

<https://pubmed.ncbi.nlm.nih.gov/11292373/#:~:text=It%20is%20postulated%20that%20the>

42. Kedige S, Anand S, Bansal J. Hyaluronic acid: A promising mediator for periodontal regeneration. *Indian Journal of Dental Research*. 2010;21(4):575.
43. Guo T, Gulati K, Arora H, Han P, Fournier B, Ivanovski S. Race to invade: Understanding soft tissue integration at the transmucosal region of titanium dental implants. *Dental Materials*. 2021 May;37(5):816–31.
44. Jayaraman S. Interventions for replacing missing teeth: Antibiotics in dental implant placement to prevent complications: Evidence summary of Cochrane review. *The Journal of Indian Prosthodontic Society*. 2015;15(2):179.
45. Grischke J, Eberhard J, Stiesch M. Antimicrobial dental implant functionalization strategies —A systematic review. *Dental Materials Journal*. 2016;35(4):545–58.
46. Bergemann C, Zaatreh S, Wegner K, Arndt K, Podbielski A, Bader R, et al. Copper as an alternative antimicrobial coating for implants - an in vitro study. *World Journal of Transplantation*. 2017;7(3):193.
47. Jing H, Yu Z, Li L. Antibacterial properties and corrosion resistance of Cu and Ag/Cu porous materials. *Journal of Biomedical Materials Research Part A*. 2008 Oct;87A(1):33–7.
48. Vítězslav Straňák, Wulff H, Henrike Rebl, Zietz C, Arndt K, Bogdanowicz R, et al. Deposition of thin titanium–copper films with antimicrobial effect by advanced magnetron sputtering methods. *Materials Science and*

- Engineering: C. 2011 Oct 1;31(7):1512–9.
49. Nikolova MP, Chavali MS. Recent advances in biomaterials for 3D scaffolds: A review. *Bioactive Materials* [Internet]. 2019 Oct 25;4:271–92. Available from: <https://www.ncbi.nlm.nih.gov/pmc/articles/PMC6829098/>
 50. Almouemen N, Kelly HM, O’Leary C. Tissue Engineering: Understanding the Role of Biomaterials and Biophysical Forces on Cell Functionality Through Computational and Structural Biotechnology Analytical Methods. *Computational and Structural Biotechnology Journal* [Internet]. 2019 Apr 17;17:591–8. Available from: <https://www.ncbi.nlm.nih.gov/pmc/articles/PMC6502738/>
 51. Kim YS, Smoak MM, Melchiorri AJ, Mikos AG. An Overview of the Tissue Engineering Market in the United States from 2011 to 2018. *Tissue Engineering Part A*. 2019 Jan;25(1-2):1–8.
 52. Ma PX. Scaffolds for tissue fabrication. *Materials Today*. 2004 May;7(5):30–40.
 53. Yadav P, Beniwal G, Saxena KK. A review on pore and porosity in tissue engineering. *Materials Today: Proceedings*. 2021;44:2623–8.
 54. Sultana N. Mechanical and biological properties of scaffold materials. Elsevier eBooks. 2018 Jan 1;1–21.
 55. Nasonova MV, Glushkova TV, Borisov VV, Velikanova EA, A. Yu. Burago, Kudryavtseva YA. Biocompatibility and Structural Features of Biodegradable Polymer Scaffolds. *Bulletin of Experimental Biology and Medicine*. 2015 Nov 1;160(1):134–40.
 56. Farzin A, Bahrami N, Mohamadnia A, Mousavi S, Gholami M, Ai J, et al. Scaffolds in Dental Tissue Engineering: A Review. *Archives of*

- Neuroscience. 2019 Nov 2;7(1).
57. Wu DT, Munguia-Lopez JG, Cho YW, Ma X, Song V, Zhu Z, et al. Polymeric Scaffolds for Dental, Oral, and Craniofacial Regenerative Medicine. *Molecules*. 2021 Nov 22;26(22):7043.
 58. Weigel T, Schinkel G, Lendlein A. Design and preparation of polymeric scaffolds for tissue engineering. *Expert Review of Medical Devices*. 2006 Nov;3(6):835–51.
 59. O'Brien FJ. Biomaterials & scaffolds for tissue engineering. *Materials Today*. 2011 Mar;14(3):88–95.
 60. Pei B, Wang W, Fan Y, Wang X, Watari F, Li X. Fiber-reinforced scaffolds in soft tissue engineering. *Regenerative Biomaterials*. 2017 Aug 1;4(4): 257–68.
 61. Ratner BD, Hoffman AS, Schoen FJ, Lemons JE. *Biomaterials Science : an Introduction to Materials in Medicine*. Saint Louis: Elsevier Science; 2014.
 62. Lanza RP, Langer RS, Chick WL. *Principles of tissue engineering*. San Diego: Academic Press ; Austin; 1997.
 63. Jun I, Han HS, Edwards J, Jeon H. Electrospun Fibrous Scaffolds for Tissue Engineering: Viewpoints on Architecture and Fabrication. *International Journal of Molecular Sciences* [Internet]. 2018 Mar 6;19(3):745. Available from: <https://www.ncbi.nlm.nih.gov/pmc/articles/PMC5877606/>
 64. Panagiotis Sofokleous, Matthew H.W. Chin, Day R. Phase-separation technologies for 3D scaffold engineering. *Elsevier eBooks*. 2018 Jan 1; 101–26.
 65. Akbarzadeh R, Yousefi AM. Effects of processing parameters in thermally induced phase separation technique on porous architecture of scaffolds for

- bone tissue engineering. *Journal of Biomedical Materials Research Part B: Applied Biomaterials*. 2014 Jan 15;102(6):1304–15.
66. Raeisdasteh Hokmabad V, Davaran S, Ramazani A, Salehi R. Design and fabrication of porous biodegradable scaffolds: a strategy for tissue engineering. *Journal of Biomaterials Science, Polymer Edition*. 2017 Jul 24;28(16):1797–825.
67. Yeong WY, Chua CK, Leong KF, Chandrasekaran M. Rapid prototyping in tissue engineering: challenges and potential. *Trends in Biotechnology*. 2004 Dec;22(12):643–52.
68. Eltom A, Zhong G, Muhammad A. Scaffold Techniques and Designs in Tissue Engineering Functions and Purposes: A Review. *Advances in Materials Science and Engineering [Internet]*. 2019 Mar 7;2019:1–13. Available from: <https://www.hindawi.com/journals/amse/2019/3429527/>
69. Alaribe FN, Manoto SL, Motaung SCKM. Scaffolds from biomaterials: advantages and limitations in bone and tissue engineering. *Biologia*. 2016 Jan 1;71(4).
70. Smith JA, Mele E. Electrospinning and Additive Manufacturing: Adding Three-Dimensionality to Electrospun Scaffolds for Tissue Engineering. *Frontiers in Bioengineering and Biotechnology [Internet]*. 2021 Nov 30 [cited 2023 Mar 24];9:674738. Available from: <https://www.ncbi.nlm.nih.gov/pmc/articles/PMC8670169/>
71. Elsadek NE, Nagah A, Ibrahim TM, Chopra H, Ghonaim GA, Emam SE, et al. Electrospun Nanofibers Revisited: An Update on the Emerging Applications in Nanomedicine. *Materials [Internet]*. 2022 Jan 1;15(5):1934. Available from: <https://www.mdpi.com/1996-1944/15/5/1934>

72. Tomoyuki Kohgo, Yamada Y, Ito K, Yajima A, Yoshimi R, Okabe K, et al. Bone regeneration with self-assembling peptide nanofiber scaffolds in tissue engineering for osseointegration of dental implants. PubMed. 2011 Aug 13;31(4):e9-16.
73. Ikeda H, Yamaza T, Yoshinari M, Ohsaki Y, Ayukawa Y, Kido MA, et al. Ultrastructural and Immunoelectron Microscopic Studies of the Peri-Implant Epithelium-Implant (Ti-6Al-4V) Interface of Rat Maxilla. Journal of Periodontology. 2000 Jun;71(6):961–73.
74. Atieh MA, Alsabeeha NHM, Faggion CM, Duncan WJ. The Frequency of Peri-Implant Diseases: A Systematic Review and Meta-Analysis. Journal of Periodontology. 2012 Dec 13;1–15.
75. Albertini M, López-Cerero L, O'Sullivan MG, Chereguini CF, Ballesta S, Ríos V, et al. Assessment of periodontal and opportunistic flora in patients with peri-implantitis. Clinical Oral Implants Research. 2014 Apr 10;26(8):937–41.
76. Wang Y, Zhang Y, Miron RJ. Health, Maintenance, and Recovery of Soft Tissues around Implants. Clinical Implant Dentistry and Related Research. 2015 Apr 15;18(3):618–34.
77. Shibli J, Ivanovski S, Park YB, Alarcon M, KM C, Duncan W. Group D. Consensus report. Implants--peri-implant (hard and soft tissue) interactions in health and disease: the impact of explosion of implant manufacturers. PubMed. 2015 Jan 1;17(1 Suppl):71–3.
78. Ivanovski S, Lee R. Comparison of peri-implant and periodontal marginal soft tissues in health and disease. Periodontology 2000. 2017 Nov 30;76(1):116–30.

79. Lafaurie GI, Sabogal MA, Castillo DM, Rincón MV, Gómez LA, Lesmes YA, et al. Microbiome and Microbial Biofilm Profiles of Peri-Implantitis: A Systematic Review. *Journal of Periodontology*. 2017 Oct;88(10):1066–89.
80. Hatayama T, Nakada A, Nakamura H, Mariko W, Tsujimoto G, Nakamura T. Regeneration of gingival tissue using in situ tissue engineering with collagen scaffold. *Oral Surgery, Oral Medicine, Oral Pathology and Oral Radiology*. 2017 Oct;124(4):348-354.e1.
81. Makita R, Akasaka T, Tamagawa S, Yoshida Y, Miyata S, Miyaji H, et al. Preparation of micro/nanopatterned gelatins crosslinked with genipin for biocompatible dental implants. *Beilstein Journal of Nanotechnology*. 2018 Jun 11;9:1735–54.
82. Sharan J, Koul V, Dinda AK, Kharbanda OP, Lale SV, Duggal R, et al. Bio-functionalization of grade V titanium alloy with type I human collagen for enhancing and promoting human periodontal fibroblast cell adhesion – an in-vitro study. *Colloids and Surfaces B: Biointerfaces*. 2018 Jan;161:1–9.
83. Hameed HA, Ariffin A, Luddin N, Husein A. Evaluation of Antibacterial Properties of Copper Nanoparticles Surface Coating on Titanium Dental Implant. *Journal of Pharmaceutical Sciences and Research*. 2018 May;10(5):1157–60.
84. Dinh TN, Hou S, Park S, Shalek BA, Kyung Jae Jeong. Gelatin Hydrogel Combined with Polydopamine Coating To Enhance Tissue Integration of Medical Implants. *ACS Biomaterials Science & Engineering*. 2018 Sep 12;4(10):3471–7.
85. Jayanti Mendhi, Srinivas Sulugodu Ramachandra, Prasad I, Saso Ivanovski, Yang Y, Xiao Y. Endogenous nitric oxide-generating surfaces via

- polydopamine-copper coatings for preventing biofilm dispersal and promoting microbial killing. *Materials Science and Engineering: C*. 2021 Sep 1;128:112297–7.
86. Sánchez-Fernández E, Magán-Fernández A, O'Valle F, Bravo M, Mesa F. Hyaluronic acid reduces inflammation and crevicular fluid IL-1 β concentrations in peri-implantitis: a randomized controlled clinical trial. *Journal of Periodontal & Implant Science*. 2021;51(1):63.
 87. Lin J, He Y, He Y, Feng Y, Wang X, Yuan L, et al. Janus functional electrospun polyurethane fibrous membranes for periodontal tissue regeneration. *Journal of Materials Chemistry B*. 2023 Jan 1;
 88. C.W Brian Webb, Katya D'Costa, Tawagi E, Antonyshyn J, O.P Stefan Hofer, J Paul Santerre. Electrospun methacrylated natural/synthetic composite membranes for gingival tissue engineering. *Acta Biomaterialia*. 2024 Jan 1;173:336–50.
 89. Caton JG, Armitage G, Berglundh T, Chapple ILC, Jepsen S, Kornman KS, et al. A new classification scheme for periodontal and peri-implant diseases and conditions - Introduction and key changes from the 1999 classification. *Journal of Periodontology* [Internet]. 2018 Jun;89:S1–8. Available from: <https://aap.onlinelibrary.wiley.com/doi/full/10.1002/JPER.18-0157>
 90. Weinstein MP, Lewis JS. The Clinical and Laboratory Standards Institute Subcommittee on Antimicrobial Susceptibility Testing: Background, Organization, Functions, and Processes. Kraft CS, editor. *Journal of Clinical Microbiology*. 2020 Feb 24;58(3).
 91. Gristina Ag, Naylor P, Myrvik Q. Infections from biomaterials and implants: a race for the surface. *PubMed*. 1988 Jan 1;14(3-4):205–24.

92. Guruprakash Subbiahdoss, Grijpma DW, van, Busscher HJ, Roel Kuijer. Microbial biofilm growth versus tissue integration on biomaterials with different wettabilities and a polymer-brush coating. *Journal of Biomedical Materials Research Part A*. 2010 Feb 22;94A(2):533–8.
93. Mireia Hoyos-Nogués, Velasco F, Maria-Pau Ginebra, José María Manero, F. Javier Gil, Mas-Moruno C. Regenerating Bone via Multifunctional Coatings: The Blending of Cell Integration and Bacterial Inhibition Properties on the Surface of Biomaterials. *ACS Applied Materials & Interfaces*. 2017 Jun 21;9(26):21618–30.
94. Tesmer M, Wallet S, Koutouzis T, Lundgren T. Bacterial Colonization of the Dental Implant Fixture–Abutment Interface: An In Vitro Study. *Journal of Periodontology*. 2009 Dec;80(12):1991–7.
95. Kensara A, Saito H, Mongodin EF, Masri R. Microbiological profile of peri-implantitis: Analyses of microbiome within dental implants. *Journal of Prosthodontics*. 2023 Feb 10;
96. Tallarico M, Canullo L, Caneva M, Özcan M. Microbial colonization at the implant-abutment interface and its possible influence on periimplantitis: A systematic review and meta-analysis. *Journal of Prosthodontic Research*. 2017 Jul;61(3):233–41.
97. Passos SP, Gressler May L, Faria R, Özcan M, Bottino MA. Implant-abutment gap versus microbial colonization: Clinical significance based on a literature review. *Journal of Biomedical Materials Research Part B: Applied Biomaterials*. 2013 May 10;101(7):1321–8.
98. Koutouzis T, Gadalla H, Kettler Z, Elbarasi A, Nonhoff J. The Role of Chlorhexidine on Endotoxin Penetration to the Implant-Abutment Interface

- (IAI). Clinical Implant Dentistry and Related Research. 2013 Sep 23;17(3):476–82.
99. Escobar A, Muzzio N, Moya SE. Antibacterial Layer-by-Layer Coatings for Medical Implants. *Pharmaceutics*. 2020 Dec 24;13(1):16.
 100. Nakhaei K, Ishijima M, Ikeda T, Ghassemi A, Saruta J, Ogawa T. Ultraviolet Light Treatment of Titanium Enhances Attachment, Adhesion, and Retention of Human Oral Epithelial Cells via Decarbonization. *Materials*. 2020 Dec 31;14(1):151.
 101. Kurup A, Dhatrak P, Khasnis N. Surface modification techniques of titanium and titanium alloys for biomedical dental applications: A review. *Materials Today: Proceedings*. 2020 Jul;
 102. Zhou L, Li X, Wang K, Shen F, Zhang L, Li P, et al. CuII-loaded polydopamine coatings with in situ nitric oxide generation function for improved hemocompatibility. *Regenerative Biomaterials*. 2020 Jan 17;7(2):153–60.
 103. Crisan MC, Teodora M, Lucian M. Copper Nanoparticles: Synthesis and Characterization, Physiology, Toxicity and Antimicrobial Applications. *Applied Sciences*. 2021 Dec 24;12(1):141.
 104. Lutsenko S, Barnes NL, Bartee MY, Dmitriev OY. Function and Regulation of Human Copper-Transporting ATPases. *Physiological Reviews*. 2007 Jul;87(3):1011–46.
 105. Lai MJ, Huang YW, Chen HC, Tsao LI, Chih-Fang Chang Chien, Singh B, et al. Effect of Size and Concentration of Copper Nanoparticles on the Antimicrobial Activity in *Escherichia coli* through Multiple Mechanisms. *Nanomaterials*. 2022 Oct 22;12(21):3715–5.

106. Chen H, Zhang J, Wu H, Li Y, Li X, Zhang J, et al. Fabrication of a Cu Nanoparticles/Poly(ϵ -caprolactone)/Gelatin Fiber Membrane with Good Antibacterial Activity and Mechanical Property *via* Green Electrospinning. *ACS Applied Bio Materials*. 2021 Aug 1;4(8):6137–47.
107. Singh I, Dhawan G, Gupta S, Kumar P. Recent Advances in a Polydopamine-Mediated Antimicrobial Adhesion System. *Frontiers in Microbiology*. 2021 Jan 12;11.
108. Zamboni F, Wong CK, Collins MN. Hyaluronic acid association with bacterial, fungal and viral infections: Can hyaluronic acid be used as an antimicrobial polymer for biomedical and pharmaceutical applications? *Bioactive Materials*. 2023 Jan;19:458–73.
109. Wang Y, Zhang W, Yao Q. Copper-based biomaterials for bone and cartilage tissue engineering. *Journal of Orthopaedic Translation* [Internet]. 2021 Jul;29:60–71. Available from: <https://www.ncbi.nlm.nih.gov/pmc/articles/PMC8164005/>
110. Davidenko N, Schuster CF, Bax DV, Farndale RW, Hamaia S, Best SM, et al. Evaluation of cell binding to collagen and gelatin: a study of the effect of 2D and 3D architecture and surface chemistry. *Journal of Materials Science: Materials in Medicine*. 2016 Aug 31;27(10).
111. Jawad A. *Dental implantology and biomaterial*. Rijeka, Croatia: Intech; 2016.
112. Halake K, Kim HJ, Birajdar M, Kim BS, Bae H, Lee C, et al. Recently developed applications for natural hydrophilic polymers. *Journal of Industrial and Engineering Chemistry*. 2016 Aug;40:16–22.
113. Bazmandeh AZ, Mirzaei E, Fadaie M, Shirian S, Ghasemi Y. Dual spinneret electrospun nanofibrous/gel structure of chitosan-gelatin/chitosan-hyaluronic

- acid as a wound dressing: In-vitro and in-vivo studies. *International Journal of Biological Macromolecules*. 2020 Nov;162:359–73.
114. Loh QL, Choong C. Three-Dimensional Scaffolds for Tissue Engineering Applications: Role of Porosity and Pore Size. *Tissue Engineering Part B: Reviews* [Internet]. 2013 Dec;19(6):485–502. Available from: <https://www.ncbi.nlm.nih.gov/pmc/articles/PMC3826579/>
 115. Bai H, Wang D, Delattre B, Gao W, J. De Coninck, Li S, et al. Biomimetic gradient scaffold from ice-templating for self-seeding of cells with capillary effect. *Acta Biomaterialia*. 2015 Jul 1;20:113–9.
 116. Chen G, Ushida T, Tateishi T. Scaffold Design for Tissue Engineering. *Macromolecular Bioscience*. 2002 Feb 1;2(2):67–77.
 117. Bružauskaitė I, Bironaitė D, Bagdonas E, Bernotienė E. Scaffolds and cells for tissue regeneration: different scaffold pore sizes—different cell effects. *Cytotechnology*. 2015 Jun 20;68(3):355–69.
 118. Lukin I, Erezuma I, Maeso L, Zarate J, Desimone MF, Al-Tel TH, et al. Progress in Gelatin as Biomaterial for Tissue Engineering. *Pharmaceutics*. 2022 May 31;14(6):1177.
 119. Lee J, Kim D, Jang CH, Kim GH. Highly elastic 3D-printed gelatin/HA/placental-extract scaffolds for bone tissue engineering. *Theranostics*. 2022;12(9):4051–66.
 120. Takuro Hozumi, Kageyama T, Ohta S, Fukuda J, Ito T. Injectable Hydrogel with Slow Degradability Composed of Gelatin and Hyaluronic Acid Cross-Linked by Schiff's Base Formation. *Biomacromolecules*. 2018 Jan 18;19(2):288–97.

121. Abatangelo G, Vindigni V, Avruscio G, Pandis L, Brun P. Hyaluronic Acid: Redefining Its Role. *Cells* [Internet]. 2020 Jul 1;9(7):1743. Available from: <https://www.mdpi.com/2073-4409/9/7/1743>
122. Alfieri ML, Weil T, Ng DYW, Ball V. Polydopamine at biological interfaces. *Advances in Colloid and Interface Science*. 2022 Jul;305:102689.

A.B. SHETTY MEMORIAL INSTITUTE OF DENTAL SCIENCES**DEPARTMENT OF PERIODONTICS**

STUDY TITLE- FABRICATION AND EVALUATION OF A NOVEL BI-LAYER TISSUE ENGINEERED SCAFFOLD FOR IMPROVED BIO SEAL AND ANTIMICROBIAL PROPERTIES OF DENTAL IMPLANTS: AN IN VITRO STUDY

CASE SHEET

Name:

Case no:

Age:

Date:

Gender:

Address:

Education:

Marital status:

Occupation:

Height:

Weight:

Medical history:

- a. Systemic diseases:
- b. Menopause:

Personal history:

1. Oral hygiene practices –
 - a. Type:
 - b. Frequency:
 - c. Method:
2. History of smoking:
3. Diet:

Intraoral examination:

1. Tongue:
2. Palate:
3. Buccal mucosa:

Probing depth

[illegible]

Clinical attachment loss

[illegible]

PISA SCORE

	tooth	18	17	16	15	14	13	12	11	21	22	23	24	25	26	27	28	tooth	
³PD	buccal palatal																	buccal palatal	PPD
³PD	lingual buccal tooth																	lingual buccal tooth	PPD
		48	47	46	45	44	43	42	41	31	32	33	34	35	36	37	38		

tooth	18	17	16	15	14	13	12	11	21	22	23	24	25	26	27	28	tooth
surface area (mm ²)	0	0.0000	0.0000	0.0000	0.0000	0.0000	0.0000	0.0000	0.0000	0.0000	0.0000	0.0000	0.0000	0.0000	0.0000	0	surface area (mm ²)
surface area (mm ²)	0	0.0000	0.0000	0.0000	0.0000	0.0000	0.0000	0.0000	0.0000	0.0000	0.0000	0.0000	0.0000	0.0000	0.0000	0	surface area (mm ²)
tooth	48	47	46	45	44	43	42	41	31	32	33	34	35	36	37	38	tooth

tooth	PESA	nr of sites with BOP	PISA (mm2)
18	0		0.00
17	0		0.00
16	0		0.00
15	0		0.00
14	0		0.00
13	0		0.00
12	0		0.00
11	0		0.00
21	0		0.00
22	0		0.00
23	0		0.00
24	0		0.00
25	0		0.00
26	0		0.00
27	0		0.00
28	0		0.00

tooth	PESA	nr of sites with BOP	PISA (mm2)
38	0		0.00
37	0		0.00
36	0		0.00
35	0		0.00
34	0		0.00
33	0		0.00
32	0		0.00
31	0		0.00
41	0		0.00
42	0		0.00
43	0		0.00
44	0		0.00
45	0		0.00
46	0		0.00
47	0		0.00
48	0		0.00

Total Periodontal Epithelial Surface Area (mm2)
0.0

Total Periodontal Inflamed Surface Area (mm2)
0.0



A B SHETTY MEMORIAL INSTITUTE OF DENTAL SCIENCES

INSTITUTIONAL ETHICAL COMMITTEE

CHAIRPERSON

Prof. (Dr.) Laxmikanth Chatra
Department of Oral Medicine & Radiology
Yenepoya Dental College, Mangalore

MEMBER SECRETARY

Prof. Dr. Amarshree A Shetty
Associate Dean, Student Welfare
Dept. of Pediatric & Preventive Dentistry.

MEMBERS

Prof. (Dr.) U. S. Krishna Nayak
Principal & Dean

Prof. (Dr.) Chethan Hegde
HOD, Prosthodontics and Crown and Bridge

Prof. (Dr.) Manoj Shetty
HOD, Oral Implantology

Prof. (Dr.) Pushparaj Shetty
HOD, Oral & Maxillofacial Pathology
and Oral Medicine

Prof. Dr R. Narayana Charyulu
Vice Principal, Nitte Gulabi Shetty Memorial
Institute of Pharmaceutical Sciences

Prof. (Dr.) Vijaya Hegde
HOD, Public Health Dentistry,
A.J. Institute of Dental Sciences

Dr. Aniban Chakraborty
Deputy Director, Nitte University Centre for
Science Education and Research

Prof. (Dr.) Audrey Madonna D'cruz
HOD, Public Health Dentistry

Dr. Tripti Shetty
Reader, Oral & Maxillofacial Surgery

Dr. Vivek Nambiar
Lawyer

Mrs. Judith Shaila Lobo
Regional Operations Manager,
Indian Cancer Society

Mr. Ramdas Aithal
Priest, Karkala

Ref. No. ETHICS/ABSMIDS/250/2022

Date: 22.04.2022

To,

Dr. Geethu Venugopalan, Principal Investigator,
Department of Periodontics
A B Shetty Memorial Institute of Dental Sciences.

Dear Dr. Geethu Venugopalan,

**Ref : Fabrication and evaluation of a Novel BI-Layer Tissue -
Engineered Scaffold for improved Bio Seal and Antimicrobial
Properties of Dental Implants : An in vitro study.**

At the ethics Committee meeting held on 14th April 2022 where your study
was discussed, the Committee has decided to **Approve and Grant Ethical
Clearance** for the study to be carried out by the Principal Investigator at
A B Shetty Memorial Institute of Dental Sciences, Deralakatte, Mangalore.

Yours Truly,

Prof. Dr. Amarshree A Shetty

MEMBER SECRETARY
INSTITUTIONAL ETHICAL COMMITTEE
ABSMIDS

Ph: 0824 2204572 - 267. Fax: 0824 2204776
E-mail: ethics.absmids@nitte.edu.in
Website: www.nitte.ac.in



DISSERTATION SYNOPSIS

DR. GEETHU VENUGOPALAN
(NU21DPER04)

DEPARTMENT OF PERIODONTICS



**A B SHETTY MEMORIAL
INSTITUTE OF DENTAL SCIENCES**

A.B SHETTY MEMORIAL INSTITUTE OF DENTAL SCIENCES
(A constituent of college of Nitte University)

NITTE
(DEEMED TO BE UNIVERSITY)

Estb. under section 3, UGC Act, 1956

(Placed under category 'A' by MHRD, Govt. of India,

Accredited as 'A⁺⁺' Grade University by NAAC)

MANGALURU, KARNATAKA, INDIA-575018

ANNEXURE-II**PROFORMA FOR REGISTRATION OF SUBJECTS FOR DISSERTATION**

1.	Name of the candidate and Address (in block letters)	DR. GEETHU VENUGOPALAN POSTGRADUATE STUDENT DEPARTMENT OF PERIODONTICS A.B. SHETTY MEMORIAL INSTITUTE OF DENTAL SCIENCES DERALAKATTE, MANGALURU - 575018
2.	Name of the institution	A.B. SHETTY MEMORIAL INSTITUTE OF DENTAL SCIENCES NITYANANDA NAGAR POST DERALAKATTE, MANGALURU- 575018
3.	Course of the study and subject	MASTER OF DENTAL SURGERY-PERIODONTICS
4.	Date of admission of course	05 November 2021
5.	Title FABRICATION AND EVALUATION OF A NOVEL BI-LAYER TISSUE ENGINEERED SCAFFOLD FOR IMPROVED BIO SEAL AND ANTIMICROBIAL PROPERTIES OF DENTAL IMPLANTS: AN IN VITRO STUDY	

6.	BRIEF RESUME OF THE INTENDED STUDY
6.1	<p data-bbox="339 293 691 327">NEED FOR THE STUDY</p> <p data-bbox="339 360 1455 533">Peri-implantitis is a pathological condition occurring in tissues around dental implants, characterized by inflammation in the peri-implant connective tissue with progressive loss of supporting bone around an osseointegrated functional implant. It has been considered a major risk factor for the late failure of dental implants. ^[1-3]</p> <p data-bbox="339 544 1455 674">The prevention of peri-implant disease involves preventing the occurrence of peri-implant mucositis and its conversion to further stages of peri-implant disease, leading to implant failure ^[4]. The prevalence rate of peri-mucositis ranges from 19 to 65% and around 1 to 47% for peri-implantitis. ^[5]</p> <p data-bbox="339 701 1455 965">The term ‘biological seal’ refers to the soft tissue around a dental implant, which provides an essential physiological and biological barrier from the external environment. ^[6,7] However, ultrastructural studies have shown that solid epithelial attachments are present only in the lower one-third of an implant-mucosal junction, thereby compromising its strength and integrity and making it prone to bacterial ingress. ^[4,6] Insufficient soft tissue attachment and the direction of gingival fibres as compared to a natural tooth results in compromised biological properties ^[3,4,6]</p> <p data-bbox="339 992 1455 1122">In recent years, investigations into the soft tissue responses to oral implant surfaces have shown that the physicochemical properties of implant materials can significantly influence the quality of soft tissue seals. ^(4,8,9,10)</p> <p data-bbox="339 1133 1455 1352">A biocompatible scaffold may be constructed using tissue engineering to allow cell adhesion and promote cell proliferation and differentiation without triggering inflammatory reactions or rejection by the body, resulting in an enhanced soft-tissue response. Tissue engineering approaches have been developed to enhance regeneration via micro-engineered topographical features, purposely designed to guide the insertion of the regenerated ligament to the root surface. ^[8,10,11,12]</p> <p data-bbox="339 1406 1455 1671">Ultimately, the outcome of an implant depends on the so-called “race for the surface” between the integration of tissue and bacterial growth on the implant surface. ^[13] Therefore, the most effective strategy to combat periimplantitis would be a prevention of biofilm formation on the implant material and provide an environment that promotes native cell proliferation. Systemic antibiotics are commonly used for this purpose in practice. ^[13,14,15] However, the risk of systemic toxicity and microbial resistance has led to the search for alternatives, such as antimicrobial metal nanoparticles (NPs) ^[15]</p>

	<p>Therefore, this study aims to fabricate a bilayer tissue-engineered scaffold and assess its effect on enhancing the proliferation and attachment of soft tissue cells to Titanium implants, with increased angiogenesis, reduced edema, and anti-bacterial colonization to provide biologically stable and aesthetically well-appearing implants.</p>
--	--

7. REVIEW OF LITERATURE

1. Michele Iafisco *et al.* in 2012 researched the effect of Electrospun Nanostructured Fibers of Collagen-Biomimetic Apatite on Titanium Alloy. The characterization results showed that the obtained mineralized scaffolds have morphological, structural, and chemical compositional features similar to the natural bone extracellular matrix. ^[16]
2. Matteo Albertini *et al.*, in 2015 assessed periodontal and opportunistic flora in patients with peri-implantitis and identified periodontal and opportunistic flora in patients with peri-implantitis including the presence of *Pseudomonas aeruginosa*, *Candida albicans*, *Staphylococcus aureus*, and *Staphylococcus warneri*. ^[17]
3. Jitendra Sharan *et al.*, in 2018 studied the effect of Bio-functionalization of grade V titanium alloy with type I human collagen for enhancing and promoting human periodontal fibroblast cell adhesion and concluded that bio-functionalization help improves cell growth and in turn formation of soft tissue gingival seal-like structure. ^[18]
4. Shirin Mahmoodi *et al.*, in 2018 studied the antibacterial activity of copper nanoparticles and concluded that the copper nanoparticles possess potent antimicrobial activities and can be used for controlling and treating different infectious diseases in the future. ^[19]
5. Thanh Dinh, *et al.*, in 2018 studied Gelatin Hydrogel Combined with Polydopamine Coating to Enhance Tissue Integration of Medical Implants and concluded that a combination of PDA coating with gelatin hydrogel can be used to enhance the integration of various medical implants. ^[20]
6. Jayanti Mendhi *et al.*, in 2021 studied Endogenous nitric oxide-generating surfaces via polydopamine-copper coatings for preventing biofilm dispersal and promoting microbial killing and concluded that PDAM@Cu coatings with NO generating surfaces have a dual anti-biofilm function, with a synergistic effect on biofilm dispersal from regulated NO generation and bactericidal effects from Cu ions from the coatings. ^[21]

8.	AIM AND OBJECTIVES
8.1	<p><u>AIM</u></p> <p>Fabrication and characterization of a bilayer tissue-engineered scaffold incorporating Polydopamine and Gelatin-hyaluronic acid-copper nanofibers, for enhanced bio seal and antimicrobial properties of dental implants</p>
8.2	<p><u>OBJECTIVES</u></p> <ol style="list-style-type: none"> 1. To synthesize and characterize a tissue-engineered bi-layer scaffold containing polydopamine and Copper nanoparticle embedded Gelatin-Hyaluronic acid electrospun mat. 2. To evaluate the cell proliferation, attachment, and cytotoxicity of this tissue-engineered bilayer scaffold against gingival fibroblasts 3. To investigate the antimicrobial efficacy of the tissue-engineered bilayer scaffold coated titanium Dental implant surface
8.3	<p><u>NULL HYPOTHESIS (H₀):</u></p> <p>The biomodification of the surface of Grade V titanium alloy with tissue-engineered bi-layer scaffold does not improve cell proliferation and attachment at the implant site and promotes microbial activity, resulting in an incomplete implant bio-seal.</p>
8.4	<p><u>ALTERNATE HYPOTHESIS (H₁):</u></p> <p>The biomodification of Grade V titanium alloy surface with bilayer tissue engineered scaffold enhances cell proliferation and attachment at the implant site while providing anti-microbial action, thereby improving the peri-implant mucosal seal.</p>

9.	MATERIALS AND METHODS
9.1	<p data-bbox="352 387 1345 461"><u>SAMPLE COLLECTION FOR THE DEVELOPMENT OF A GINGIVAL FIBROBLAST CELL LINE</u></p> <p data-bbox="352 517 1418 678">Gingival tissue samples (n = 3) will be collected from periodontally and systemically healthy subjects reporting to the Department of Periodontics, A.B. Shetty Memorial Institute of Dental Sciences, undergoing Premolar extraction as a part of orthodontic treatment or crown lengthening procedure after obtaining their consent.</p> <p data-bbox="352 734 550 763">Inclusion criteria:</p> <ol data-bbox="352 779 1418 1025" style="list-style-type: none"> 1. Periodontally healthy patients with probing depth $\leq 3\text{mm}$, with no clinical attachment loss and $<10\%$ bleeding sites.* 2. Patients undergoing therapeutic extraction of premolars for orthodontic purposes or undergoing crown lengthening procedures. 3. Systemically healthy individuals. 4. 18-40 years of age. <p data-bbox="352 1066 1418 1140">*(Classified based on the 2017 world workshop on the classification of periodontal and peri-implant diseases and conditions.)</p> <p data-bbox="352 1196 555 1225">Exclusion criteria:</p> <ol data-bbox="391 1281 1054 1442" style="list-style-type: none"> 1. Gingivitis/periodontitis patients with probing depth $> 3\text{mm}$. 2. Systemically compromised patients. 3. Pregnant and lactating women. 4. Patients under antibiotic drug therapy.

9.2	FABRICATION OF THE BILAYER SCAFFOLD
9.2.1	<p><u>PREPARATION OF MODIFIED TI ALLOY DISCS</u></p> <p>Grade V medical alloy (Ti6Al4V) discs (10 × 2 mm) will be used as a Titanium dental implant prototype in the study. Sequential polishing of the discs shall be performed using 200 to 2,000 grit SiC abrasive sheets and 1-micron oil-based diamond paste, to mimic the smooth surface of the neck of the implant and to provide a homogeneous surface for reactions.</p> <p>Ti disks will be ultrasonically cleaned stepwise using acetone, ethanol, and deionized water</p> <p>Cleaned disks will then be air-dried and stored in a desiccator</p>
9.2.2	<p><u>POLYDOPAMINE COATING TREATMENT</u></p> <p>Polydopamine (PDAM) can bind strongly to virtually all substrates and provide secondary reactivity for conjugating biomolecules. The polydopamine coating strategy can assist in cell attachment and proliferation additionally. ^[22,23]</p> <p>To prepare the polydopamine coating solution, Dopamine HCl will be dissolved in 10 mM-Tris buffer at the ratio of 1 mg Dopamine HCl : 1 mL Tris buffer, followed by adjustment of the pH to 8.5. The cleaned Ti disks will then be soaked in the dopamine/Tris buffer solution for 24 hours.</p> <p>The PDA-coated Ti substrates (Ti-PDA) will be collected and ultrasonically cleaned using deionized water and then air-dried at room temperature.</p>
9.2.3	<p><u>SYNTHESIS OF GE/HA/CU ELECTROSPUN MAT</u></p> <p>Hyaluronic acid (HA) is known to participate in many biological responses, including angiogenesis, cell adhesion, proliferation, and differentiation, by binding with surface receptors of target cells. ^[24,25] Gelatin in the scaffold can mimic RGD bio signaling and provide a site for cell attachment, causing myofibroblasts to migrate, and get recruited at the healing site. ^[26,27] The presence of copper nanoparticles can regulate endogenous NO generation, leading to a significant reduction in biofilm metabolic activity, viability, thickness, and attachment. Along with this, copper itself allows for antimicrobial action on the dispersed bacteria resulting in effective biofilm control and anti-microbial activity. ^[28,29,30]</p> <p>An electrospinning method will be utilized to prepare GE/HA/Cu nanofibrous scaffolds.</p> <p>Pure Gelatin (type A) and Hyaluronic acid (Sodium salt) will be blended with a weight ratio (GE/HA: 6: 4). This solution shall then be dissolved in 2,2,2- trifluoroethanol (TFE)/water (1: 1; v/v) solvents with the Copper Nanoparticles [CuNP] at room temperature, with constant stirring to expedite dissolution and to obtain a homogeneous solution. The solution will then be sonicated for 15 minutes and loaded into a 5mL syringe for electrospinning. The electrospun nanofibers will be collected onto the polydopamine coated Ti alloy disc. The study proposes the use of 1 wt % glutaraldehyde (GTA/ethanol) for a time</p>

period of 30 minutes in a closed chamber for crosslinking, after which the samples will be placed in a laminar airflow overnight to remove residual GTA vapors. The prepared samples will then be immersed in a 1-M glycine solution for 1 hour to quench the residual aldehyde groups.

Although glutaraldehyde provides good improvement in mechanical properties, contradictory evidence has been provided on the cytotoxicity of glutaraldehyde-crosslinked materials. Nevertheless, cytotoxicity of glutaraldehyde is dependent on the concentration used, and up to 8% glutaraldehyde was shown to be non-cytotoxic.^[31] Furthermore, since GTA toxicity seems to be related to its release from the material, it is important to point out that no GTA release has been determined from films submitted to crosslinking up to a GTA concentration of 1.5 wt%.^[32]

However, alternative strategies for crosslinking the scaffold may be used if cytotoxicity to glutaraldehyde vapors is established during the course of the study. Alternative strategies would include adopting either one of the approaches listed below.

1. 1-Ethyl-3-(3-dimethyl aminopropyl) carbodiimide hydrochloride (EDC) and N-hydroxy succinimide (NHS): The biomodified Ti disc with the bilayer scaffold will be immersed into the crosslinking medium containing EDC/NHS (50mM/50mM) at 4°C and kept for 24 hours to fulfill the crosslinking reactions. After crosslinking, the crosslinked membranes will be washed with water and ethanol three times, and shall then be dried in a vacuum at room temperature for three days to remove the residual solvents.
2. Ammonium carbonate: The biomodified Ti disc with the bilayer scaffold will be placed in a sealed desiccator containing ~5 g of (NH₄)₂CO₃ powder for 24 h. the crosslinked mats will then be vacuum dried for 24 h and used for further studies.

9.3	CHARACTERIZATION OF THE BILAYER SCAFFOLD
	<p>Scanning Electron Microscopy (SEM)</p> <p>The morphology of the electrospun nanofibers will be studied by scanning electron microscopy (SEM) equipped with image analyser software at an accelerating voltage of 20 kV.</p> <p>The diameter, diameter distribution, and uniformity will be measured with an image analyser software.</p> <p>Fourier-transform infrared spectroscopy</p> <p>FTIR spectra will be recorded using a Fourier transform infrared (FTIR) spectrometer to determine the surface composition of the mats. The functional groups formed and the nature of bonding on Ti alloy discs before and after surface modifications will be determined by this method.</p>
9.4	CELL CULTURE OF HUMAN GINGIVAL FIBROBLASTS:
	<p>Gingival fibroblasts will be established and cultured in DMEM (Dulbecco's Modified Eagle's Medium) supplemented with 10% fetal bovine serum, 100 ug/ml penicillin, 100 mg/ml streptomycin, in a 5% CO₂ at 37°C. Cultured cells will then be harvested by treating them with 0.25% trypsin-0.025% EDTA in phosphate-buffered saline (PBS). The subculture of gingival fibroblasts shall be carried out once a week with a 1:4 ratio and medium change between the sub-cultures.</p>
9.5	CYTOTOXICITY AND CELL PROLIFERATION
	<p><u>Cytotoxicity assay:</u></p> <p>MTT (3-(4,5-dimethylthiazol-2-yl)-2,5-diphenyltetrazolium bromide) assay is measured by dehydrogenase activity to monitor the cell viability. A human gingival fibroblast cell line will be used to evaluate the biocompatibility of the coating.</p> <p>Cells will be cultured in Dulbecco's Modified Eagle medium (DMEM) with 10% FBS and 1% penicillin-streptomycin in an incubator at 37°C and 5% CO₂. Ti alloy discs sterilized by gamma irradiation shall then be placed in a 24- well microtiter plates. Each disc will be incubated with 1×10^4 cells counted on a hemocytometer at 24 hours, and 72 hours.</p> <p>After incubation, 5mg/ml MTT reagent will be added to each well and allowed to react for 2 hrs. After pipetting off the reagent, the violet formazan product will be dissolved in 0.2mL dimethyl sulfoxide for 10 minutes at room temperature. The solution shall then be transferred to a 96-well microtiter plate, and the optical density (OD) at 570 nm will be measured.</p>

	<p>A minimum of triplicates will be performed for each study group i.e. :</p> <p>Control Group (CG): Uncoated Ti alloy disc</p> <p>Study Group (SG): Tissue-engineered Polydopamine- Gel/HA/Cu scaffold coated Ti alloy disc</p> <p><u>Cell proliferation</u></p> <p>Human gingival fibroblast cells will be seeded on the substrates (Control Group: Uncoated Ti alloy disc and Study Group: Tissue-engineered Polydopamine- Gel/HA/Cu scaffold coated Ti alloy disc) at a density of 4000 cells/cm² in a 24 well culture plate. The number of cells adhered will be counted using hemocytometers equipped with improved Neubauer grids at the end of 12, 24, 48, and 72 hours.</p>
9.6	ANTIMICROBIAL EVALUATION
	<p>The antibacterial effect CuNPs will be assessed using broth dilution and serial dilution plate methods. The minimum inhibitory concentrations (MICs) of CuNPs will be calculated for two reference standard microbial cultures, S.aureus (ATCC-29213) and P. aeruginosa (ATCC 27853). Bacterial cultures will be individually streaked on nutrient agar (NA) slants and set at 0.5 McFarland using a densitometer to determine the final concentration. All cultures shall be subject to validation by the plate count method and adjusted to achieve 1×10^8 CFU/mL. Colony counts will be taken at time point 0 hours initially, thereafter at 4, 24, and 48 hours.</p> <p>The gamma sterilized, disc-shaped samples will be placed on Mueller Hinton agar plates and incubated at $37^\circ\text{C} \pm 2^\circ\text{C}$ for 48 hours. The absence of bacterial colonies around the scaffold will be measured by the “zone of inhibition” at a time of 48 hours and shall be taken as the measure of antimicrobial activity of the scaffold. Each of the assays will be done in triplicates.</p>
10.	STATISTICAL ANALYSIS:
	<p>Data will be entered in Microsoft excel Software and analyzed using SPSS Statistics Software version 22.</p> <p>The cell proliferation will be measured as n and expressed as percentages. The comparison of the increase in the proportion of cells between the two groups will be done using the Chi-Squared test.</p> <p>The cytotoxicity will be measured by counting the number of dead/viable fibroblasts. The cytotoxicity will be compared using the Chi-squared test. The mean number of viable cells will be compared using a t-test.</p> <p>The antimicrobial efficiency will be measured using “ Zone of Inhibition” and a cut-off will be constructed for each material at specific time points of time 0,4,24 and 48 hours.</p> <p>A receiver operating curve will be constructed for each material and their respective area under the curve (AUC) will be calculated. AUCs at various time will be compared between the two materials.</p>


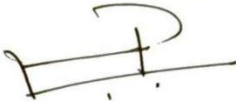



11.	<p>1. Does the study require any investigations or interventions to be conducted on patients or other humans or animals?</p> <p>Yes, the study requires gingival tissue samples from healthy patients.</p> <p>2. Does the study require any ethical clearance?</p> <p>Yes, Ethical clearance has been granted.</p>
12.	RESEARCH GAPS
	<p>A fundamental part of dental implant integration, namely developing a soft tissue seal around the implant, is often overlooked. There is a lack of a comprehensive approach to healing that includes coagulation, decreased inflammation, cell proliferation, increased soft tissue attachment, bacterial attachment prevention, and biofilm creation, all of which are important phases in implant integration.</p> <p>There is currently no micro or macrostructural surface modifications that will support perpendicularly directed collagen attachment. In addition, most of the studies incorporate silver nanoparticles for an antimicrobial effect. Several research and reports, however, imply that silver nanoparticles can have negative impacts on individuals and the environment.</p>
13.	NOVELTY
	<p>The Polydopamine and Gelatin-Hyaluronic acid-Copper nanofiber scaffold can mimic both the form and functionality of the native ECM with increased stability. They will have appropriate porosities to guide cellular migration and penetration by perpendicular connective tissue attachment at the implant/abutment interface similar to natural teeth. The scaffold will have sufficient surface area and the proper surface chemistry to promote cell adhesion, growth, migration, and differentiation; and a rate of degradation that closely matches the rate of native tissue regeneration to promote proper tissue ingrowth.</p> <p>The use of copper nanoparticles for their broad-spectrum antimicrobial and capacity to cross-link collagen. Copper is found to be generally less toxic and more biocompatible than other metals.</p>

12. REFERENCES

1. Sakka S, Coulthard PJMOPOCB. Implant failure: etiology and complications. 2011;16(1):e42-4
2. Mombelli A, Lang NP. The diagnosis and treatment of peri-implantitis. *Periodontology* 2000. 1998 Jun;17(1):63-76\
3. Schwarz F, Derks J, Monje A, Wang HL. Peri-implantitis. *Journal of clinical periodontology*. 2018 Jun;45:S246-66.
4. Wang Y, Zhang Y, Miron RJ. Health, maintenance, and recovery of soft tissues around implants. *Clinical implant dentistry and related research*. 2016;18(3):618-34.
5. Jepsen S, Berglundh T, Genco R, Aass AM, Demirel K, Derks J, et al. Primary prevention of peri-implantitis: Managing peri-implant mucositis. 2015;42(S16):S152-S7.
6. Yamaza T, Kido MA. Biological sealing and defense mechanisms in peri-implant mucosa of dental implants. *Implant Dentistry-The Most Promising Discipline of Dentistry*. London, UK: Intech Open. 2011 ct 3:219-42.
7. Alva H, Prasad KD, Prasad AD. Bioseal: The physiological and biological barrier for an osseointegrated supported prosthesis. *Journal of Dental Implants*. 2013 Jul 1;3(2):148.
8. Salvi GE, Bosshardt DD, Lang NP, Abrahamsson I, Berglundh T, Lindhe J, et al. Temporal sequence of hard and soft tissue healing around titanium dental implants. *Periodontology* 2000. 2015;68(1):135-52
9. Newman MG, Takei H, Klokkevold PR. Carranza's Clinical Periodontology: Elsevier Health Sciences; 2014.
10. Hosoyama K, Lazurko C, Muñoz M, McTiernan CD, Alarcon EI. Peptide-based functional biomaterials for soft-tissue repair. *Frontiers in Bioengineering and Biotechnology*. 2019:205.
11. Staples RJ, Ivanovski S, Vaquette C. Fibre guiding scaffolds for periodontal tissue engineering. *Journal of periodontal research*. 2020 Jun;55(3):331-41.
12. Ceccarelli G, Presta R, Benedetti L, Casella De Angelis MG, Lupi SM, Rodriguez y Baena R. Emerging perspectives in scaffold for tissue engineering in oral surgery. *Stem Cells International*. 2017 Oct;2017.
13. **Guo T, Gulati K, Arora H, Han P, Fournier B, Ivanovski S. Race to invade: Understanding soft tissue integration at the transmucosal region of titanium dental implants. *Dental Materials*. 2021 May 1;37(5):816-31**
14. Esposito M, Grusovin MG, Worthington HV. Interventions for replacing missing teeth: antibiotics at dental implant placement to prevent complications. *Cochrane Database Syst Rev*. 2013(7):CD004152
15. Grischke J, Eberhard J, Stiesch M. Antimicrobial dental implant functionalisation strategies -A systematic review. *Dent Mater J*. 2016;35(4):545-558.
16. Iafisco M, Foltran I, Sabbatini S, Tosi G, Roveri N. Electrospun nanostructured fibers of collagen-biomimetic apatite on titanium alloy. *Bioinorganic chemistry and Applications*. 2012 Jan 1;2012.

17. Albertini M, López-Cerero L, O'Sullivan MG, Chereguini CF, Ballesta S, Ríos V, Herrero-Climent M, Bullón P. Assessment of periodontal and opportunistic flora in patients with peri-implantitis. *Clinical oral implants research*. 2015 Aug;26(8):937-41.
18. Sharan, J., Koul, V., Dinda, A.K., Kharbanda, O.P., Lale, S.V., Duggal, R., Mishra, M., Gupta, G. and Singh, M.P., 2018. Bio-functionalization of grade V titanium alloy with type I human collagen for enhancing and promoting human periodontal fibroblast cell adhesion—an in-vitro study. *Colloids and Surfaces B: Biointerfaces*, 161, pp.1-9.
19. Mahmoodi S, Elmi A, Hallaj-Nezhadi S. Copper nanoparticles as antibacterial agents. *J. Mol. Pharm. Org. Process. Res.* 2018;6(1):140.
20. Dinh TN, Hou S, Park S, Shalek BA, Jeong KJ. Gelatin hydrogel combined with polydopamine coating to enhance tissue integration of medical implants. *ACS biomaterials science & engineering*. 2018 Sep 12;4(10):3471-7.
21. Mendhi J, Ramachandra SS, Prasadani I, Ivanovski S, Yang Y, Xiao Y. Endogenous nitric oxide-generating surfaces via polydopamine-copper coatings for preventing biofilm dispersal and promoting microbial killing. *Materials Science and Engineering: C*. 2021 Sep 1;128:112297.
22. Lee H, Dellatore SM, Miller WM, Messersmith PB. Mussel-inspired surface chemistry for multifunctional coatings. *Science*. 2007;318(5849):426-30.
23. Zhang S, Xu K, Darabi MA, Yuan Q, Xing M. Mussel-inspired alginate gel promoting the osteogenic differentiation of mesenchymal stem cells and antiinfection. *Mater Sci Eng C Mater Biol Appl*. 2016;69:496-504.
24. Xing F, Zhou C, Hui D, Du C, Wu L, Wang L, Wang W, Pu X, Gu L, Liu L, Xiang Z. Hyaluronic acid as a bioactive component for bone tissue regeneration: Fabrication, modification, properties, and biological functions. *Nanotechnology Reviews*. 2020 Jan 1;9(1):1059-79
25. Cooper CA, Brown KK, Meletis CD, Zabriskie N. Inflammation and hyaluronic acid. *Alternative & complementary therapies*. 2008 Apr 1;14(2):78-84.
26. Altomare L, Bonetti L, Campiglio CE, De Nardo L, Draghi L, Tana F, Farè S. Biopolymer-based strategies in the design of smart medical devices and artificial organs. *The International Journal of Artificial Organs*. 2018 Jun;41(6):337-59.
27. Mathur A, Kharbanda OP, Koul V, Dinda AK, Anwar MF, Singh S. Fabrication and evaluation of antimicrobial biomimetic nanofiber coating for improved dental implant bioseal: An in vitro study. *Journal of periodontology*. 2021 Dec 2.
28. Giannousi K, Pantazaki A, Dendrinou-Samara C. Copper-based nanoparticles as antimicrobials. In *Nanostructures for Antimicrobial Therapy* 2017 Jan 1 (pp. 515-529). Elsevier.
29. Mendhi JA. Polydopamine-copper coatings for soft tissue regeneration and infection prevention in dental implants (Doctoral dissertation, Queensland University of Technology)
30. Mahmoodi S, Elmi A, Hallaj-Nezhadi S. Copper nanoparticles as antibacterial agents. *J. Mol. Pharm. Org. Process. Res.* 2018;6(1):140.

- | | |
|--|--|
| | <p>31. Reddy N, Reddy R, Jiang Q. Crosslinking biopolymers for biomedical applications. Trends in biotechnology. 2015 Jun 1;33(6):362-9.</p> <p>32. Bigi A, Cojazzi G, Panzavolta S, Rubini K, Roveri N. Mechanical and thermal properties of gelatin films at different degrees of glutaraldehyde crosslinking. Biomaterials. 2001 Apr 1;22(8):763-8.</p> |
|--|--|

13.	Signature of the candidate	
14	Remarks of the guide	<i>Satisfactory</i>
15	Name and designation of:	
15.1	Guide (In block letter)	PROF. (DR.) RAHUL BHANDARY PROFESSOR-DEPARTMENT OF PERIODONTICS A.B SHETTY MEMORIAL INSTITUTE OF DENTAL SCIENCES, MANGALORE
15.2	Signature	
15.3	Co-guide	PROF. (DR.) A. VEENA SHETTY COORDINATOR- NITTE UNIVERSITY CENTRE FOR STEM CELL RESEARCH AND REGENERATIVE MEDICINE
15.4	Signature	
15.5	Head of the Department	PROF. (DR.) AMITHA RAMESH PROFESSOR AND HEAD DEPARTMENT OF PERIODONTICS A.B SHETTY MEMORIAL INSTITUTE OF DENTAL SCIENCES, MANGALORE
15.6	Signature	
15.7	Remarks of the chairman and Principal	<i>Feasible study</i>
15.8	Signature	 PROF.(DR.) U.S. KRISHNA NAYAK

A.B. SHETTY MEMORIAL INSTITUTE OF DENTAL SCIENCES**DEPARTMENT OF PERIODONTICS**

STUDY TITLE- FABRICATION AND EVALUATION OF A NOVEL BI-LAYER TISSUE ENGINEERED SCAFFOLD FOR IMPROVED BIO SEAL AND ANTIMICROBIAL PROPERTIES OF DENTAL IMPLANTS: AN IN VITRO STUDY

CASE SHEET**Name:****Case no:****Age:****Date:****Gender:****Address:****Education:****Marital status:****Occupation:****Height:****Weight:****Medical history:**

- a. Systemic diseases:
- b. Menopause:

Personal history:

- 1. Oral hygiene practices –
 - a. Type:
 - b. Frequency:
 - c. Method:
- 2. History of smoking:
- 3. Diet:

Intraoral examination:

- 1. Tongue:
- 2. Palate:
- 3. Buccal mucosa:

Probing depth

[illegible]

Clinical attachment loss

[illegible]

PISA SCORE

PPD	tooth	18	17	16	15	14	13	12	11	21	22	23	24	25	26	27	28	tooth	PPD
	buccal palatal																	buccal palatal	
PPD	lingual																	lingual	PPD
	buccal tooth	48	47	46	45	44	43	42	41	31	32	33	34	35	36	37	38	buccal tooth	

tooth surface area (mm ²)	tooth	18	17	16	15	14	13	12	11	21	22	23	24	25	26	27	28	tooth
	surface area (mm ²)	0	0.0000	0.0000	0.0000	0.0000	0.0000	0.0000	0.0000	0.0000	0.0000	0.0000	0.0000	0.0000	0.0000	0.0000	0	surface area (mm ²)
surface area (mm ²)	tooth	48	47	46	45	44	43	42	41	31	32	33	34	35	36	37	38	tooth

tooth	PESA	nr of sites with BOP	PISA (mm ²)
18	0		0.00
17	0		0.00
16	0		0.00
15	0		0.00
14	0		0.00
13	0		0.00
12	0		0.00
11	0		0.00
21	0		0.00
22	0		0.00
23	0		0.00
24	0		0.00
25	0		0.00
26	0		0.00
27	0		0.00
28	0		0.00

tooth	PESA	nr of sites with BOP	PISA (mm ²)
38	0		0.00
37	0		0.00
36	0		0.00
35	0		0.00
34	0		0.00
33	0		0.00
32	0		0.00
31	0		0.00
41	0		0.00
42	0		0.00
43	0		0.00
44	0		0.00
45	0		0.00
46	0		0.00
47	0		0.00
48	0		0.00

Total Periodontal Epithelial Surface Area (mm ²)	
0.0	

Total Periodontal Inflamed Surface Area (mm ²)	
0.0	

A.B SHETTY MEMORIAL INSTITUTE OF DENTAL SCIENCES
DEPARTMENT OF PERIODONTICS

STUDY TITLE- FABRICATION AND EVALUATION OF A NOVEL BI-LAYER TISSUE ENGINEERED SCAFFOLD FOR IMPROVED BIO SEAL AND ANTIMICROBIAL PROPERTIES OF DENTAL IMPLANTS: AN IN VITRO STUDY

INFORMED CONSENT FORM

Name of the volunteer:

Age:

Sex:

This informed consent is intended to protect yourself, the investigator who asks you to take part in the study, and the members of the committee (institutional ethics committee) who are responsible for permitting the study. You should certify your agreement with the following statement by signing below.

I have received a verbal description of the study in which I have been asked to participate. I agree that the verbal description:

1. Describes the purpose, nature of the study
2. Indicates the number of people who will also be participating in this study
3. Indicates the location of the study
4. Explains the test procedures (GINGIVAL TISSUE COLLECTION METHOD) and mentions the possibility of unforeseeable risks.
5. I have had an opportunity to ask questions, and my questions have been satisfactorily answered.
6. I have disclosed to those considering my participation in this study details of any adverse or unusual reactions to any medicaments used by me, whether obtained on prescription, or over-the-counter treatments.
7. I will be able to follow the procedures required of me, including visits for assessment, agree to follow instructions as required.
8. I understand that my participation in the study is voluntary and that I am free to withdraw at any time, without giving any reason, without my medical care or legal rights being affected.

I am willing to take part in this study.

Signature of the volunteer:

Date:

A.B SHETTY MEMORIAL INSTITUTE OF DENTAL SCIENCES**DEPARTMENT OF PERIODONTICS**

STUDY TITLE- FABRICATION AND EVALUATION OF A NOVEL BI-LAYER TISSUE ENGINEERED SCAFFOLD FOR IMPROVED BIO SEAL AND ANTIMICROBIAL PROPERTIES OF DENTAL IMPLANTS: AN IN VITRO STUDY

അറിയിച്ച സമ്മത ഫോം

സന്നദ്ധപ്രവർത്തകന്റെ പേര്:

വയസ്സ്:

ലൈംഗികത:

ഈ അറിവോടെയുള്ള സമ്മതം നിങ്ങളെയും പഠനത്തിൽ പങ്കെടുക്കാൻ നിങ്ങളോട് ആവശ്യപ്പെടുന്ന അന്വേഷകനെയും പഠനത്തിന് അനുമതി നൽകുന്നതിന് ഉത്തരവാദികളായ കമ്മിറ്റിയിലെ (ഇൻസ്റ്റിറ്റ്യൂഷണൽ എത്തിക്സ് കമ്മിറ്റി) അംഗങ്ങളെയും സംരക്ഷിക്കാൻ ഉദ്ദേശിച്ചുള്ളതാണ്. താഴെ ഒപ്പിട്ടുകൊണ്ട് ഇനിപ്പറയുന്ന പ്രസ്താവനയുമായുള്ള നിങ്ങളുടെ കരാർ നിങ്ങൾ സാക്ഷ്യപ്പെടുത്തണം. എന്നോട് പങ്കെടുക്കാൻ ആവശ്യപ്പെട്ട പഠനത്തിന്റെ വാക്കാലുള്ള വിവരണം എനിക്ക് ലഭിച്ചു. വാക്കാലുള്ള വിവരണം ഞാൻ സമ്മതിക്കുന്നു:

1. പഠനത്തിന്റെ ഉദ്ദേശ്യം, സ്വഭാവം എന്നിവ വിവരിക്കുന്നു
2. ഈ പഠനത്തിൽ പങ്കെടുക്കുന്ന ആളുകളുടെ എണ്ണം സൂചിപ്പിക്കുന്നു, പഠനത്തിന്റെ സ്ഥാനം സൂചിപ്പിക്കുന്നു
3. പരിശോധനാ നടപടിക്രമങ്ങൾ (ജിംഗൈവൽ ടിഷ്യൂ ശേഖരണ രീതി) വിശദീകരിക്കുകയും മുൻകൂട്ടിക്കാണാൻ കഴിയാത്ത അപകടസാധ്യതകൾ സൂചിപ്പിക്കുകയും ചെയ്യുന്നു.
4. എനിക്ക് ചോദ്യങ്ങൾ ചോദിക്കാനുള്ള അവസരം ലഭിച്ചു, എന്റെ ചോദ്യങ്ങൾക്ക് തൃപ്തികരമായ ഉത്തരം ലഭിച്ചു.
5. ഈ പഠനത്തിൽ എന്റെ പങ്കാളിത്തം പരിഗണിക്കുന്നവരോട് ഞാൻ ഉപയോഗിക്കുന്ന ഏതെങ്കിലും മരുന്നുകളോട് എന്തെങ്കിലും പ്രതികൂലമോ അസാധാരണമോ ആയ പ്രതികരണങ്ങളുടെ വിശദാംശങ്ങൾ ഞാൻ വെളിപ്പെടുത്തിയിട്ടുണ്ട്, കുറിപ്പടിയിലൂടെയോ അല്ലെങ്കിൽ കൗണ്ടർ ചികിത്സകളിലൂടെയോ ലഭിച്ചതാണോ.
6. മൂല്യനിർണ്ണയത്തിനുള്ള സന്ദർശനങ്ങൾ ഉൾപ്പെടെ, എനിക്ക് ആവശ്യമായ നടപടിക്രമങ്ങൾ പാലിക്കാൻ എനിക്ക് കഴിയും, ആവശ്യാനുസരണം നിർദ്ദേശങ്ങൾ പാലിക്കാൻ സമ്മതിക്കുന്നു.
7. പഠനത്തിൽ എന്റെ പങ്കാളിത്തം സ്വമേധയാ ഉള്ളതാണെന്നും ഒരു കാരണവും പറയാതെ, എന്റെ മെഡിക്കൽ പരിചരണത്തെയോ നിയമപരമായ അവകാശങ്ങളെയോ ബാധിക്കാതെ എപ്പോൾ വേണമെങ്കിലും പിൻവലിക്കാൻ എനിക്ക് സ്വാതന്ത്ര്യമുണ്ടെന്നും ഞാൻ മനസ്സിലാക്കുന്നു.

ഈ പഠനത്തിൽ പങ്കെടുക്കാൻ ഞാൻ തയ്യാറാണ്.

സന്നദ്ധപ്രവർത്തകന്റെ ഒപ്പ്:

തീയതി:

A.B SHETTY MEMORIAL INSTITUTE OF DENTAL SCIENCES**DEPARTMENT OF PERIODONTICS**

STUDY TITLE- FABRICATION AND EVALUATION OF A NOVEL BI-LAYER TISSUE ENGINEERED SCAFFOLD FOR IMPROVED BIO SEAL AND ANTIMICROBIAL PROPERTIES OF DENTAL IMPLANTS: AN IN VITRO STUDY

सूचित सहमति प्रपत्र

स्वयंसेवक का नाम:

उम्र:

लिंग:

इस सूचित सहमति का उद्देश्य स्वयं की रक्षा करना है, अन्वेषक जो भी आपको अध्ययन में भाग लेने के लिए कहता है और समिति के सदस्य (संस्थागत नैतिकता समिति) जो अध्ययन की अनुमति देने के लिए जिम्मेदार हैं। आपको निम्नलिखित कथन के साथ अपने अनुबंध को नीचे हस्ताक्षर करके प्रमाणित करना चाहिए।

मुझे उस अध्ययन का मौखिक विवरण प्राप्त हुआ है जिसमें मुझे भाग लेने के लिए कहा गया है। मैं सहमत हूँ कि मौखिक विवरण:

1. अध्ययन के उद्देश्य, प्रकृति का वर्णन करता है
2. उन लोगों की संख्या को दर्शाता है जो इस अध्ययन में भी भाग लेंगे
3. अध्ययन के स्थान को इंगित करता है
4. परीक्षण प्रक्रियाओं (जिजिवल ऊतक संग्रह विधि) की व्याख्या करता है और अप्रत्याशित जोखिमों की संभावना का उल्लेख करता है।
5. मुझे प्रश्न पूछने का अवसर मिला है, और मेरे प्रश्नों का संतोषजनक उत्तर दिया गया है।
6. मैंने इस अध्ययन में मेरी भागीदारी पर विचार करने वालों को मेरे द्वारा उपयोग की जाने वाली किसी भी दवा के प्रतिकूल या असामान्य प्रतिक्रियाओं के विवरण का खुलासा किया है, चाहे वह नुस्खे पर या काउंटर उपचार पर प्राप्त किया गया हो।
7. मैं अपने लिए आवश्यक प्रक्रियाओं का पालन करने में सक्षम होऊंगा, जिसमें मूल्यांकन के लिए दौरे शामिल हैं, आवश्यकतानुसार निर्देशों का पालन करने के लिए सहमत हूँ।
8. मैं समझता हूँ कि अध्ययन में मेरी भागीदारी स्वैच्छिक है और मैं बिना कोई कारण बताए, मेरी चिकित्सा देखभाल या कानूनी अधिकारों को प्रभावित किए बिना किसी भी समय वापस लेने के लिए स्वतंत्र हूँ।

मैं इस अध्ययन में भाग लेने के लिए तैयार हूँ।

स्वयंसेवक के हस्ताक्षर:

तारीख:

A.B SHETTY MEMORIAL INSTITUTE OF DENTAL SCIENCES**DEPARTMENT OF PERIODONTICS**

STUDY TITLE- FABRICATION AND EVALUATION OF A NOVEL BI-LAYER TISSUE ENGINEERED SCAFFOLD FOR IMPROVED BIO SEAL AND ANTIMICROBIAL PROPERTIES OF DENTAL IMPLANTS: AN IN VITRO STUDY

ಮಾಹಿತಿ ನೀಡಿದ ಒಪ್ಪಿಗೆ ನಮೂನೆ

ಸ್ವಯಂಸೇವಕರ ಹೆಸರು:

ವಯಸ್ಸು:

ಲಿಂಗ:

ಈ ತಿಳುವಳಿಕೆಯುಳ್ಳ ಸಮ್ಮತಿಯು ನಿಮ್ಮನ್ನು, ಅಧ್ಯಯನದಲ್ಲಿ ಭಾಗವಹಿಸಲು ನಿಮ್ಮನ್ನು ಕೇಳುವ ತನಿಖಾಧಿಕಾರಿ ಮತ್ತು ಅಧ್ಯಯನಕ್ಕೆ ಅನುಮತಿ ನೀಡುವ ಜವಾಬ್ದಾರಿ ಹೊಂದಿರುವ ಸಮಿತಿಯ (ಸಾಂಸ್ಥಿಕ ನೈತಿಕ ಸಮಿತಿ) ಸದಸ್ಯರನ್ನು ರಕ್ಷಿಸಲು ಉದ್ದೇಶಿಸಲಾಗಿದೆ. ಕೆಳಗೆ ಸಹಿ ಮಾಡುವ ಮೂಲಕ ಕೆಳಗಿನ ಹೇಳಿಕೆಯೊಂದಿಗೆ ನಿಮ್ಮ ಒಪ್ಪಂದವನ್ನು ನೀವು ಪ್ರಮಾಣೀಕರಿಸಬೇಕು.

ನಾನು ಭಾಗವಹಿಸಲು ಕೇಳಲಾದ ಅಧ್ಯಯನದ ಮೌಖಿಕ ವಿವರಣೆಯನ್ನು ನಾನು ಸ್ವೀಕರಿಸಿದ್ದೇನೆ. ಮೌಖಿಕ ವಿವರಣೆಯನ್ನು ನಾನು ಒಪ್ಪುತ್ತೇನೆ:

1. ಅಧ್ಯಯನದ ಉದ್ದೇಶ, ಸ್ವರೂಪವನ್ನು ವಿವರಿಸುತ್ತದೆ
2. ಈ ಅಧ್ಯಯನದಲ್ಲಿ ಭಾಗವಹಿಸುವ ಜನರ ಸಂಖ್ಯೆಯನ್ನು ಸೂಚಿಸುತ್ತದೆ
3. ಅಧ್ಯಯನದ ಸ್ಥಳವನ್ನು ಸೂಚಿಸುತ್ತದೆ
4. ಪರೀಕ್ಷಾ ವಿಧಾನಗಳನ್ನು ವಿವರಿಸುತ್ತದೆ (ಜಿಂಗ್ಸ್‌ವಲ್ ಟೆಶ್ಟ್, ಕಲೆಕ್ಷನ್ ಮಥಡ್) ಮತ್ತು ಅನಿರೀಕ್ಷಿತ ಅಪಾಯಗಳ ಸಾಧ್ಯತೆಯನ್ನು ಉಲ್ಲೇಖಿಸುತ್ತದೆ.
5. ಪ್ರಶ್ನೆಗಳನ್ನು ಕೇಳಲು ನನಗೆ ಅವಕಾಶವಿದೆ ಮತ್ತು ನನ್ನ ಪ್ರಶ್ನೆಗಳಿಗೆ ತೃಪ್ತಿಕರವಾಗಿ ಉತ್ತರಿಸಲಾಗಿದೆ.
6. ಈ ಅಧ್ಯಯನದಲ್ಲಿ ನನ್ನ ಭಾಗವಹಿಸುವಿಕೆಯನ್ನು ಪರಿಗಣಿಸುವವರಿಗೆ ನಾನು ಬಳಸಿದ ಯಾವುದೇ ಔಷಧಿಗಳಿಗೆ ಯಾವುದೇ ಪ್ರತಿಕ್ರೋಧ ಅಥವಾ ಅಸಾಮಾನ್ಯ ಪ್ರತಿಕ್ರಿಯೆಗಳ ವಿವರಗಳನ್ನು ನಾನು ಬಹಿರಂಗಪಡಿಸಿದ್ದೇನೆ, ಪ್ರಿಸ್ಟಿಪ್ಷನ್ ಅಥವಾ ಕೌಂಟರ್ ಟ್ರೀಟ್ಮೆಂಟ್ ಮೂಲಕ ಪಡೆಯಲಾಗಿದೆ.
7. ಮೌಲ್ಯಮಾಪನಕ್ಕಾಗಿ ಭೇಟಿಗಳು ಸೇರಿದಂತೆ ನನಗೆ ಅಗತ್ಯವಿರುವ ಕಾರ್ಯವಿಧಾನಗಳನ್ನು ಅನುಸರಿಸಲು ನನಗೆ ಸಾಧ್ಯವಾಗುತ್ತದೆ, ಅಗತ್ಯವಿರುವಂತೆ ಸೂಚನೆಗಳನ್ನು ಅನುಸರಿಸಲು ಒಪ್ಪಿಕೊಳ್ಳುತ್ತೇನೆ.
8. ಅಧ್ಯಯನದಲ್ಲಿ ನನ್ನ ಭಾಗವಹಿಸುವಿಕೆಯು ಸ್ವಯಂಪ್ರೇರಿತವಾಗಿದೆ ಮತ್ತು ಯಾವುದೇ ಕಾರಣವನ್ನು ನೀಡದೆ, ನನ್ನ ವೈದ್ಯಕೀಯ ಆರೈಕೆ ಅಥವಾ ಕಾನೂನು ಹಕ್ಕುಗಳ ಮೇಲೆ ಪರಿಣಾಮ ಬೀರದಂತೆ ನಾನು ಯಾವುದೇ ಸಮಯದಲ್ಲಿ ಹಿಂಪಡೆಯಲು ಸ್ವತಂತ್ರನಾಗಿದ್ದೇನೆ ಎಂದು ನಾನು ಅರ್ಥಮಾಡಿಕೊಂಡಿದ್ದೇನೆ.

ನಾನು ಈ ಅಧ್ಯಯನದಲ್ಲಿ ಭಾಗವಹಿಸಲು ಸಿದ್ಧನಿದ್ದೇನೆ.

ಸ್ವಯಂಸೇವಕರ ಸಹಿ:

ದಿನಾಂಕ

A.B SHETTY MEMORIAL INSTITUTE OF DENTAL SCIENCES**DEPARTMENT OF PERIODONTICS**

TITLE: - FABRICATION AND EVALUATION OF A NOVEL BI-LAYER TISSUE ENGINEERED SCAFFOLD FOR IMPROVED BIO SEAL AND ANTIMICROBIAL PROPERTIES OF DENTAL IMPLANTS: AN IN VITRO STUDY

SUBJECT INFORMATION SHEET

We would like you to inform that this study is being conducted by _____

This study consists of case history taking, intraoral examination, scaling, and minor surgical procedures like crown lengthening and operculectomy by giving local anesthesia.

Your response to this study or any individual questions is completely voluntary.

You will not be individually identified and your participation in this study will be used for statistical purposes only.

You are free to refuse to participate in this study at any given time. There are no risks in taking part in the study

Joining the trial will not result in any expenses for you. None of the participants will receive any payment

If you have any questions regarding our study, please contact:

A.B SHETTY MEMORIAL INSTITUTE OF DENTAL SCIENCES**DEPARTMENT OF PERIODONTICS**

TITLE: - FABRICATION AND EVALUATION OF A NOVEL BI-LAYER TISSUE ENGINEERED SCAFFOLD FOR IMPROVED BIO SEAL AND ANTIMICROBIAL PROPERTIES OF DENTAL IMPLANTS: AN IN VITRO STUDY

ವಿಷಯ ಮಾಹಿತಿ ಕಾಗದ

ಈ ಅಧ್ಯಯನ ವನ್ನು ಪೆರಿಯೊಡಾಂಟಿಕ್ಸ್ ವಿಭಾಗ, A.B Shetty Memorial Institute of Dental Sciences, ದೇರಳಕಟ್ಟೆ, ಮಂಗಳೂರು ಇದರಿಂದ ನಡೆಸಲಾಗುತ್ತಿದೆ ಎಂದು ತಿಳಿಸಲು ಬಯಸುತ್ತೇವೆ. ಈ ಅಧ್ಯಯನ ಕೇಸ ಹಿಸ್ಟರಿ ಟೇಕಿಂಗ್, ಇಂಟ್ರಾರಲ್ ಪರೀಕ್ಷೆ, ಸ್ಟೇಲಿಂಗ್ ಮತ್ತು ಸ್ಥಳೀಯ ಅರಿವಳಿಕೆ ನೀಡುವ ಮೂಲಕ ಕ್ರೌನ್ ಲೆಂಗ್ತ್‌ನಿಂಗ್ ಮತ್ತು ಆಪರ್ಯುಲೆಕ್ಟಮಿಯಂಟ್‌ಹ ಸಣ್ಣ ಶಸ್ತ್ರಚಿಕಿತ್ಸಾ ವಿಧಾನಗಳನ್ನು ಒಳಗೊಂಡಿದೆ. ಈ ಅಧ್ಯಯನ ಅಥವಾ ಯಾವುದೇ ವೈಯಕ್ತಿಕ ಪ್ರಶ್ನೆಗಳಿಗೆ ನಿಮ್ಮ ಪ್ರತಿಕ್ರಿಯೆ ಸಂಪೂರ್ಣವಾಗಿ ಸ್ವಯಂಪ್ರೇರಿತವಾಗಿದೆ. ನಿಮ್ಮನ್ನು ಪ್ರತ್ಯೇಕವಾಗಿ ಗುರುತಿಸಲಾಗುವುದಿಲ್ಲ ಮತ್ತು ಈ ಅಧ್ಯಯನದಲ್ಲಿ ನಿಮ್ಮ ಭಾಗವಹಿಸುವಿಕೆಯನ್ನು ಸಂಖ್ಯಾಶಾಸ್ತ್ರೀಯ ಉದ್ದೇಶಗಳಿಗಾಗಿ ಮಾತ್ರ ಬಳಸಲಾಗುತ್ತದೆ.

ಯಾವುದೇ ಸಮಯದಲ್ಲಿ ಈ ಅಧ್ಯಯನದಲ್ಲಿ ಭಾಗವಹಿಸಲು ನಿರಾಕರಿಸಲು ನೀವು ಸ್ವತಂತ್ರರು. ಅಧ್ಯಯನದಲ್ಲಿ ಪಾಲ್ಗೊಳ್ಳುವುದರಿಂದ ಯಾವುದೇ ಅಪಾಯಗಳಿಲ್ಲ

ಪ್ರಯೋಗಕ್ಕೆ ಸೇರುವುದರಿಂದ ನಿಮಗೆ ಯಾವುದೇ ವೆಚ್ಚವಾಗುವುದಿಲ್ಲ. ಭಾಗವಹಿಸುವವರಲ್ಲಿ ಯಾರೂ ಯಾವುದೇ ಪಾವತಿಯನ್ನು ಸ್ವೀಕರಿಸುವುದಿಲ್ಲ

ನಮ್ಮ ಅಧ್ಯಯನಕ್ಕೆ ಸಂಬಂಧಿಸಿದಂತೆ ನೀವು ಯಾವುದೇ ಪ್ರಶ್ನೆಗಳನ್ನು ಹೊಂದಿದ್ದರೆ, ದಯವಿಟ್ಟು ಸಂಪರ್ಕಿಸಿ:

ಡಾ.ಗೀತು ವೇಣುಗೋಪಾಲನ್

ಸ್ನಾತಕೋತ್ತರ ಪದವಿ

ಪೆರಿಯೊಡಾಂಟಿಕ್ಸ್ ವಿಭಾಗ

A.B Shetty Memorial Institute of Dental Sciences

NITTE Deemed to be University, ಮಂಗಳೂರು.

ದೂರವಾಣಿ ಸಂಖ್ಯೆ: 9895663152

ಇಮೇಲ್ ಐಡಿ: geethu.21dper04@student.nitte.edu.in

A.B SHETTY MEMORIAL INSTITUTE OF DENTAL SCIENCES**DEPARTMENT OF PERIODONTICS**

TITLE: - FABRICATION AND EVALUATION OF A NOVEL BI-LAYER TISSUE ENGINEERED SCAFFOLD FOR IMPROVED BIO SEAL AND ANTIMICROBIAL PROPERTIES OF DENTAL IMPLANTS: AN IN VITRO STUDY

विषय सूचना पत्र

हम आपको सूचित करना चाहेंगे कि यह अध्ययन पीरियोडॉन्टिक्स विभाग, ए बी शेट्टी मेमोरियल इंस्टीट्यूट ऑफ डेंटल साइंसेज, डेरेलकट्टे, मैंगलोर द्वारा किया जा रहा है।

इस अध्ययन में केस हिस्ट्री लेना, अंतर्गर्भाशयी परीक्षा, स्केलिंग, और स्थानीय एनेस्थीसिया देकर क्राउन को लंबा करना और ऑपरेशन जैसी छोटी शल्य प्रक्रियाएं शामिल हैं।

इस अध्ययन या किसी भी व्यक्तिगत प्रश्न पर आपकी प्रतिक्रिया पूरी तरह से स्वैच्छिक है।

आपकी व्यक्तिगत रूप से पहचान नहीं की जाएगी और इस अध्ययन में आपकी भागीदारी का उपयोग केवल सांख्यिकीय उद्देश्यों के लिए किया जाएगा।

आप किसी भी समय इस अध्ययन में भाग लेने से इंकार करने के लिए स्वतंत्र हैं। अध्ययन में भाग लेने में कोई जोखिम नहीं है

परीक्षण में शामिल होने से आपके लिए कोई खर्च नहीं होगा। किसी भी प्रतिभागी को कोई भुगतान प्राप्त नहीं होगा

यदि हमारे अध्ययन के संबंध में आपके कोई प्रश्न हैं, तो कृपया संपर्क करें:

डॉ. गीतू वेणुगोपालन

पोस्ट ग्रेजुएट

पीरियोडॉन्टिक्स विभाग

ए बी शेट्टी मेमोरियल इंस्टीट्यूट ऑफ डेंटल साइंसेज

एनआईटीटीई डीमड टू बी यूनिवर्सिटी डेरेलकट्टे, मैंगलोर।

फोन नंबर: 9895663152

ईमेल आईडी: geethu.21dper04@student.nitte.edu.

A.B SHETTY MEMORIAL INSTITUTE OF DENTAL SCIENCES**DEPARTMENT OF PERIODONTICS**

TITLE: - FABRICATION AND EVALUATION OF A NOVEL BI-LAYER TISSUE ENGINEERED SCAFFOLD FOR IMPROVED BIO SEAL AND ANTIMICROBIAL PROPERTIES OF DENTAL IMPLANTS: AN IN VITRO STUDY

സബ്ജക്ട് ഇൻഫർമേഷൻ ഷീറ്റ്

മംഗലാപുരത്തെ ദേരലക്കാട്ടെ, എ ബി ഷെട്ടി മെമ്മോറിയൽ ഇൻസ്റ്റിറ്റ്യൂട്ട് ഓഫ് ഡെന്റൽ സയൻസസിലെ ഡിപ്പാർട്ട്മെന്റ് ഓഫ് റിയോഡോണ്ടിക്സ് ആണ് ഈ പഠനം നടത്തുന്നതെന്ന് നിങ്ങളെ അറിയിക്കാൻ ഞങ്ങൾ ആഗ്രഹിക്കുന്നു. ഈ പഠനത്തിൽ കേസ് ഹിസ്റ്ററി എടുക്കൽ, ഇൻട്രാറൽ പരിശോധന, സ്കെയിലിംഗ്, ലോക്കൽ അനസ്തേഷ്യ നൽകി ക്രൗൺ നീളം കൂട്ടൽ, ഓപ്പർക്യൂലക്ടമി തുടങ്ങിയ ചെറിയ ശസ്ത്രക്രിയകൾ എന്നിവ ഉൾപ്പെടുന്നു. ഈ പഠനത്തിനോ ഏതെങ്കിലും വ്യക്തിഗത ചോദ്യത്തിനോ ഉള്ള നിങ്ങളുടെ പ്രതികരണം പൂർണ്ണമായും സ്വമേധയാ ഉള്ളതാണ്. നിങ്ങളെ വ്യക്തിപരമായി തിരിച്ചറിയില്ല കൂടാതെ ഈ പഠനത്തിലെ നിങ്ങളുടെ പങ്കാളിത്തം സ്ഥിതിവിവരക്കണക്കുകൾക്കായി മാത്രം ഉപയോഗിക്കും.

എപ്പോൾ വേണമെങ്കിലും ഈ പഠനത്തിൽ പങ്കെടുക്കാൻ വിസമ്മതിക്കാൻ നിങ്ങൾക്ക് സ്വാതന്ത്ര്യമുണ്ട്. പഠനത്തിൽ പങ്കെടുക്കുന്നതിൽ അപകടങ്ങളൊന്നുമില്ല. ട്രെയിനിൽ ചേരുന്നത് നിങ്ങൾക്ക് ഒരു ചെലവും ഉണ്ടാക്കില്ല. പങ്കെടുക്കുന്ന ആർക്കും ഒരു പേയ്മെന്റും ലഭിക്കില്ല.

ഞങ്ങളുടെ പഠനവുമായി ബന്ധപ്പെട്ട് നിങ്ങൾക്ക് എന്തെങ്കിലും ചോദ്യങ്ങളുണ്ടെങ്കിൽ, ദയവായി ബന്ധപ്പെടുക:

ഡോ.ഗീതു വേണുഗോപാലൻ

ബിരുദാനന്തര ബിരുദം

ഡിപ്പാർട്ട്മെന്റ് ഓഫ് പെരിയോഡോണ്ടിക്സ്

എ ബി ഷെട്ടി മെമ്മോറിയൽ ഇൻസ്റ്റിറ്റ്യൂട്ട് ഓഫ് ഡെന്റൽ സയൻസസ്

NITTE മംഗലാപുരത്തെ ദേരലക്കാട്ടെ സർവ്വകലാശാലയായി കണക്കാക്കുന്നു.

ഫോൺ നമ്പർ: 9895663152

ഇമെയിൽ ഐഡി: geethu.21dper04@student.nitte.edu.in

CERTIFICATE

This is to certify that the dissertation titled “Fabrication and evaluation of a novel bi-layer tissue-engineered scaffold for improved bio seal and antimicrobial properties of dental implants: An in vitro study” submitted by Dr. Geethu Venugopalan (US No. NU21DPER04), Department of Periodontology, A.B. Shetty Memorial Institute of Dental Sciences, Deralakatte, has been subjected to TURNITIN software for Anti-Plagiarism and it is found to have a similarity index of 7%

This is within the 15% permitted by Nitte (Deemed to be University) for the acceptance of Dissertation.



Prof. (Dr.) Amitha Ramesh

Head of Department

Department of Periodontics

A.B. Shetty Memorial Institute of Dental Sciences
 Department of Periodontics
 Nitte (Deemed to be University)
 Deralakatte, Mangalore - 575 018



Mrs. Shashikala K

Librarian

ABSMIDS

Librarian

A.B. Shetty Memorial Institute of
 Dental Sciences Deralakatte
 MANGALORE 575 018

Fabrication and evaluation of a novel bilayer tissue engineered scaffold for improved bioseal and antimicrobial porpoerties of dental implants

ORIGINALITY REPORT

7 %	6 %	4 %	0 %
SIMILARITY INDEX	INTERNET SOURCES	PUBLICATIONS	STUDENT PAPERS

PRIMARY SOURCES

1	new.esp.org Internet Source	2 %
2	www.researchgate.net Internet Source	1 %
3	eprints.qut.edu.au Internet Source	1 %
4	Apoorva Mathur, Om Prakash Kharbanda, Veena Koul, Amit Kumar Dinda, Mohammad Faiyaz Anwar, Suchita Singh. "Fabrication and evaluation of antimicrobial biomimetic nanofiber coating for improved dental implant bioseal: An in vitro study", Journal of Periodontology, 2022 Publication	1 %
5	Ahmed Saad, Carolina Penaloza Arias, Min Wang, Osama ElKashty, Davide Brambilla, Faleh Tamimi, Marta Cerruti. "Biomimetic Strategy to Enhance Epithelial Cell Viability	1 %

and Spreading on PEEK Implants", ACS Biomaterials Science & Engineering, 2022

Publication

6	journals.innovareacademics.in	1 %
	Internet Source	
7	jpsr.pharmainfo.in	1 %
	Internet Source	

Exclude quotes On

Exclude matches < 1%

Exclude bibliography On



धातुकी एवं पदार्थ अभियांत्रिकी विभाग
राष्ट्रीय प्रौद्योगिकी संस्थान कर्नाटक, सुरतकल
DEPARTMENT OF METALLURGICAL & MATERIALS ENGINEERING
NATIONAL INSTITUTE OF TECHNOLOGY KARNATAKA, SURATHKAL

S Anandhan PhD FRSC
Professor & Former Head
Metallurgical & Materials Engineering
Phone: +91-824-2473762
anandhan@nitk.edu.in

15 February, 2024

TO WHOMSOEVER IT MAY CONCERN

This is to certify that Dr. Geethu Venugopalan, who has been pursuing her M.D.S. at the A.B. Shetty Memorial Institute of Dental Sciences, Nitte Deemed to be University, Deralakatte, Mangaluru – 575018, Karnataka, India, has carried out the following experiments in my department with our collaboration (2023-24) as part of her master's research project: synthesis of biocompatible nanofibrous scaffolds, FTIR spectroscopy, contact angle measurements, and x-ray diffraction. She has used the field emission scanning electron microscopy in our central research facility with our assistance. We wish Dr. Geethu all the best for her master's thesis.

Sincerely,

Prof. S. Anandhan PhD FRSC
Department of Metallurgical & Materials Engineering
National Institute of Technology Karnataka
Surathkal, Srinivasnagar (P.O.)
Mangaluru-575025, Karnataka, India.

To,

**DR. GEETHU VENUGOPALAN
POST GRADUATE
NU21DPER04
DEPARTMENT OF PERIODONTICS**

Dear Dr. Geethu Venugopalan,

Sub: Permission to use the facilities at NUCSReM for MDS dissertation- Reg.

With reference to your letter dated 19/04/2022, I hereby provide the consent to use the facilities at NUCSReM to conduct the research pertaining to PG dissertation on the topic **"FABRICATION AND EVALUATION OF A NOVEL BI-LAYER TISSUE ENGINEERED SCAFFOLD FOR IMPROVED BIO SEAL AND ANTIMICROBIAL PROPERTIES OF DENTAL IMPLANTS - AN IN VITRO STUDY"** . The research expenses of the study will be borne by the student.

With best regards,



Dr. A. Veena Shetty

CRL Scientific officer
Research Co-ordinator
NUCSReM, KSHEMA

Copy to:

1. PROF. (DR) RAHUL BHANDARY, Guide, Dept. of Periodontics, ABSMIDS

COMPARISONS OF CELL VIABILITY					
Tukey's multiple comparisons test	Mean Diff.	95.00% CI of diff.	Below threshold?	Summary	Adjusted P Value
24 hrs:Control vs. 24 hrs:Ti coated	12.85	4.011 to 21.69	Yes	**	0.0049
24 hrs:Control vs. 24 hrs:Ti uncoated	31.76	22.92 to 40.59	Yes	****	<0.0001
24 hrs:Control vs. 48 hrs:Control	1.505	-7.334 to 10.34	No	ns	0.998
24 hrs:Control vs. 48 hrs:Ti coated	9.465	0.6258 to 18.30	Yes	*	0.0343
24 hrs:Control vs. 48 hrs:Ti uncoated	32.88	24.04 to 41.72	Yes	****	<0.0001
24 hrs:Control vs. 72 hrs:Control	0.9	-7.939 to 9.739	No	ns	>0.9999
24 hrs:Control vs. 72 hrs:Ti coated	8.565	-0.2742 to 17.40	No	ns	0.0591
24 hrs:Control vs. 72 hrs:Ti uncoated	23.31	14.47 to 32.15	Yes	****	<0.0001
24 hrs:Ti coated vs. 24 hrs:Ti uncoated	18.91	10.07 to 27.74	Yes	***	0.0003
24 hrs:Ti coated vs. 48 hrs:Control	-11.35	-20.18 to -2.506	Yes	*	0.0114
24 hrs:Ti coated vs. 48 hrs:Ti coated	-3.385	-12.22 to 5.454	No	ns	0.825
24 hrs:Ti coated vs. 48 hrs:Ti uncoated	20.03	11.19 to 28.87	Yes	***	0.0002
24 hrs:Ti coated vs. 72 hrs:Control	-11.95	-20.79 to -3.111	Yes	**	0.0081
24 hrs:Ti coated vs. 72 hrs:Ti coated	-4.285	-13.12 to 4.554	No	ns	0.62
24 hrs:Ti coated vs. 72 hrs:Ti uncoated	10.46	1.621 to 19.30	Yes	*	0.019
24 hrs:Ti uncoated vs. 48 hrs:Control	-30.25	-39.09 to -21.41	Yes	****	<0.0001
24 hrs:Ti uncoated vs. 48 hrs:Ti coated	-22.29	-31.13 to -13.45	Yes	****	<0.0001
24 hrs:Ti uncoated vs. 48 hrs:Ti uncoated	1.125	-7.714 to 9.964	No	ns	0.9997
24 hrs:Ti uncoated vs. 72 hrs:Control	-30.86	-39.69 to -22.02	Yes	****	<0.0001
24 hrs:Ti uncoated vs. 72 hrs:Ti coated	-23.19	-32.03 to -14.35	Yes	****	<0.0001
24 hrs:Ti uncoated vs. 72 hrs:Ti uncoated	-8.445	-17.28 to 0.3942	No	ns	0.0635

48 hrs:Control vs. 48 hrs:Ti coated	7.96	-0.8792 to 16.80	No	ns	0.0853
48 hrs:Control vs. 48 hrs:Ti uncoated	31.38	22.54 to 40.21	Yes	****	<0.0001
48 hrs:Control vs. 72 hrs:Control	-0.605	-9.444 to 8.234	No	ns	>0.9999
48 hrs:Control vs. 72 hrs:Ti coated	7.06	-1.779 to 15.90	No	ns	0.1468
48 hrs:Control vs. 72 hrs:Ti uncoated	21.81	12.97 to 30.64	Yes	****	<0.0001
48 hrs:Ti coated vs. 48 hrs:Ti uncoated	23.42	14.58 to 32.25	Yes	****	<0.0001
48 hrs:Ti coated vs. 72 hrs:Control	-8.565	-17.40 to 0.2742	No	ns	0.0591
48 hrs:Ti coated vs. 72 hrs:Ti coated	-0.9	-9.739 to 7.939	No	ns	>0.9999
48 hrs:Ti coated vs. 72 hrs:Ti uncoated	13.85	5.006 to 22.68	Yes	**	0.0029
48 hrs:Ti uncoated vs. 72 hrs:Control	-31.98	-40.82 to -23.14	Yes	****	<0.0001
48 hrs:Ti uncoated vs. 72 hrs:Ti coated	-24.32	-33.15 to -15.48	Yes	****	<0.0001
48 hrs:Ti uncoated vs. 72 hrs:Ti uncoated	-9.57	-18.41 to -0.7308	Yes	*	0.0322
72 hrs:Control vs. 72 hrs:Ti coated	7.665	-1.174 to 16.50	No	ns	0.102
72 hrs:Control vs. 72 hrs:Ti uncoated	22.41	13.57 to 31.25	Yes	****	<0.0001
72 hrs:Ti coated vs. 72 hrs:Ti uncoated	14.75	5.906 to 23.58	Yes	**	0.0019

COMPARISONS OF CELL PROLIFERATION					
Tukey's multiple comparisons test	Mean Diff.	95.00% CI of diff.	Below threshold?	Summary	Adjusted P Value
24hrs:Control vs. 24hrs:Ti coated	3250	-5386 to 11886	No	ns	0.8366
24hrs:Control vs. 24hrs:Ti uncoated	62750	54114 to 71386	Yes	****	<0.0001
24hrs:Control vs. 48hrs:Control	-74500	-83136 to -65864	Yes	****	<0.0001
24hrs:Control vs. 48hrs:Ti coated	425	-8211 to 9061	No	ns	>0.9999
24hrs:Control vs. 48hrs:Ti uncoated	65250	56614 to 73886	Yes	****	<0.0001
24hrs:Control vs. 72hrs:Control	-89500	-98136 to -80864	Yes	****	<0.0001
24hrs:Control vs. 72hrs:Ti coated	-14500	-23136 to -5864	Yes	**	0.0018
24hrs:Control vs. 72hrs:Ti uncoated	56500	47864 to 65136	Yes	****	<0.0001
24hrs:Ti coated vs. 24hrs:Ti uncoated	59500	50864 to 68136	Yes	****	<0.0001
24hrs:Ti coated vs. 48hrs:Control	-77750	-86386 to -69114	Yes	****	<0.0001
24hrs:Ti coated vs. 48hrs:Ti coated	-2825	-11461 to 5811	No	ns	0.9103
24hrs:Ti coated vs. 48hrs:Ti uncoated	62000	53364 to 70636	Yes	****	<0.0001
24hrs:Ti coated vs. 72hrs:Control	-92750	-101386 to -84114	Yes	****	<0.0001
24hrs:Ti coated vs. 72hrs:Ti coated	-17750	-26386 to -9114	Yes	***	0.0004
24hrs:Ti coated vs. 72hrs:Ti uncoated	53250	44614 to 61886	Yes	****	<0.0001
24hrs:Ti uncoated vs. 48hrs:Control	-137250	-145886 to -128614	Yes	****	<0.0001
24hrs:Ti uncoated vs. 48hrs:Ti coated	-62325	-70961 to -53689	Yes	****	<0.0001
24hrs:Ti uncoated vs. 48hrs:Ti uncoated	2500	-6136 to 11136	No	ns	0.9506
24hrs:Ti uncoated vs. 72hrs:Control	-152250	-160886 to -143614	Yes	****	<0.0001
24hrs:Ti uncoated vs. 72hrs:Ti coated	-77250	-85886 to -68614	Yes	****	<0.0001
24hrs:Ti uncoated vs. 72hrs:Ti uncoated	-6250	-14886 to 2386	No	ns	0.2164

48hrs:Control vs. 48hrs:Ti coated	74925	66289 to 83561	Yes	****	<0.0001
48hrs:Control vs. 48hrs:Ti uncoated	139750	131114 to 148386	Yes	****	<0.0001
48hrs:Control vs. 72hrs:Control	-15000	-23636 to -6364	Yes	**	0.0014
48hrs:Control vs. 72hrs:Ti coated	60000	51364 to 68636	Yes	****	<0.0001
48hrs:Control vs. 72hrs:Ti uncoated	131000	122364 to 139636	Yes	****	<0.0001
48hrs:Ti coated vs. 48hrs:Ti uncoated	64825	56189 to 73461	Yes	****	<0.0001
48hrs:Ti coated vs. 72hrs:Control	-89925	-98561 to -81289	Yes	****	<0.0001
48hrs:Ti coated vs. 72hrs:Ti coated	-14925	-23561 to -6289	Yes	**	0.0014
48hrs:Ti coated vs. 72hrs:Ti uncoated	56075	47439 to 64711	Yes	****	<0.0001
48hrs:Ti uncoated vs. 72hrs:Control	-154750	-163386 to -146114	Yes	****	<0.0001
48hrs:Ti uncoated vs. 72hrs:Ti coated	-79750	-88386 to -71114	Yes	****	<0.0001
48hrs:Ti uncoated vs. 72hrs:Ti uncoated	-8750	-17386 to -114.2	Yes	*	0.0466
72hrs:Control vs. 72hrs:Ti coated	75000	66364 to 83636	Yes	****	<0.0001
72hrs:Control vs. 72hrs:Ti uncoated	146000	137364 to 154636	Yes	****	<0.0001
72hrs:Ti coated vs. 72hrs:Ti uncoated	71000	62364 to 79636	Yes	****	<0.0001